Received 20 June 2023; revised 12 July 2023; accepted 12 July 2023. Date of publication 17 July 2023; date of current version 7 August 2023.

Digital Object Identifier 10.1109/OJCOMS.2023.3296061

Error Rate Analysis of NOMA: Principles, Survey and Future Directions

HAMAD YAHYA [1] (Graduate Student Member, IEEE), ASHFAQ AHMED [2] (Senior Member, IEEE), EMAD ALSUSA [1] (Senior Member, IEEE), ARAFAT AL-DWEIK [3,4] (Senior Member, IEEE), AND ZHIGUO DING [1,2] (Fellow, IEEE)

[1]Department of Electrical and Electronic Engineering, The University of Manchester, M13 9PL Manchester, U.K.

[2]Department of Electrical Engineering and Computer Science, Khalifa University, Abu Dhabi, UAE

[3]Center for Cyber Physical Systems, Khalifa University, Abu Dhabi, UAE

[4]Department of Electrical and Computer Engineering, Western University, London, ON N6A 3K7, Canada

CORRESPONDING AUTHOR: H. YAHYA (e-mail: hamad.mohamadaliyahya@manchester.ac.uk)

The work of Arafat Al-Dweik was supported by the Technology Innovation Institute (TII) Project 'PHY Layer Security for Heterogeneous UAV-Ground Wireless Networks,' under Grant EX2020-036.

ABSTRACT Non-orthogonal multiple access (NOMA) continues to receive enormous attention as a potential technique for improving the spectral efficiency (SE) of wireless networks. Although for several years most research efforts on the performance of NOMA systems focused on the ergodic sum-rate and outage probability, recent works have shifted towards error rate analysis of various NOMA configurations and designs. While the influx of publications on this topic is rich in lessons and innovations, the sheer volume of it makes it easy to get caught up in the details, so much so that one often loses sight of the overall picture. This paper serves as a survey on NOMA error rate analysis, painted in the large with bold and immediately recognizable strokes of insights to facilitate for the reader to understand and follow the up-to-date progress in this area. In addition to summarizing the principles of NOMA error rate analysis, this work aims to minimize redundancy and overlaps, identify research gaps, and outline future research directions.

INDEX TERMS Non-orthogonal multiple access (NOMA), bit error rate (BER), power assignment (PA), enhanced performance.

I. INTRODUCTION

THE EMERGENCE of revolutionary wireless applications is the driver behind the need for wider connectivity to enable new breeds of advanced technologies, in addition to the increasingly demanding traditional communications devices such as mobile phones and tablets. Examples of current new technologies include holographic applications, telemedicine, massive machine-type communications, and autonomous systems [1], [2], where the Internet of Things (IoT) is at the core of these applications [2]. Consequently, the demand for data access has been growing rapidly in the past few years, driven by the increasing number of new subscribers, high data rate systems, and IoT applications. According to the Ericsson mobility report [3], mobile network data traffic grew 44% between 2020 and 2021, and reached 72 Exabyte per month generated by about 8 billion subscribers. Also, in [4], it was reported that 50% of all IoT networked devices in 2023 will be connected to cellular networks. This indicates that the wireless network is expected to support about 15 billion IoT devices in addition to 8 billion mobile users. Although the advances achieved by fifth generation (5G) wireless networks are considered substantial compared to the fourth generation (4G) ones, the 5G networks capacity improvement is still way below the 1000× increase specified by the International Mobile Telecommunications-2020 (IMT-2020) vision.

In light of such expectations, Non-orthogonal multiple access (NOMA) has attracted tremendous attention as a promising candidate for future mobile networks because of its inherent ability to provide high spectral efficiency (SE), massive connectivity, and low latency [5], [6], [7]. Much research in this area was focused on the integration of NOMA in various applications, such as IoT, short packet communication (SPC), satellite communications, unmanned aerial vehicle communications, visible light communication (VLC), underwater communications, intelligent reflecting surface (IRS) communications and cooperative communications [8], [9], [10], [11], [12].

The error rate performance is a fundamental indicator of the reliability of wireless communication systems. Given its critical importance, there has been a recent surge in the interest in the error rate analysis of broad NOMA configurations and designs. Such an emerging trend in research is driven by the dedication of the community to improving the reliability of NOMA systems. This article provides a comprehensive review of the state-of-the-art research conducted on error rate performance analysis of power and code-domain NOMA.

A. MOTIVATION AND CONTRIBUTION

As can be noted from the published literature, several survey papers have been published covering the progress on new concepts, advancements, and integration of NOMA into various technologies and applications. The most relevant survey papers are listed in Table 1, where the focus of each article is highlighted. While metrics such as the sum rate and outage probability have been extensively surveyed, the progress on the error performance of NOMA has only been briefly mentioned in some papers without any comprehensiveness. For example, the error propagation caused by successive interference cancellation (SIC), and its variations, is briefly discussed by Islam et al. [15] and Liu et al. [18]. Whereas, the NOMA resilience to errors caused by imperfect channel state information (CSI) is studied by Ding et al. [16]. On the other hand, Maraqa et al. [25] considered that symbol error rate (SER) and bit error rate (BER) analysis are out of their paper scope.

Based on an extensive literature search, and to the best of the authors' knowledge, no survey papers reported in the literature capture the statistical-based error rate performance analysis of NOMA holistically. Thus, this article aims to shed light on the current understanding of NOMA error rate performance and provide comprehensive coverage and classification of analytical work. Table 2 is a comparative matrix that provides insights about the contributions of this survey as compared to other relevant survey papers. The main contributions of this work can be summarized as follows:

- Section III provides a tutorial on the fundamentals of error rate analysis for NOMA in the downlink (DL) and uplink (UL), where the important metrics, including BER, SER, pairwise error probability (PEP) and block error rate (BLER) analyses, are used. In addition, we highlight the power assignment (PA) and the user pairing processes.
- Section IV presents a comprehensive survey of existing work for conventional NOMA schemes in DL and UL,

TABLE 1. Areas of focus for relevant overview papers on NOMA.

Survey Paper	Area of Focus
Dai *et al.* [13]–2015	• Comparison of power and code domains NOMA • Complexity of various receivers
Wang *et al.* [14]–2016	• General framework for different NOMA schemes • Summary of NOMA standardization and prototyping efforts
Islam *et al.* [15]–2017	• Power-domain NOMA • PA and user pairing • NOMA integration with cooperative communications, MIMO, beamforming, space-time and network coding
Ding *et al.* [16]–2017	• Power and code-domain • Design of single and multicarrier NOMA • NOMA integration with MIMO, cooperative communications and millimeter-wave
Ding *et al.* [17]–2017	• Power-domain • Single and multi-cell NOMA networks • Interference management techniques for multi-cell networks
Liu *et al.* [18]–2017	• Power-domain • Design of NOMA with multiple antennas, cooperative communications • Resource management
Islam *et al.* [19]–2018	• Power-domain • User pairing and power allocation • Integration with MIMO
Basharat *et al.* [20]–2018	• NOMA optimization problems including objective function, constraints, problem type, and solution approaches
Dai *et al.* [21]–2018	• Principles power and code-domain NOMA • Receiver complexity
Cai *et al.* [22]–2018	• Major candidates for 5G including power and code-domain NOMA
Ye *et al.* [23]–2018	• NOMA schemes for UL grant-free • Operations at BS and receivers
Vaezi *et al.* [24]–2019	• Integration of NOMA with massive MIMO, VLC, cooperative, cognitive and millimeter-wave communication, physical layer security, EH and mobile edge computing
Maraqa *et al.* [25]–2020	• Power-domain • Rate optimization of NOMA combined with other technologies
Shahab *et al.* [26]–2020	• Design of grant-free NOMA for mMTC
Makki *et al.* [27]–2020	• Welch-bound equality spread multiple access-based NOMA • Detector complexity
Liaqat *et al.* [28]–2020	• Power-domain • Resources allocation and relay selection • EH
Akbar *et al.* [29]–2021	• Classify the NOMA work methodology, i.e. analytical, optimization, etc. • Resource allocation, signaling and security of NOMA • Experimental trails of NOMA
Sadat *et al.* [30]–2022	• Power-domain • PA, clipping effect, MIMO and security of VLC-NOMA
Mohsan *et al.* [31]–2023	• Power-domain • Deep learning approaches • Resource allocation and PA • Transceiver design • NOMA integration with IRS, mobile edge computing, SWIPT, OFDM and MIMO

TABLE 2. Comparative matrix for existing surveys on NOMA.

Ref.	Year	Metrics	Principles	Analysis	PD-NOMA Classification		Integration with Other Technologies						Topic Density	No. Papers
					Conventional	Improved	Optical	IRS and Backscat.	Cooperative	IM	SPC	Code Domain		
[13]	2015	BER, capacity, fairness	✓	×	✓	×	×	×	×	×	×	✓	×	15
[14]	2016	Capacity	✓	✓	✓	✓	×	×	×	×	×	✓	×	43
[15]	2017	Capacity, fairness, outage	✓	✓	✓	✓	✓	×	✓	×	×	✓	×	88
[16]		Capacity, fairness, outage	✓	✓	✓	✓	✓	×	✓	×	×	✓	×	142
[17]		Capacity, fairness	✓	✓	✓	✓	×	×	×	×	×	×	×	15
[18]		Capacity, fairness	✓	✓	✓	✓	✓	×	✓	×	×	✓	×	241
[19]	2018	Capacity, fairness, outage	✓	×	✓	×	×	×	×	×	×	×	×	22
[20]		Error rate, capacity, fairness, outage	✓	×	✓	✓	×	×	✓	×	×	✓	×	113
[21]		Error rate, capacity, fairness, outage	✓	✓	✓	✓	×	×	✓	×	×	✓	×	172
[22]		Error rate, capacity, fairness, outage	✓	✓	✓	×	×	×	✓	×	×	✓	×	128
[23]		Capacity, fairness	✓	×	✓	✓	×	×	×	×	×	✓	×	122
[24]	2019	Capacity, fairness, outage, energy efficiency	✓	×	✓	✓	✓	✓	✓	×	×	×	×	199
[25]	2020	Capacity, fairness	✓	×	✓	×	✓	✓	✓	×	×	×	×	325
[26]		Capacity, energy efficiency, latency	✓	×	✓	✓	×	×	✓	×	×	✓	×	261
[27]		BLER, capacity, fairness	✓	✓	✓	✓	×	×	×	×	×	✓	×	59
[28]		Capacity, fairness, outage, energy efficiency	✓	✓	×	×	×	×	✓	×	×	✓	×	139
[29]	2021	Capacity, fairness, outage, energy efficiency	✓	×	✓	×	✓	✓	✓	×	×	×	×	319
[30]	2022	Error rate, capacity, fairness, outage, energy efficiency	✓	✓	✓	✓	✓	×	✓	×	×	×	✓	121
[31]	2023	Error rate, capacity, fairness, outage, energy efficiency	✓	×	✓	✓	✓	✓	✓	×	×	×	×	185
This work	2023	Error rate, capacity, fairness	✓	✓	✓	✓	✓	✓	✓	✓	✓	✓	✓	265

where classifications based on the number of users, channel models, and modulation orders are provided. In addition, optimization-oriented works are grouped based on their optimization objectives.

- Section V surveys state-of-the-art work on improved NOMA schemes, including labeling, constellation rotation, interference alignment, channel coding, multicarrier NOMA designs, and detector designs.
- Section VI studies state-of-the-art work on the interplay between NOMA and other technologies including optical communications, IRS and backscatter communications, cooperative communications, index modulation, SPC and code domain.
- Section VII provides a holistic error rate literature classification of NOMA that captures the system model traits based on antenna setup, number of users, error rate performance metrics, modulation schemes, channel models, and receiver design.
- Section VIII discusses NOMA future research directions and open challenges while focusing on analytical and system integration.

B. ARTICLE ORGANIZATION

The rest of the article is organized as follows. Section II provides an overview of the NOMA operation principles and considers selected NOMA applications. Section III explains the fundamentals of error rate analysis for NOMA. Section IV reviews the state-of-the-art analytical work on conventional NOMA. In contrast, Section V reviews the improved NOMA schemes. Section VI highlights the state-of-the-art analytical work on NOMA integrated with other technologies. Section VII classifies the different NOMA

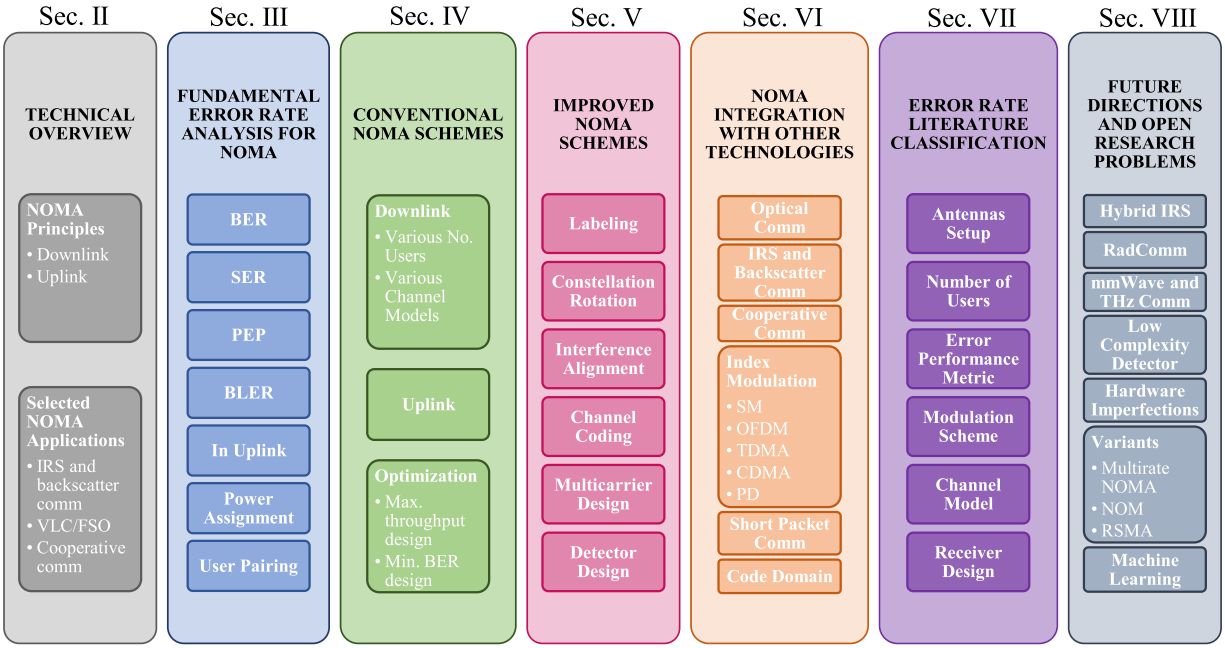

FIGURE 1. The structure of the paper.

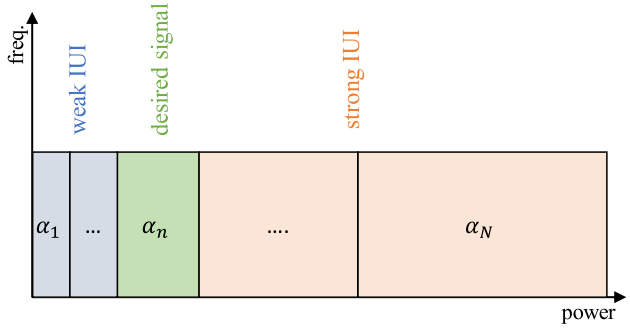

FIGURE 2. Observing DL SC at *n*th user.

system model traits reported in the literature. Future research directions and open research problems are discussed in Section VIII. Finally, Section IX concludes the article with a summary and the main remarks. Fig. 1 illustrates the article organization graphically.

II. TECHNICAL OVERVIEW

To provide the readers with sufficient technical background, this section presents the basic principles of power-domain NOMA in the DL and UL. In addition, it highlights important and selected emerging applications for NOMA. Interested readers can refer to [32] for more details on the principles of NOMA.

A. NOMA PRINCIPLES

1) DOWNLINK NOMA

Unlike orthogonal multiple access (OMA), NOMA allows the users to share the same resource block in a non-orthogonal manner. For example, the transmitter in DL-NOMA multiplexes the data of N users in the power-domain by allocating each user a distinct power coefficient, $\alpha_n, n \in \{1, \ldots, N\}$. This process is commonly known as superposition coding (SC) which can be mathematically described as $x_{sc} = \sum_{n=1}^{N} \sqrt{\alpha_n} x_n$, where $\sum_{n=1}^{N} \alpha_n = 1$ to normalize the transmitted power, x_n is the nth user information symbol, which has a unity average power, i.e., $\mathbb{E}[|x_n|^2]$, $\mathbb{E}[\cdot]$ denotes the statistical expectation process. The information symbols for each user are selected from a symbol alphabet χ_n that corresponds to a certain constellation set, such as M-ary phase shift keying (M_n-PSK) or M-ary quadrature amplitude modulation (M_n-QAM). The process of allocating the power coefficients and modulation orders is performed by the scheduler at the base station (BS), which is typically configured to ensure fairness and efficient use of resources. Fig. 2 shows the SC process at the BS for the case of N users where $\alpha_1 < \alpha_2, \ldots < \alpha_N$. The received signal at the nth user is $y_n = h_n x_{sc} + w_n$, where h_n is the channel coefficient between the BS and nth user, and $w_n \sim \mathcal{CN}(0, N_0)$ is the additive white Gaussian noise (AWGN).

The received signal at the nth user is given by

$$y_n = \underbrace{h_n \sum_{i=1}^{n-1} \sqrt{\alpha_i} x_i}_{\text{weak IUI}} + \underbrace{h_n \sqrt{\alpha_n} x_n}_{\text{desired signal}} + \underbrace{h_n \sum_{i=n+1}^{N} \sqrt{\alpha_i} x_i}_{\text{strong IUI}} + w_n. \quad (1)$$

As can be noted from (1), the users experience two types of interference, weak inter-user interference (IUI) and strong IUI, except for the first and Nth users whose received signals suffer only from one interference type.

The IUI is classified as strong or weak based on its power as compared to the desired signal power as shown in Fig. 2, where the signals of users 1 to $n-1$, i.e., $s_i = \sqrt{\alpha_i} x_i$,

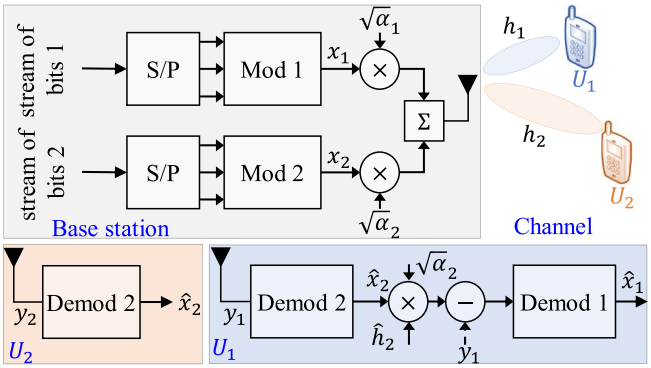

FIGURE 3. SC and SIC schematic for $N = 2$ case.

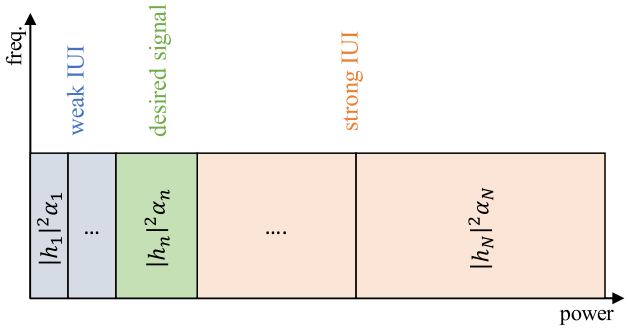

FIGURE 4. Observing UL SC at the BS.

are considered as weak IUIs to user n, while the signals of users $n+1$ to N are considered as strong IUIs to user n. Hence, s_1 to s_{n-1} are treated as unknown additive noise when detecting s_n. Moreover, the user with the maximum power, i.e., user N is the interference-limited user, and its symbols can be detected directly by all users using a single-user maximum likelihood detector (MLD) such that

$$\hat{x}_N = \arg \min_{x_N \in \chi_N} \left| y_N - \hat{h}_N \sqrt{\alpha_N} x_N \right|^2 \tag{2}$$

where $\hat{h}_n$ is the estimated channel coefficient, which can be written as $\hat{h}_n = h_n + \epsilon_n$, ϵ_n is the channel estimation error. The MLD selects $\hat{x}_N$ as the trial value of x_N that minimizes the Euclidean distance (ED).

Furthermore, SIC can be used to cancel the strong IUIs where residual interference is caused when erroneous estimates of strong IUIs are used. The detection of the nth user signal can be written as

$$\hat{x}_n = \arg \min_{x_n \in \chi_n} \left| y_n - \hat{h}_n \underbrace{\sum_{i=n+1}^{N} \sqrt{\alpha_i} \hat{x}_i}_{\text{residual interference}} - \hat{h}_n \sqrt{\alpha_n} x_n \right|^2 \tag{3}$$

Fig. 4 shows a schematic of the SC process at the BS for $N = 2$ and the detection process at the users as explained in (2)–(3). It is worth mentioning that the SIC chain will get longer for $N > 2$ and hence complexity and delay will increase [33]. Alternatively, a joint-multiuser maximum likelihood detector (JMLD) can be applied to detect the signals jointly [34, eq. (5)].While Fig. 4 refers to the baseband processes at the NOMA BS and receivers, interested readers can refer to [35, Fig. 1] for the baseband-passband chain of processes of NOMA which is critical to conduct experimental studies.

2) UPLINK NOMA

On the other hand, NOMA in the UL uses the channel gains to multiplex the different users' signals as seen in Fig. 3. Assuming that $|h_1|^2\alpha_1 < \ldots < |h_N|^2\alpha_N$, the received signal at the BS for the synchronized UL-NOMA with respect to the nth user is given as

$$y = \underbrace{\sum_{i=1}^{n-1} h_i \sqrt{\alpha_i} x_i}_{\text{weak IUI}} + \underbrace{h_n \sqrt{\alpha_n} x_n}_{\text{desired signal}} + \underbrace{\sum_{i=n+1}^{N} h_i \sqrt{\alpha_i} x_i}_{\text{strong IUI}} + w. \tag{4}$$

Hence, the nth user received signal power at the BS depends on the $|h_n|^2\alpha_n$. Therefore, the SIC decoding order depends on the received signal power. Therefore, detecting user N signal can be performed as follows,

$$\hat{x}_N = \arg \min_{x_N \in \chi_N} \left| y - \hat{h}_N \sqrt{\alpha_N} x_N \right|^2 \tag{5}$$

while the detection of the nth user signal can be done using SIC such that

$$\hat{x}_n = \arg \min_{x_n \in \chi_n} \left| y - \underbrace{\sum_{i=n+1}^{N} \hat{h}_i \sqrt{\alpha_i} \hat{x}_i}_{\text{residual interference}} - \hat{h}_n \sqrt{\alpha_n} x_n \right|^2. \tag{6}$$

Alternatively, JMLD can be used for detection [36, eq. (4)].It is straightforward to extend the aforementioned formulas to the multi-antenna setup as described in [34], [37].

B. SELECTED NOMA APPLICATIONS

1) IRS AND BACKSCATTER COMMUNICATIONS

IRS and backscatter communications can be considered key solutions for enhancing the spectrum and energy efficiencies of future wireless communications systems [38], [39]. The main principle of both technologies is based on reflecting the incident signals towards an intended destination. While IRS aims at improving the signal-to-noise ratio (SNR) at the destination, backscatter communications aim at reflecting radio frequency (RF) signals to a passive or low-power backscatter communications device. IRS consists of passive metasurface elements that control the reflection angle of the incident signals, whereas backscatter communications devices consist of an antenna and an energy harvesting (EH) circuit with or without a dedicated power source to support the communications and sensory systems.

Combining NOMA with IRS or backscatter communications can improve the coverage and energy efficiency of the system by facilitating the delivery of several coherent

copies of the signal to the receiver. Furthermore, an IRS-assisted NOMA system with multiple transmit antennas enable channel manipulation to achieve the capacity region [40]. Therefore, NOMA combined with IRS or backscatter communications are considered energy, spectrum and cost-efficient solution for future wireless networks.

2) VLC AND FSO

The evolution of light emitting diodes (LEDs) and photodetectors have made it possible to use light sources for communications [41], [42]. Unlike optical fiber communications, VLC and free space optical (FSO) communications are performed wirelessly, where the former is mostly used for indoor mobile user applications, while the latter is used for outdoor applications such as backhauling for fixed point-to-point communications [43]. The frequency band for the VLC is 430 THz to 790 THz which corresponds to the unlicensed visible light spectrum, while the band for FSO includes infrared and ultraviolet. Such a wide free spectrum can provide a promising solution to the spectrum scarcity problem. Nonetheless, the main limitation of VLC and FSO systems is that the achievable data rates are constrained by the modulation bandwidth of the LEDs which spans a few hundred megahertz, hence can only utilize a small fraction of the available bandwidth at such frequencies [44]. It is worth noting that NOMA is particularly suitable for DL-VLC systems that aim at connecting a few users in a small cell, which is aligned with the principle of NOMA and small cell densification.

3) COOPERATIVE COMMUNICATIONS

Utilizing some devices to relay the signals of other ones is an effective solution to extend the network range and overcome channel impairments such as fading, pathloss and shadowing. There are two main categories of such a solution, which are user relaying and dedicated relaying [45]. In the former, idle users act as relays, while in the latter category, dedicated relay nodes are distributed in the network. In general, two time slots are needed to relay the signal to the destination when half-duplex (HD) mode is considered, whereas one time slot is needed by the full-duplex (FD) mode. It is worth noting that high complexity and self-interference are the two main limitations for the FD mode. A simple network structure for dedicated user relaying in NOMA is that the near-user acts as a HD relay for the far-user either through decode-and-forward (DF) or amplify-and-forward (AF). In AF, a scaled version of the received signal is sent to the destination, while an attempt to detect the signal is made, then retransmission of the detected information takes place for DF. Various such network structures are discussed in [45].

III. FUNDAMENTAL ERROR RATE ANALYSIS FOR NOMA

Several fundamental error rate performance metrics have been considered in the literature to provide insights about NOMA under a broad range of channel conditions and operating scenarios. These main error performance metrics are BER, SER, PEP and BLER. For example, BER requires considering the transmitted signal constellation diagram at the bit-level, whereas the SER computation is performed at the symbol level. PEP is usually employed as an upper bound on the BER and SER when the exact analysis is intractable. In the following subsections, a brief tutorial is provided to review the error rate analysis DL-NOMA.

A. BER

To evaluate the BER in NOMA systems, the following steps should be considered:

- Divide the NOMA constellation diagram into regions using maximum likelihood (ML) rule. The regions can be labeled as $\mathcal{R}_k^{(1)}$ such that the kth bit is 1, i.e., $b_k = 1$, and $\mathcal{R}_k^{(0)}$ where $b_k = 0$. Note that $k \in \{1, \ldots, \mathcal{M}\}$ and $\mathcal{M} = \sum_n \mathcal{M}_n = \sum_n \log_2 M_n$.
- Find the probability that for a given transmitted NOMA symbol, bit b_k is incorrectly received. In other words, $\Pr(\hat{b}_k \neq b_k | x_{sc} \rightarrow b)$ where $b = b_1 b_2 \ldots b_{\mathcal{M}}$ is the NOMA symbol in binary representation.
- Due to symmetry, we can repeat the previous steps for all NOMA symbols in the first quadrant only, and the BER of the specific bit would be the average of all these probabilities because all symbols are assumed to be equally likely.
- The user BER would be the average of its all bits' BERs.

To illustrate this process, consider the case shown in Fig. 5a where two NOMA users are using QPSK. The red cross represents the symbols of user 2 who is given a higher power coefficient, while the black squares represent the NOMA symbols. The amplitudes mentioned are defined as $A_{\nu_1,\nu_2,\ldots,\nu_N} = \sum_{n=1}^{N} \nu_n \sqrt{\frac{\alpha_n}{\kappa_n}}$, $\nu_n \in \{0, \pm 1, \pm 3, \ldots, \pm \Lambda_n\}$, Λ_n is the nth user constellation width, κ_n is a scaling factor that is used to normalize the data symbols such that $\mathbb{E}[|x_n|^2] = 1$. For simplicity, we define $\grave{\nu}_n \triangleq -\nu_n$ [34]. For example, $A_{\grave{1}1} = \frac{1}{\sqrt{2}}(-\sqrt{\alpha_1} + \sqrt{\alpha_2})$. As can be seen from the figure, the binary representation of the NOMA symbol $\mathbf{b}$ is given, where the first two bits belong to user 1 while the last two bits belong to user 2. Considering the first bit of user 2, which is b_3. As noted from Fig. 5a, $\mathcal{R}_3^{(1)}$ is in the negative part of the quadrature-axis, whereas $\mathcal{R}_3^{(0)}$ is in the positive part. Meaning that for a given channel realization, the imaginary component of the AWGN, $\tilde{w}_n$, will decide whether the transmitted bit is received correctly or not. Therefore,

$$\begin{aligned}\Pr\left(b_3 \neq \hat{b}_3 | x_{sc} \rightarrow 0100\right) &= \Pr\left(b_3 \neq \hat{b}_3 | x_{sc} \rightarrow 0000\right) \\ &= \Pr(\tilde{w}_n < -A_{11}). \end{aligned} \tag{7}$$

Similarly,

$$\begin{aligned}\Pr\left(b_3 \neq \hat{b}_3 | x_{sc} \rightarrow 1100\right) &= \Pr\left(b_3 \neq \hat{b}_3 | x_{sc} \rightarrow 1000\right) \\ &= \Pr\left(\tilde{w}_n < -A_{\grave{1}1}\right). \end{aligned} \tag{8}$$

The same steps are repeated for b_4 where the results are found identical to (7)–(8). Since circularly symmetric AWGN

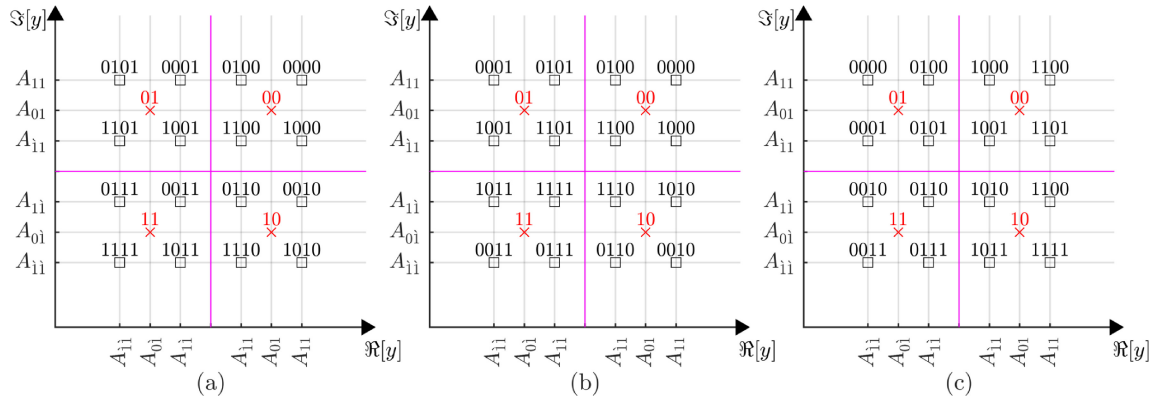

FIGURE 5. NOMA constellation diagram with different symbol-to-bit mapping schemes. (a) NOMA non-Gray labeling. (b) Joint Gray labeling. (c) Natural labeling.

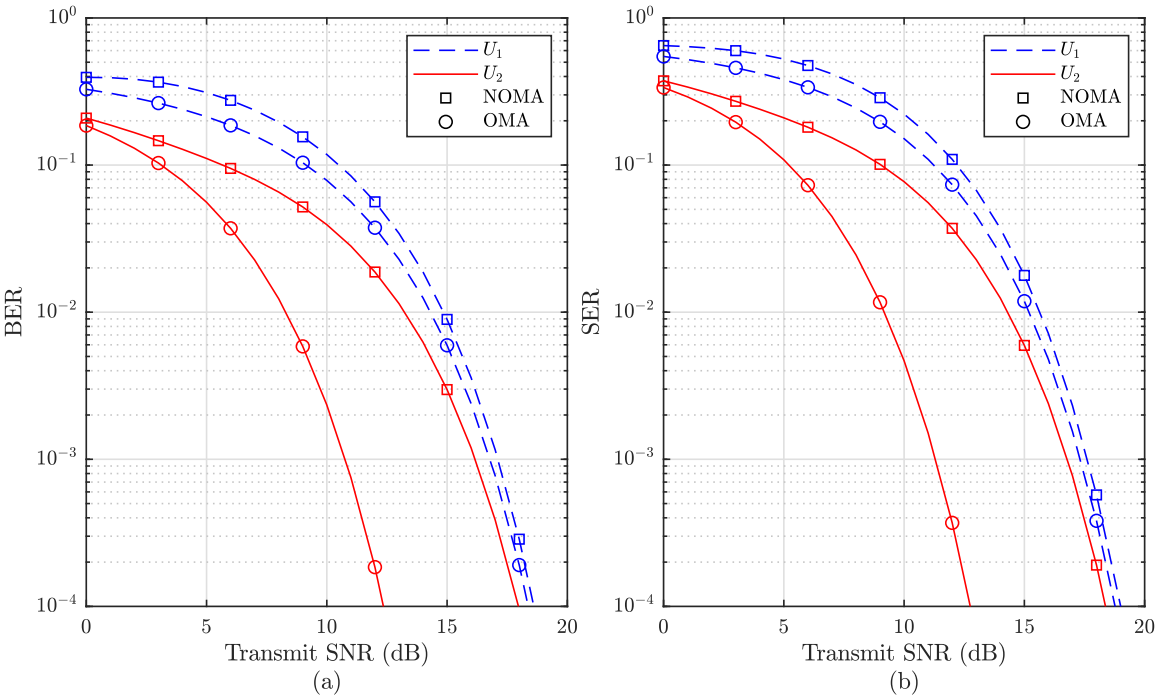

FIGURE 6. The exact NOMA and OMA performance over AWGN channel QPSK for two-user scenario with power coefficients of $[\alpha_1, \alpha_2] = [0.2, 0.8]$: a) BER. b) SER.

is assumed, the real and imaginary components are random variables with $\mathcal{N}(0, N_0/2)$. Hence, these probabilities can be calculated as $\Pr(\tilde{w}_n < -\mathcal{A}) = \Pr(\check{w}_n < -\mathcal{A}) = Q(\sqrt{\mathcal{A}^2\gamma_n})$, where $\check{w}_n$ is the real component of the AWGN, $\gamma_n = \frac{2\mathbb{E}[|h_n|^2]}{N_0}$. Therefore, the BER for user 2 is computed by finding the average of (7)–(8). Hence, $P_{B_2} = \frac{1}{2}\sum_{i=1}^{2} Q(\sqrt{\mathcal{A}_{i,2}^2\gamma_2})$, where $\mathcal{A}_{1,2} = A_{11}$ and $\mathcal{A}_{2,2} = A_{\grave{1}\grave{1}}$. The same steps can be applied for different labeling schemes and for other users in different N settings when considering JMLD. The readers are referred to references [33], [34], [46] for more details about the derivations when considering SIC and higher modulation orders. The NOMA BER for the example discussed above is compared to the OMA counterpart in Fig. 6a where $[\alpha_1, \alpha_2] = [0.2, 0.8]$. While ensuring that both systems are normalized in terms of average power, it can be seen that the performance of the interference-free user, user 1, is degraded due to the imperfections in SIC and error propagation. Furthermore, such degradation reduces as the SNR gets larger. On the other hand, the interference-limited user, user 2, is suffering from the interference caused by user 1.

B. SER

The SER of each user can be found by considering the following steps:

- Divide the constellation diagram to regions, $\mathcal{R}_n^{(s_n)}$ where $x_n \rightarrow s_n$ and $s_n \in \{0, \ldots, M_n - 1\}$ is the decimal representation of the nth user symbol.
- Find the probability that a given transmitted symbol is correctly received, i.e., $\Pr(x_n = \hat{x}_n | x_{sc} \rightarrow s) = \Pr(y_n \in \mathcal{R}_n^{(s_n)} | x_{sc} \rightarrow s)$, where s is the decimal representation of the NOMA symbol.

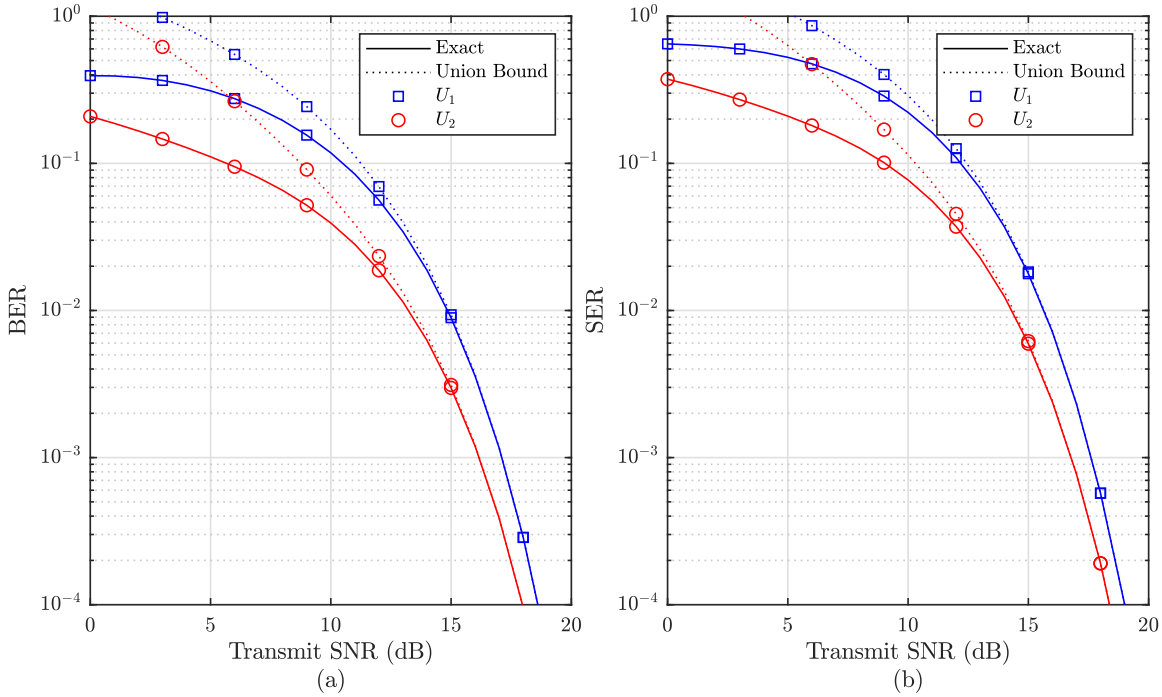

FIGURE 7. The exact and approximate NOMA performance over AWGN channel QPSK for two-user scenario with power coefficients of $[\alpha_1, \alpha_2] = [0.2, 0.8]$: a) BER. b) SER.

- Find the complementary of the previous probability such that $\Pr(x_n \neq \hat{x}_n | x_{sc} \to s) = 1 - \Pr(x_n = \hat{x}_n | x_{sc} \to s)$.
- Repeat the previous steps for all NOMA symbols in the first quadrant, and the SER would be the average of all these probabilities because the symbols are equally likely.

To illustrate the process, consider the same example used for the BER case. The decimal representation of user 1, given by s_1, can be found by converting $b_1 b_2$ to decimal, whereas s_2 can be found by converting $b_3 b_4$ to decimal. Therefore, the regions are found to be: $\mathcal{R}_2^{(0)}$ which is the first quadrant, $\mathcal{R}_2^{(1)}$ which is the second quadrant, $\mathcal{R}_2^{(2)}$ which is the fourth quadrant and $\mathcal{R}_2^{(3)}$ which is the third quadrant. Furthermore, the probability of correctly received symbol for $x_{sc} \to 0$ is

$$\begin{aligned}
&\Pr\left(y_2 \in \mathcal{R}_2^{(0)} | x_{sc} \to 0\right) \\
&= \Pr(\tilde{w}_2 > -A_{11} \cap \check{w}_2 > -A_{11}) \\
&= \Pr(\tilde{w}_2 > -A_{11}) \Pr(\check{w}_2 > -A_{11}) \\
&= \left(1 - Q\left(\sqrt{\mathcal{A}_{1,2}^2 \gamma_2}\right)\right)^2. \qquad (9)
\end{aligned}$$

The same steps can be repeated for all other symbols in the first quadrant. Therefore, the SER of user 2 is computed by averaging over the complements of $\Pr(y_2 \in \mathcal{R}_2^{(0)} | x_{sc} \to s)$, $s \in (0, 4, 8, 12)$. Thus,

$$\begin{aligned}
P_{S_2} = &\, Q\left(\sqrt{\mathcal{A}_{1,2}^2 \gamma_2}\right) + Q\left(\sqrt{\mathcal{A}_{2,2}^2 \gamma_2}\right) \\
&- \frac{1}{2} Q\left(\sqrt{\mathcal{A}_{1,2}^2 \gamma_2}\right) Q\left(\sqrt{\mathcal{A}_{2,2}^2 \gamma_2}\right) \\
&- \frac{1}{4} Q^2\left(\sqrt{\mathcal{A}_{1,2}^2 \gamma_2}\right) - \frac{1}{4} Q^2\left(\sqrt{\mathcal{A}_{2,2}^2 \gamma_2}\right). \qquad (10)
\end{aligned}$$

These steps can be applied for user 1 and for different labeling schemes [47], [48], [49], [50]. The NOMA SER for the example discussed above is compared to the OMA counterpart in Fig. 6b where $[\alpha_1, \alpha_2] = [0.2, 0.8]$. While similar observations to the BER are made for SER as well, the justification is the same.

C. PEP

The union of PEPs is an upper bound of the BER and SER. To compute the PEP, consider a pair of NOMA symbols, x_{sc} and $\check{x}_{sc}$, such that the bit-wise or symbol-wise decision on the pair is erroneous. Such condition is met if $\tilde{w}_n > \frac{\Delta_n}{2}$, where $\Delta_n = |x_{sc} - \check{x}_{sc}|$. Therefore, the PEP is generally given by $Q(\frac{\Delta_n}{2}\sqrt{\gamma_n})$. To compute the union bound on the PEPs, all possible pairs should be considered and the average should be taken [51], [52], [53], [54]. To illustrate, Fig. 7 shows the exact NOMA BER and SER of a two-user system with QPSK and $[\alpha_1, \alpha_2] = [0.2, 0.8]$ is compared to the approximation which is computed following the previous discussion. It can be seen that union bound provides a tight approximation at moderate SNR values while it converges to the exact solution at high SNR values. Therefore, the union bound can provide an accurate yet simple estimate to analyze the performance of NOMA systems.

D. BLER

The BLER can be computed by either considering the BER or SER which both lead to the same final solution. Considering the BER then the block is in error if all bits in the block are in error. In other words, $P_{e_n} = 1 - (1 - P_{B_n})^{L\mathcal{M}_n}$ where L is the block length in symbols. On the other hand,

when considering the SER, the BLER can be computed as $P_{e_n} = 1 - (1 - P_{S_n})^L$. Note that this approach can be applied to uncoded systems, whereas some approximations are applied to coded SPCs as will be discussed in the following sections. It is worth noting that all metrics discussed in this section are conditioned for a given γ_n. Hence, to derive the average performance, then an integration over the probability density function (PDF) of γ_n should take place. For example, the average BLER considering coherent detection can be computed as $\bar{P}_{e_n} = \int_0^\infty P_{e_n} \times p_{\gamma_n}(\gamma_n) d\gamma_n$.

E. IN UPLINK

When considering the analysis for given channel realizations, the DL analysis can be extended to UL directly. However, to get the average performance, then N-fold integration should be considered because N channel realizations affect the received signal at the BS. This makes the analysis challenging, therefore, different approaches are introduced to solve this issue. For example, the authors of [55] used the union bound for the outer integration and exponential bound for the inner integration. The total probability theorem and Taylor series expansion are then applied to get the average BER. Kara and Kaya in [46] utilized the fact that the channel realizations are independent and got the PDF of the joint channels. Hence, they were able to get the exact average BER in a single-integral form, in addition to deriving an approximate closed-form.

F. POWER ASSIGNMENT

The PA scheme affects the error rate performance, and hence, it is a crucial aspect to discuss. Generally speaking, there are two main PA schemes, which are fixed PA and adaptive PA. The former ensures minimum signaling overhead and low complexity owing to its non-optimality, whereas the latter can ensure optimality or sub-optimality but with higher signaling overhead and complexity [34]. A number of issues should be considered when designing both schemes. First, ambiguity at the receivers. For example, ambiguity can be caused at the receivers for two NOMA users with binary phase shift keying (BPSK) if equal power coefficients are given when $x_1 = -x_2$. Hence, two NOMA symbols will coincide on the same constellation point.

Moreover, enabling reliable detection using SIC requires abiding by certain power coefficient bounds (PCBs) [34], [47], [56], [57], [58]. Considering the previous example, when $\alpha_1 < \alpha_2$ the order of the NOMA symbols is as follows from the negative in-phase axis: 11, 01, 10, 00. In such a scenario, MLD can detect b_2 reliably because $b_2 = 0$ is always in the positive side. Hence, SIC can cancel the interference caused by b_2 and detect b_1 reliably. In contrast, when $\alpha_1 > \alpha_2$, the two middle symbols swap order causing $b_2 = 0$ to fall in two different regions. Therefore, MLD will not be able to detect b_2 correctly, and hence the SIC performance will be unreliable. It is worth noting that this problem is not encountered when JMLD is used.

G. USER PAIRING

User pairing is the scheduler's process of selecting a set of users to share the same communication resource. In a DL/UL coordinated scenario, the BS acts as a centralized unit to coordinate the user pairing process to achieve a certain objective. For example, the objective could be the sum rate maximization while satisfying certain quality of service (QoS) constraints such as minimum rate per user or maximum BER per user. Also, user pairing can aim to ensure fairness among users. Furthermore, the satisfaction of such objectives and constraints depends on the network knowledge available at the scheduler. For instance, user pairing can satisfy certain criteria instantaneously if the CSI knowledge of all links is available instantaneously. Alternatively, such criteria can be satisfied on average if statistical CSI knowledge is available. For instance, it is reported that pairing users with the most distinct channel gains would maximize the sum rate in NOMA systems. The concept of prioritizing users with different priorities is known as cognitive radio (CR)-NOMA in which the primary user is given the highest priority while the secondary user is served opportunistically. Moreover, CR-NOMA tends to pair the best channel user with the second best channel user [59]. On the other hand, the UL decentralized scenario usually refers to the grant free access (GFA) in which the users are allowed random access to the channel without resource allocation. Hence, collisions might occur where the BS needs to detect collisions and resolve them in order to detect the messages.

IV. CONVENTIONAL NOMA

The error rate performance of conventional NOMA has been widely studied in the literature, focusing mainly on DL with less attention to UL. Additionally, power allocation and modulation order optimization based on error performance metrics has attracted the interest of many researchers. This section reviews the work that considered the DL and UL conventional NOMA, as well as its optimization.

A. DOWNLINK

The main work that considers DL-NOMA with a various number of users and modulation orders is given in [46], [47], [48], [51], [52], [59], [60], [61], [62], [63], [64], [65], [66], [67], [68], [69], [33], [34], [54], [58], [70], [71], [72], [73], [74], [75], [76], [77], [78], [79], [80], [81], [53], [82], [83].

1) VARIOUS NUMBER OF USERS

The error rate performance of two-user NOMA is extensively considered in the literature [46], [47], [48], [59], [60], [61], [62], [63], [64], [65], [66], [67], [68], [69], unlike the three-user [51], [52], [70], [71], [72], [73], [82] and an arbitrary number of users cases [34], [54], [58], [74], [75]. All the aforementioned references consider single-input-single-output (SISO) channels except [34] which considers the case of multiple receiving antennas. Table 3 provides a comprehensive summary of the work that

TABLE 3. Summary of DL-NOMA work.

[#]	Metric	Antennas	Channel	M	N	Receiver	CSI
[47]	SER	SISO	Rayleigh	$\forall M$	2	Imperf. SIC	Perf.
[48]	SER	SISO	AWGN	$\forall M$	2	Imperf. SIC	-
[60]	SER	SISO	AWGN	$\forall M^{\bullet}$	2	Imperf. SIC	-
[61]	SER	SISO	Nakagami-m	$\forall M$	2	Imperf. SIC	Perf.
[62]	BER	SISO	Rayleigh	$\forall M$	2	Impref. SIC	Perf.
[46]	BER	SISO	Rayleigh	$4 + 2$	2	Imperf. SIC	Perf.
[63]	BER	SISO	Rayleigh	≤ 4	2	Imperf. SIC	Perf.
[64]	BER	SISO	AWGN	4	2	Imperf. SIC	Perf.
[65]	BER	SISO	Rayleigh	2	2	Perf. SIC	Imperf.
[66], [67]	BER	SISO	Rayleigh	2	2	Perf. SIC	Perf.
[68]	BER	SISO,MISO	Double Nakagami-m	$\forall M^{\bullet}$, M^{*}	2	Imperf. SIC	Perf.
[69]	PEP	2×1	Rayleigh	2, 4	2	Imperf. SIC	Perf.
[59]	PER	SISO	Nakagami-m	2	2	Imperf. SIC	Perf.
[51]	PEP	SISO	Nakagami-m	$\forall M$	2, 3	Imperf. SIC	Perf.
[52]	PEP	SISO	Rayleigh	$\forall M$	2, 3	Imperf. SIC	Perf.
[70]	PEP	SISO	Rayleigh	≤ 4	2, 3	Imperf. SIC	Perf.
[71]	PEP	SISO	Rician	2	2, 3	Imperf. SIC	Imperf.
[72]	SER	SISO	Nakagami-m	$\forall M^{\bullet}$, $\forall M$	2, 3	Imperf. SIC	Perf.
[73]	BER	SISO	Nakagami-m	4	2, 3	Imperf. SIC	Perf.
[34]	BER	SIMO	Rayleigh	$\forall M$	$\forall N$	MRC–JMLD	Perf.
[74]	BER	SISO	AWGN	4	$\forall N$	Imperf. SIC	-
[75]	BER	SISO	Rayleigh	2	$\forall N$	Perf. SIC	Perf.
[54]	PEP	SISO	Nakagami-m	$\forall M$	$\forall N$	JMLD, Imperf. SIC,	Perf.
[58]	PEP	SISO	Nakagami-m	$\forall M^{*}$ (Identical)	$\forall N$	JMLD	Perf.

considered DL-NOMA. For each of the listed references, the table shows the error metric, antenna setup, channel model, modulation scheme and order M, number of users N, receiver model and CSI availability if applicable when considering fading channels. It is worth mentioning that this table structure will be adopted throughout the paper. Furthermore, a certain superscript is adopted to distinguish the modulation schemes, for example $\star$ is for on-off keying (OOK), $\bullet$ is for M-ary pulse amplitude modulation (M_n-PAM), $*$ is for M_n-PSK, $\diamond$ is for M-ary pulse position modulation (M_n-PPM), $\dagger$ is for multiple pulse position modulation (MPPM), and finally no superscript corresponds to M_n-QAM.

Two-user: Starting off with the two-user scenario, the closed-form SER expressions are derived for the imperfect SIC case in [47], [48], [60], [61]. The authors of [47], [48] consider rectangular M_n-QAM, whereas [61] considers hexagonal M_n-QAM. Meanwhile M_n-PAM is considered in [60]. It is worth noting that the average SER is derived for Rayleigh fading channel in [47] and Nakagami–m fading channel in [61], while the instantaneous SER is derived in [48], [60].

For the BER, Assaf et al. [62] derive the exact closed-form BER expressions for imperfect SIC considering rectangular M_n-QAM. Kara and Kaya [46] derive the BER of the near and far-users which use QPSK and BPSK, respectively. Furthermore, the authors of [63] extend the work in [46] to consider the identical BPSK and QPSK cases. The authors of [64] study the high-power amplifier non-linear distortions in a DL orthogonal frequency division multiplexing (OFDM)-NOMA system, where the distortions are modeled with memory polynomial model. The exact closed-form BER expressions are derived for the two-user case with QPSK considering perfect and imperfect SIC. Chung [65], [66], [67] studies the BER performance assuming BPSK for both users and perfect SIC. For example, [65] quantifies the impact of imperfect CSI, while [66], [67] consider users with correlated information symbols, where [67] focuses on the negative correlation mapping performance. On the other hand, Jaiswal and Purohit [68] investigates a two-user vehicle-to-vehicle (V2V) communications system with NOMA. The proposed model considers SISO and multiple-input single-output (MISO) scenarios. Due to the vehicular nature of the nodes, this work considers an independent and non-identical double Nakagami-m fading channels. The source broadcasts the NOMA signal through an opportunistically selected antenna. The proposed system performance is assessed in terms of the average BER in the SISO and MISO cases. Exact expressions for both users under SISO are derived in which the infinite summation is presumed to be convergent to allow tractable analysis. Finally, the average BER is calculated by utilizing the average BER expressions of both users.

A further in-depth analysis is carried out of the system's average BER performance for the two proposed transmitting antenna selection procedures, which were verified using numerical and simulation results. Reference [69] explores the error performance of orthogonal space-time block code (OSTBC) in a DL-NOMA system. The system consists of a transmitter with two antennas and two NOMA users, each equipped with a single receiving antenna. The study evaluates the SER performance using PEP considering imperfect SIC for QPSK-BPSK and BPSK-BPSK modulations at the near-user and far-user over Rayleigh fading channels. The authors of [59] study a two-user cognitive NOMA system, where opportunistic transmissions are considered based on the users' priorities. While assuming imperfect detection at the users' ends, closed-form packet error rate (PER) expressions are derived for BPSK case over Nakagami-m fading channels.

Two and three-user: References [51], [73] consider ordered Nakagami-m fading channels, while [52], [70], [72] consider Rayleigh fading channels. Meanwhile [71] studied Rician fading channels. The authors of [51], [52], [70], [71] derive upper bound BER expressions using the union bound of the PEPs assuming imperfect SIC. Assaf et al. [73] derive exact closed-form BER expressions considering QPSK for all users. The authors of [70], [71] propose integrating physical layer security with NOMA to degrade the performance of internal unknown eavesdroppers without affecting the legitimate users' performance. The scheme is based on utilizing the random phase of the channel between the users and the base station, which is known to both ends but not to illegitimate users. Hence, the scheme introduces phase shifts of multiples of $2\pi/M$ to the users' transmitted symbols based on their instantaneous channel phases before SC. Therefore, the eavesdroppers will not be able to detect the symbols, as each user symbol will appear as a different symbol in the constellation diagram. Furthermore, privacy is ensured between legitimate users. In [70], the exact closed-form union bound of the PEPs in insecure conventional NOMA is derived for the unknown eavesdroppers considering arbitrary location. Furthermore, the worst-case scenario union bound of the PEPs is derived for the proposed scheme. Reference [71] derives the exact closed-form union bound on the PEPs for the proposed scheme considering the unknown eavesdroppers to the intended users, while the impact of imperfect channel phase estimation is evaluated at one of the users.

Reference [72] considers the SER analysis under equally-spaced constellations condition because only the outer constellation points are considered in the analysis. Nonetheless, the equal PA for such condition is only found for M_n-PAM with $M_1 = M_2 = 2$. Exact and approximate expressions of the SER are presented for the two-user case considering M_n-PAM with $M_n \in (2, 4)$ and M_n-QAM with $M_n \in (4, 16)$, while for the three-user case the expressions are presented for M_n-PAM with $M_1 = 2$, $M_2 = 4$ and $M_3 = 8$ only.

Arbitrary number of users: References [34], [74], [75] derive exact closed-form BER expressions of an arbitrary number of users, whereas references [54], [58] considers an upper bound using PEPs. The authors of [34] consider users with rectangular M_n-QAM. Reference [54] derives PEP assuming M_n-QAM while [58] assumes users with identical M_n-PSK orders. Garnier et al. [74] consider users with QPSK. The BER is derived considering the real part only, as the in-phase and quadrature-phase components are independent in QPSK and have identical analyses. Additionally, an iterative algorithm using gradient descent is developed to find optimal power coefficients to minimize the overall system BER for two and three-user cases. The theoretical results are verified by Monte-Carlo simulations and over-the-air experimental results through a software-defined-radio (SDR) testbed. Aldababsa et al. [75] consider users employing BPSK and perfect SIC in Rayleigh fading channels. SDR experiments are conducted to validate the derived analytical expressions. Besides [74], [75], several articles have considered the implementation and testing of NOMA over-the-air. Interested readers can refer to Qi et al. [35] which provides a comprehensive review of experimental works related to NOMA. It is noted from the literature that while the analysis is generally tractable and results in closed-form solutions for the DL scenario, it becomes cumbersome and tedious for higher number of users and higher modulation orders. Therefore, deriving a closed-form expression that is applicable to all cases is challenging.

2) VARIOUS CHANNEL MODELS

Furthermore, various channel models are considered in the literature. For example, the BER of the two-user case is derived for the κ-μ fading [77], α-η-μ fading [78] and $\kappa - \mu$ shadowed fading [79]. In addition, the two-user SER for shadowed Rician fading is derived in [80]. The BER of two and three-user scenarios is considered for α-μ fading channels in [81], for Rician fading channels in [33], and for two-wave with diffused power channel model in [82]. Bariah et al. [53] derived upper bound BER expressions using the union bound of PEPs while considering generalized Gaussian noise (GGN) with Rayleigh fading.

Aslan and Gucluoglu [83] derive approximate and asymptotic SER expressions over the generalized K fading channel by replacing the SNR of the single-user instantaneous SER with the signal-to-interference-plus-noise ratio (SINR) of multiuser NOMA. The PDF of the SINR is derived, but it is limited by a boundary condition. The SER analysis is validated using Monte-Carlo simulation for BPSK with an arbitrary number of users, and the results show a close match to the exact solution. However, this approach is not valid for higher modulation orders. Similarly, the authors of [76] derive the BER of two-user NOMA over double Rayleigh fading channels by integrating the BER expression over the PDF of the SINR. Table 4 provides a summary of various channel models used for DL-NOMA with SISO configuration.

TABLE 4. Summary of the work considering various channel models for DL SISO NOMA.

[#]	Metric	Channel	M	N	Receiver	CSI
[76]	BER	Double Rayleigh	$\forall M^{\bullet}$, $\forall M^{*}$	2	Perf. SIC	Perf.
[77]	BER	κ-μ fading	4 + 2	2	Imperf. SIC	Perf.
[78]	BER	α-η-μ fading	2	2	JMLD	Perf.
[79]	BER	κ-μ shadowed fading	$\forall M$	2	Perf. SIC	Perf.
[80]	SER	Shadowed Rician	$\forall M^{*}$	2	Perf. SIC	Perf.
[81]	BER	α-μ fading	$\forall M$	2, 3	Imperf. SIC	Perf.
[33]	BER	Rician	4	2, 3	JMLD	Perf.
[82]	BER	Two-wave with diffused power	2	2, 3	Imperf. SIC	Perf.
[53]	PEP	GGN with Rayleigh	2	3	Imperf. SIC	Perf.
[83]	SER	Generalized K	2	$\forall N$	Imperf. SIC	Perf.

TABLE 5. Summary of UL-NOMA work.

[#]	Metric	Antennas	Channel	M	N	Receiver	CSI
[84]	BER	SISO	AWGN	4	2	Imperf. SIC	-
[85]	BER	SISO	AWGN	4	2	Imperf. SIC	-
[86]	BER	SISO	AWGN	4 + 2	2	Imperf. SIC	-
[87]	BER	SISO	Rician	2	2	JMLD	Perf.
[88]	BER	SIMO	Rayleigh	4	2	JMLD	Perf.
[89]	PEP, SER	SISO	AWGN	4	2	Imperf. SIC	-
[90]	BER	SISO	Rayleigh	4	2	Perf. SIC	Perf.
[36]	PEP	SIMO	Rayleigh	$\forall M^{*}$	$\forall N$	JMLD	Perf.
[91]	PEP	SIMO	Rayleigh	$\forall M$	$\forall N$	JMLD	Perf.

B. UPLINK

Synchronous UL-NOMA is studied while considering the two-user scenario [84], [85], [86], [87], [88], [89], [90] and arbitrary number of users [36], [91]. In [84], [85], [86], closed-form BER expressions are derived for SISO setup over AWGN channels, where imperfect SIC is assumed. For example, both users use QPSK in [84], [85], whereas QPSK and BPSK are assigned to the near and far-users to account for channel asymmetry in [86]. Furthermore, accurate BER expressions over fading channels are derived for JMLD in [87], [88], where [87] considers SISO Rician channel and BPSK, while [88] considers single-input-multiple-output (SIMO) Rayleigh fading channel and QPSK.

Liu and Beaulieu [89] derive closed-form union bounds on the SER and BER of the two-user NOMA with QPSK for arbitrary relative phase offset in AWGN channel. These expressions are valid for both UL and DL, where intentional phase rotation can be applied for the former, and the channel can add phase rotation in the UL. Additionally, exact single-integral-from of the SER and BER expressions are derived for a specific power ratio. The authors of [90] study a multicarrier under-lay CR-NOMA system in the UL. By employing perfect SIC at the receiver, analytical expressions are derived over Rayleigh fading channels for the SER per sub-carrier of both the primary and secondary users with QPSK. Furthermore, closed-form approximations for these expressions are provided.

An upper bound of the BER for arbitrary number of UL users with M_n-PSK in Rayleigh fading channels is derived in [36] considering JMLD and multiple antennas at the base station. It is found that JMLD overcomes the error floor problem of the SIC. A comprehensive performance analysis of an UL-NOMA with adaptive M_n-QAM in the presence of Rayleigh fading channels is proposed in [91]. The system consists of N users, each equipped with a single antenna, transmitting data to a BS with multiple receiving antennas. The BS employs maximal ratio combining (MRC) to combine the received signals from all antennas and JMLD for jointly estimating the symbols of each user. The system's performance is evaluated in terms of PEP. The utilization of MRC-JMLD effectively eliminates the error floor. Table 5 provides a comprehensive summary of the conventional NOMA work in the UL direction.

C. OPTIMIZATION

To improve the performance of NOMA systems, finding the optimal transmission parameters such as the power coefficients and modulation orders is considered for different objectives and reliability constraints in [49], [50], [92], [93], [94], [95], [96], [97], [98], [99], [100], [101]. A comprehensive summary of the conventional NOMA optimization work is shown in Table 6.

1) MAXIMUM THROUGHPUT DESIGN

For example, references [92], [93], [94], [95], [96] study resource allocation of two-user DL-NOMA system to maximize the sum-rate using practical modulation schemes such as M_n-QAM while satisfying the BER/BLER

TABLE 6. Summary of the conventional NOMA optimization work.

[#]	Objective	Metric	Direction	Channel	M	N	Receiver	CSI
[92]	Max. Throughput	BER	DL	Rayleigh	$\forall M$	2	Imperf. SIC	Perf.
[93]	Max. Throughput	BER	DL	Rayleigh	$\forall M$	2	Imperf. SIC	Perf.
[94], [95]	Max. Throughput	BLER	DL	Rayleigh	$\forall M$	2	Imperf. SIC	Perf.
[96]	Max. Throughput	BER	DL	Rayleigh	$\forall M$	2	Imperf. SIC	Perf.
[97]	Max. Throughput	BER	UL	AWGN, Rayleigh	≤ 4	2	Imperf. SIC	Perf.
[49]	Min. SER	SER	DL	AWGN	$\forall M^{\bullet}$, $\forall M$	2	Imperf. SIC	-
[50]	Min. BER	SER, BER	DL	AWGN	4	2	Imperf. SIC	-
[98]	Min. BER	SER	DL	AWGN	$\forall M$	2	Imperf. SIC	-
[99]	Min. SER	SER	DL	Rayleigh	$\forall M$	$\forall N$	Perf. SIC	Imperf.
[100]	Min. ED	BER	UL	Rayleigh	$\forall M$	2	JMLD	Perf.
[101]	SINR balancing	BER	DL	Rayleigh	-	2	JMLD	Imperf.

constraints. Unlike single carrier systems [96], maximizing the sum-rate in multicarrier systems is a non-deterministic polynomial-time hard problem that requires highly complex exhaustive search [92], [93]. Therefore, it is important to design efficient algorithms. Cejudo et al. [92] design an efficient resource allocation algorithm to maximize the sum-rate while satisfying the BER constraints. Accurate instantaneous BER expressions are presented for square M_n-QAM considering imperfect SIC. These expressions are used to derive the exact optimal channel gain ratios between a pair of NOMA users, maximizing the achievable sum-rate for a given BER constrain. To ensure reliable SIC detection, the power coefficient for equally-spaced constellation points or highly separable constellation points groups is presented in closed-form. The exact optimal channel gain ratios and the approximated BER expressions over Rayleigh flat fading channel are used to design an efficient iterative resource allocation algorithm which involves user pairing algorithm and continuous power and rate allocation. It is worthy to mention that when NOMA is infeasible, the subcarrier is not used. Moreover, control channel is used to inform the users about the rate, power and subcarrier assignment.

Assaf et al. [93] design an efficient iterative greedy algorithm to maximize the system throughput while satisfying the users' BER constraints. Adaptive modulation, fixed power allocation and hybrid OMA/NOMA are utilized by the design. It is noteworthy to mention that relying on exact rather than approximate NOMA BER expressions induce high computational complexity.

The authors of [94] design an adaptive modulation and PA scheme for packet-based NOMA to maximize the throughput. The design considers optimizing the transmission mode (TM) by the BS which tunes the modulation orders and power coefficients while satisfying the BLER requirement for each user. Two PA schemes are considered: 1) Fixed PA based on linear mapping. 2) Adaptive PA. The former optimization is solved using integer programming while the latter is solved using mixed-integer programming. In addition, the computational complexity is reduced using an efficient terminating criterion, segment-line search, and quantized SNRs. Approximated closed-form BLER expressions are derived over Rayleigh fading channels. The authors extend their work in [95] by proposing the min-max method to solve the fixed PA optimization. Such a method reduces the complexity and the number of TMs significantly while improving the throughput of the system.

The authors of [96] propose a joint adaptive power and modulation order to maximize the SER without sacrificing the BER performance, where the BER expressions of NOMA over Rayleigh fading are approximated as OMA counterpart. This is applicable only when assuming perfect SIC. Two adaptive power schemes are proposed to guarantee the minimum target rate for one user while maximizing the rate of the other user. Continuous and discrete adaptive rate modulation are considered to adapt to the channel fade level.

Adaptive modulation is studied for UL-NOMA in [97], where an asymmetric adaptive modulation algorithm is designed for a two-user UL-NOMA system to maximize the system throughput for a given average SNRs and BER thresholds. The BER expressions are derived in closed-form for AWGN channels considering imperfect SIC and M_n-PSK with $M_n \in \{2, 4\}$. Lower bound BER expressions are derived for Rayleigh fading channels while ignoring the channel phase effect. The boundary value effect is studied, where to have reliable SIC performance, the modulation orders are selected based on ratio of the users SNRs and the boundary value.

2) MINIMUM BER DESIGN

References [49], [50], [98], [99] formulate several optimization problems to minimize the error performance of DL-NOMA systems. For example, the objective function in [49] is to minimize the instantaneous SER of the strong user while satisfying the SER requirement for the weak user. The instantaneous SER is derived in closed-form for both users considering M_n-QAM and M_n-PAM. Nonetheless, a closed-form suboptimal PA is derived. The authors of [50] propose a line search algorithm for a two-user system to find the optimal power coefficients that minimize the un/coded

TABLE 7. Summary of the labeling work.

[#]	Metric	Antennas	Direction	Channel	M	N	Receiver	CSI
[102]	SER	SISO	DL	AWGN	$\forall M^{\bullet}$	2	JMLD	-
[103]	SER, BER	SISO	DL	Rayleigh	4	2	Imperf. SIC	Perf.
[104]	SER, BER	SISO	DL,UL	AWGN	4	$\forall N$	Imperf. SIC	-
[105]	BER	SIMO	DL	Rayleigh	4	2	MRC–SIC	Perf.
[106]	BER	SISO	DL	Nakagami-m	2	2	Imperf. SIC	Perf.

NOMA system overall error performance in AWGN channels. BER is considered and derived for the uncoded QPSK, while the SPC BER approximation is considered for the coded system. The work is extended in [98] to consider square M_n-QAM, where the BER is approximated using the SER expressions derived for AWGN channels. These expressions are used to find the optimal power coefficients that minimize the instantaneous overall system BER. The optimization problem is simplified by obtaining upper and lower bounds of the overall BER.

Dutta [99] approximates the closed-form BER expressions using the SER expressions that are derived for an arbitrary number of DL-NOMA users, considering arbitrary quadrature amplitude modulation (QAM) and perfect SIC. These expressions have been used for power allocation optimization such that the average BER among all users is minimized while satisfying certain minimum rate requirements per user. Since the problem is non-convex, an upper bound approximation is used for the objective function to make it convex, while the concave rate is transformed to be convex. As the probability of error considers all the possible realizations of the input vector, it is computationally difficult to handle the objective function. Hence, a faster approach is developed to find the optimal power coefficients, which is based on splitting the data sets into subsets and running the optimization for all subsets in parallel.

Optimizing the error rate performance of the UL-NOMA system is studied in [100] which derives closed-form optimal power coefficients and phases to maximize the minimum ED of the sum of the constellations of two-user NOMA with square M_n-QAM, while JMLD is used at the receiver. The resulting sum constellation is found to be a uniform M-QAM constellation of a larger size. Mixed-integer optimization is used to formulate the problem, where the complex Rayleigh fading channel is decomposed into symmetrical real and imaginary parts. Only one part is analyzed due to symmetry.

In a different category, optimal closed-form SINR-balancing is derived in [101] for two-user case assuming imperfect CSI. This scheme can provide fairness between the users, however, the performance is not guaranteed.

V. IMPROVED NOMA SCHEMES

Improving the error rate performance of NOMA was a major research objective for the past decade. Thus, several techniques and designs were introduced for NOMA such as labeling, constellation rotation, interference alignment, channel coding, multicarrier system design and detector design. Therefore, this section provides a brief description of such approaches and summarizes the state-of-the-art research in these areas.

A. LABELING

The error rate performance of NOMA is highly impacted by the symbol-to-bit labeling strategy used, [102], [103], [104], [105], [106]. There are three main labeling strategies which are: 1) NOMA non-Gray labeling, 2) Joint Gray labeling, 3) Natural labeling. The NOMA non-Gray labeling results naturally from the SC process. An example is shown in Fig. 5a. On the other hand, the joint Gray labeling is simply performed such that the NOMA word becomes Gray coded. This is done before SC on each user stream of bits, $\mathbf{b}_n$, such that the stream of bits after joint Gray coding is

$$\mathbf{g}_n = \begin{cases} \mathbf{b}_n, & n = N \\ \mathbf{b}_n \oplus \mathbf{b}_{n+1}, & 1 \leq n < N. \end{cases} \tag{11}$$

Considering the same example in Fig. 5a, the non-Gray coded NOMA word is 1010 where $\mathbf{b}_1 = [1, 0]$ and $\mathbf{b}_2 = [1, 0]$. Then, $\mathbf{g}_1 = \mathbf{b}_1 \oplus \mathbf{b}_2 = [0, 0]$ and $\mathbf{g}_2 = \mathbf{b}_2 = [1, 0]$. Hence, the joint-Gray coded NOMA word becomes 0010. Fig. 5b shows the NOMA constellation diagram with joint Gray labeling. As can be seen, a NOMA symbol error usually results in a single bit error compared to multi bit error for the NOMA non-Gray labeling. Lastly, the natural labeling which is based on natural counting rules, and the NOMA constellation for such a labeling scheme is shown in Fig. 5c. While the use of natural labeling imposes the need for JMLD, NOMA with joint Gray labeling does not impose using JMLD. In fact, SIC can still be used, however, decoding should be performed after detection such that

$$\mathbf{b}_n = \begin{cases} \mathbf{g}_n, & n = N \\ \mathbf{g}_n \oplus \mathbf{g}_{n+1}, & 1 \leq n < N \end{cases}. \tag{12}$$

Table 7 provides a comprehensive summary of the labeling work.

State-of-the-Art on NOMA with Labeling: The authors of [102] study three labeling schemes for two NOMA users with M_n-PAM in AWGN channel with uniform NOMA constellation and a modulation order of $M = M_1 \times M_2$. Meanwhile, the simulation results are shown for SER and BLER for different modulation orders, the only closed-form expression derived is the near-user SER for $\forall M$ as the far-user performance is independent of the labeling scheme.

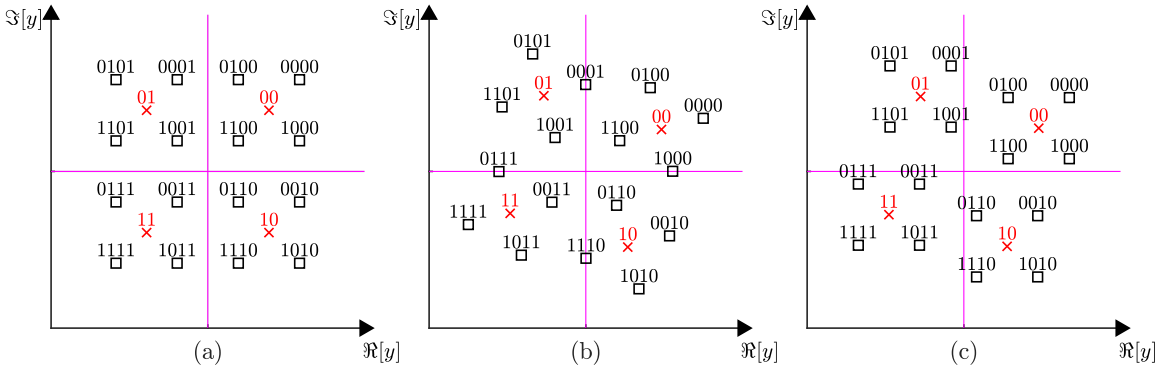

FIGURE 8. The constellation diagram of NOMA with constellation rotation utilizing different rotation angles. (a) $\theta_1 = 0°, \theta_2 = 0°$. (b) $\theta_1 = 30°, \theta_2 = 16°$. (c) $\theta_1 = 0°, \theta_2 = 15°$.

It is observed from the results that compared to other labeling schemes, joint Gray labeling improves the SER and BLER performance of the near-user. Furthermore, the authors of [105] consider Gray-labeling for a DL SIMO system assuming only two users per subcarrier, where the far-user is multiplexed with all near-users' subcarriers. The BER expressions are derived over Rayleigh fading channels for QPSK and MRC SIC detector.

In reference [103] closed-form expressions are derived for the SER and BER for joint Gray and non-Gray labeling schemes. The derived expressions are for a DL two users case with QPSK in AWGN channel. It is noted that error propagation due to SIC imperfections is eliminated at high SNRs when joint Gray labeling is used. This work was extended in [104] by considering arbitrary number of users. Closed-from expressions are presented for specific cases such as the first, second and last users; where the expressions for other users can be inferred. In addition, approximate expressions are demonstrated for the joint Gray labeling. The UL scenario is highlighted for the random phase offset case and proved that the DL expressions can be considered as an upper bound estimation of the UL case for a specific phase offset.

The authors of [106] propose symmetrical coding for two-user DL-NOMA with BPSK. The proposed scheme manipulates the transmitted symbol such that the NOMA symbols are Gray-coded for the near-user as well. Closed-form BER expressions over Nakagami-*m* fading are derived. Also, an algorithm to optimize the power coefficients based on statistical CSI is developed to achieve better BER performance for the near-user.

B. CONSTELLATION ROTATION

The basic principle of NOMA constellation rotation is to rotate the individual user constellation before SC with a specific angle. For example, in the DL, the signal transmitted from the BS is given as

$$x_{sc} = \sum_{n=1}^{N} \sqrt{\alpha_n} x_n \exp\left[-\jmath\theta_n\right] \tag{13}$$

where θ_n is the rotation angle. The phase rotation provides an additional degree of freedom to optimize performance. However, extra signaling overhead is introduced besides the higher detection complexity, because the symbols of all users have to be detected jointly. Fig. 8 shows the constellation diagram for the example in Fig. 5, but different rotation angles are used. As can be noted from the figure, the rotation angles do not affect the intra-constellation distances, whereas they directly impact the inter-constellation distances. The definition of intra-constellation and inter-constellation distances can be obtained with the aid of Fig. 8a. As can be seen from the figure, the NOMA constellation can be divided into four groups of constellation points that are centered around the constellation points of the user with a higher power coefficient. Each of the four groups is known as an intra-constellation. All the scenarios in Fig. 8 have four intra-constellations. In addition, the distance between the intra-constellation points is known as the intra-constellation distance. Whereas the inter-constellation distance is the distance between two constellation points that are from different intra-constellations. References [55], [107], [108], [109], [110], [111], [112], [113], [114], [115], [116], [117], [118], [119], [120], [121], [122], [123] study the performance of NOMA with constellation rotation, where Table 8 provides a comprehensive summary for the constellation rotation work including the optimization objective in a dedicated column.

State-of-the-Art on NOMA with Constellation Rotation: The work in [107] studies constellation rotation for the DL scenario with two users each of which is using QPSK. Because deriving exact closed-form SER expressions is challenging due to the arrangement of the NOMA constellation points, upper bounds on the SER are presented based on the union bound of the PEPs. These expressions are used for rotation angles optimization which is performed using exhaustive search. Chang and Fukawa [108] derive the optimal rotation angles that minimize ED between the NOMA constellation points for the two-user case while considering identical QPSK and QPSK with 16-QAM. Furthermore, the work is extended to the three-user case using QPSK in [109], where the optimal phase rotation is found for two schemes which are: 1) rotation for the

TABLE 8. Summary of the constellation rotation work.

[#]	Optimization	Metric	Antennas	Direction	Channel	M	N	Receiver	CSI
[107]	PEP	SER, BLER	SISO	DL	Rayleigh	4	2	ML	Perf.
[108]	ED	BER	SISO	DL	AWGN	4, 16	2	JMLD, Imperf. SIC	-
[109]	ED	BER	SISO	DL	AWGN	4	3	JMLD, Imperf. SIC	-
[110], [111]	PEP	BER	SIMO	DL,UL	Rayleigh	4	2	JMLD	Perf.
[112]	SER	SER	SISO	UL	Non-fading	4	2	Imperf. SIC	Perf.
[113]	ED	BER	SISO	UL	Rayleigh	2-D	2	JMLD	Perf.
[114]	ED	BER	SISO	UL	Rayleigh	K-D	2	JMLD	Perf.
[115]	MI	BER	SIMO	UL	Rayleigh	4	2	Imperf. SIC	Perf.
[55]	-	BER	2×1	UL	Rayleigh	4	2	JMLD	Perf.
[116]	-	SER	SISO	DL	Rayleigh	$\forall M^{\bullet}$	2	MLD	Perf.
[117]	-	BER	SISO	DL	Rayleigh	$\forall M$, M^{*}	4	Imperf. SIC	Perf.
[118]	ED	BER	SIMO	UL	Rayleigh	4	2	JMLD	Perf.
[119]	SER	SER	SIMO	DL	Correlated Rician	$\forall M^{*}$	2	MRC-MLD	Perf.
[120]	SER	SER	SISO	DL	Nakagami-m	4	2	MLD	Perf.
[121]	ED	SER	SISO	UL	Fading	≤ 16	2 streams	Imperf. SIC	Perf.
[122]	ED	SER	SISO	UL	AWGN	≤ 4	2	JMLD	-
[123]	ED	BER	SISO	DL	AWGN	4	2	JMLD	-

near-user. 2) rotation for the near-user and the composite of near and middle users. Reference [110] studies two users NOMA with QPSK and finds the rotation angle that minimizes the dominant PEP, which translates to maximizing the smallest ED. It is found that the optimal rotation angle depends on the ratio of the assigned power coefficients and phase differences between the channel coefficients for UL, while it only depends on the ratio of the assigned power coefficients for DL. The work is extended in [111] by jointly optimizing the power coefficients and rotation angles. In [112], the authors propose phase pre-distortion for UL VLC-NOMA system to improve the SER. Assuming that the phase difference between the channels of the two users is uniformly distributed, closed-form SER expressions are derived considering QPSK for both users and SIC at the receiver. The optimal rotation angle that minimizes the SER is found to be the one that ensures 0° relative phase, i.e., angle that causes co-phasing. Closed-form optimal rotation angles were derived for single and multi-receiving antenna cases. The joint optimization problem reduces to a piece-wise convex optimization problem over its sub-domains, for which the global maximum solution is obtained in closed-form. The work in [113] proposes an algebraic rotation approach to design DL-NOMA for two users while achieving full diversity and improved BER performance. This improvement gained due to the special lattice partition scheme that ensures maximum minimum product distance. The upper bound of the minimum product distance is derived in closed-form for arbitrary power coefficients for the two dimensional lattice. The work is generalized in [114] for multi-dimensional lattices. It is worthy to mention that the design and analysis are applicable to the JMLD rather than SIC, which imposes high complexity at the receiver, but reduces the decoding delay. The results show that the proposed scheme outperforms the conventional NOMA and the scheme proposed in [107] in fast and block fading channels.

Ye et al. [115] study a two-user multi-antenna UL-NOMA with SIC utilizing constellation rotation. Optimal rotation angles are found to maximize the mutual information (MI) where the signal is modeled as a Gaussian mixture model. The MI maximization problem has high computational complexity because it is a bivariate problem. Hence, it is transformed to an entropy maximization problem that involves only a single random variable. Efficient closed-form approximation is derived using variational approximation. Improved sum-rate and lower BER are obtained when compared to conventional NOMA. Constellation rotation with space-time line code (STLC) is considered in [55] for two-user UL-NOMA, where the BS is equipped with two receiving antennas and each user is equipped with a single antenna. The channel between each user and each receiving antenna at the BS is assumed to be quasi-static for two time slots and known to the user. Hence, spatial diversity can be obtained using STLC-encoding. Assuming that QPSK is used by both users and constellation rotation is applied to one user only, upper bound expressions for the average BER are derived for the JMLD using the union bound of the PEPs. Additionally, an approximation is derived for high SNRs using Taylor series.

The authors of [116] propose a novel scheme for the single antenna DL-NOMA based on coordinate interleaving for a general number of users, where M_n-pulse amplitude modulation (PAM) constellation is rotated by $\pi/4$ rad counter clock-wise. Because the real and imaginary components of the $\pi/4$ M_n-PAM constellation are equal, then coordinate interleaving for the two-user case results in $x_{sc} = \sqrt{\alpha_1}\Re[x_1] + \jmath\sqrt{\alpha_2}\Re[x_2] + \sqrt{\alpha_1}\Im[x_1] + \jmath\sqrt{\alpha_2}\Im[x_2] = 2\sqrt{\alpha_1}\Re[x_1] + 2\jmath\sqrt{\alpha_2}\Re[x_2]$. This results in a M-QAM like constellation where $M = M_1 \times M_2$. It is worth noting that x_{sc} in its current form does not have a unity average power. In fact $\mathbb{E}[|x_{sc}|^2] = 2$. Therefore, it has to be normalized for a fair comparison with the conventional

NOMA system. Additionally, this scheme eliminates the need for using SIC at the receiver for the two-user case, while it reduces the number of SIC operations by more than half when there is more than two users in the system. Furthermore, closed-form SER expressions are derived for the two-user, as well as the optimal power coefficients that achieve fairness. A DL-NOMA scheme for a cluster of four users is proposed in [117] by utilizing phase rotation to achieve a lower BER and higher sum rate. The optimal rotation angle is determined to maximize the minimum distance between symbols, thereby improving overall system performance. Furthermore, the optimal power allocation is determined by minimizing both the inter-cluster and intra-cluster distances in the NOMA signal. The proposed method reduces the overall complexity by eliminating the need for SIC between subgroup multiplexing. Exact BER and union bound on BER expressions are derived for all users using M_n-PSK or M_n-QAM in a Rayleigh fading channel.

In [118], a constellation rotation technique is proposed for an UL-NOMA based IoT network to enhance performance. It is assumed that perfect CSI is available to the transmitting nodes, where each transmitter is equipped with a single antenna and the access point employs two antennas. The upper bounds on the BER over Rayleigh fading channels are derived for the case with two transmitters and QPSK. Both dynamic and fixed constellation rotation scenarios are considered, and optimal rotation angles are determined for a given SNR to improve the BER.

Reddy et al. [119] propose optimal constellation rotation for the two-user DL-NOMA system considering M_n-PSK signaling over correlated SIMO Rician channels. By modifying the NOMA SC as follows, $x_{sc} = \sqrt{\alpha_1}[x_1] + \jmath\sqrt{\alpha_2}[x_2]$, the need for SIC at the receiver is eliminated and MRC-MLD is used instead. Assuming perfect CSI, the optimal rotation angles that minimize the SER are found using the derived closed-form SER expressions.

The authors of [120] generalize the idea in [116] for the two-user case by considering arbitrary rotation angles and more flexible choices of modulation schemes such as M_n-PSK and M_n-QAM. The need for joint multiuser detection or SIC is eliminated by rotating the constellations of both users and multiplexing the real component of user 1 in the in-phase axis, while the imaginary component of user 2 is multiplexed in the quadrature-phase axis. This results in a M-QAM-like constellation where $M = M_1 \times M_2$. Nonetheless, the symbol-to-bit mapping is unique as user 1 bits flip along the in-phase axis only, while user 2 bits flip along the quadrature-phase axis only. Additionally, the distance between the constellation points is not uniform because it depends on the allocated power coefficients and rotation angles. The exact instantaneous SER expressions are derived in closed-form for both users using QPSK. The derived expressions are used to calculate the optimal rotation angles, which can be represented by a low complexity approximation at high SNRs.

The UL is studied in [121] for a single-user having two data streams superimposed using NOMA. The objective is to maximize the minimum inter-constellation distance via constellation rotation, where the rotation angle closed-form expression is derived as a function of the power coefficients for different modulation schemes including BPSK, QPSK and 16-QAM. It is proved that the performance of such design provides more robust error performance and better fairness when compared to SNR-dependent designs such as MI maximization. Inspired by [121], the authors of [122] propose a novel simple parallelogram-structured constellation design to further improve the SER and maximize the minimum inter-constellation distance. The design is based on shifting one of two coordinates of the constellation allowing arbitrary placement of the constellation points. Furthermore, the work is extended to DL scenario in [123], where the parallelogram structured constellation is specifically tailored for DL by shifting and scaling the constellation to preserve the parallelogram-structure. The minimum distance is derived in closed-form for the identical QPSK case.

Several articles have conducted over-the-air experiments using SDR to investigate NOMA with constellation rotation [124], [125], [126] and the references therein. For instance, References [125], [126] specifically explore constellation rotation in a two-user DL-NOMA scenario. The authors propose a technique where the constellation of the lower power user, which is susceptible to phase noise, is rotated to minimize its BER and alleviate the adverse effects of phase noise caused by residual hardware impairment (RHI). These studies provide valuable insights into the experimental evaluation and feasibility of NOMA systems with constellation rotation, offering interested readers further in-depth analysis and findings in this area.

C. INTERFERENCE ALIGNMENT

Multiuser interference generally causes performance degradation for NOMA users. However, constructive interference may improve the performance as the desired signal power is boosted by the interference. On the other hand, destructive interference degrades the performance of NOMA. Therefore, the concept of interference alignment is to design the individual users' signals such that they add constructively. This can be achieved via phase rotation [127], [128], [129] or symbol scaling [130], [131]. A summary of the work on interference alignment is given in Table 9.

1) INTERFERENCE ALIGNMENT VIA PHASE ROTATION

The work in [127] proposes a constellation rotation scheme for simultaneous wireless information and power transfer (SWIPT)-assisted NOMA to maximize the energy transmitted to the wireless information transfer (WIT) users and wireless power transfer (WPT) users, while satisfying acceptable SER performance for the WIT users. To minimize the signaling overhead associated with informing the WIT receivers about the optimal rotation angles, the constellation rotation is performed jointly over a block of symbols rather

TABLE 9. Summary of the interference alignment work.

[#]	Method	Metric	Antennas	Direction	Channel	M	N	Receiver	CSI
[127]	Constellation Rotation	SER	SISO	DL	AWGN	4	2 WIT + 1 WPT	Imperf. SIC	-
[128]	Constellation Rotation	SER	SISO	DL	AWGN	$\forall M$	N WIT + 1 WPT	Imperf. SIC	-
[129]	Constellation Rotation	SER	SISO	DL	Rayleigh	4	2	JMLD	Perf.
[130]	Symbol Scaling	BER	SISO	DL	Rayleigh	≤ 4	2, 3	JMLD	Perf.
[131]	Symbol Scaling	BER	SISO	DL	Rayleigh	$2+4$	2	JMLD	-

TABLE 10. Summary of the channel coding work.

[#]	Coding	Metric	Antennas	Direction	Channel	M	N	Receiver	CSI
[132]	LDPC	PEP	MIMO	UL	Rayleigh	4	2	Novel JMLD	Imperf.
[133]	LDPC	PEP	SISO	UL	Rayleigh	$\forall M$	2	Perf. Codeword-level SIC	Perf.
[134]	TCM	BER	SISO	DL	Fading	$\forall M^*$	2	Joint Viterbi	Perf.
[135]	Polar	BLER	SISO	UL	AWGN	2	2	Adaptive List SIC	Perf.
[136]	Turbo	BLER	SISO	DL	Rayleigh	4	2	LLR-based	Perf.
[137]	Repetition	BER	SISO	DL	AWGN	2	2, 3	MLD	Perf.

than on a symbol-by-symbol basis. The optimal constellation rotation angles are derived for QPSK case assuming two NOMA WIT users and a single WPT user. The work is extended in [128] by considering a multi-carrier system, arbitrary modulation orders, and multi WIT and WPT users. A joint design of the energy interleaver and constellation rotation is proposed, where the energy interleaver is introduced to suppress the destructive interference of multiple symbols scheduled on each subcarrier. Furthermore, the receiver operations for WIT and WPT users as well as the signaling overhead are discussed thoroughly. An iterative algorithm is proposed for obtaining optimal the constellation rotation angles since the objective function is non-convex. Whereas a low-complexity greedy algorithm is proposed for the energy interleaver integer optimization. In [129], phase rotation is applied to the near-user to allow constructive interference with the far-user symbol. In addition, a nonredundunt precoding is applied to the near-user symbol to allow symbol extraction at the receiver. The authors propose a semi-blind detection scheme based on independent component analysis to detect the near-user symbols after rotation. Nonetheless, it requires 1–2 pilot symbols to remove ambiguities caused by the independent component analysis. The SER is derived in closed-form under Rayleigh fading for two users with QPSK assuming perfect ambiguity elimination. Additionally, an efficient power allocation algorithm that is based on statistical channel information is proposed to minimize the average asymptotic SER. Furthermore, the computational complexity of the scheme is studied and compared with other common benchmarks, such as [108], [111].

2) INTERFERENCE ALIGNMENT VIA SYMBOL SCALING

The authors of [130], [131] propose a data-aware power assignment for DL-NOMA to scale the NOMA symbols with different power coefficients to maximize the constructive interference. This scheme is based on the polarities of the information symbols real and imaginary components. Hence, the assignment for the in-phase component can be different from the quadrature-phase component. Yahya et al. [130] derive the BER expressions for two and three users for the identical BPSK case. In addition, the optimal power coefficients are found. Whereas [131] derives the BER for a two-user scenario given that BPSK is adopted by the near-user while QPSK is adopted by the far-user. The work also considers finding the power coefficients that maximize the constructive interference.

D. CHANNEL CODING

Channel coding is a well-known approach to reduce the error probability of digital communications systems at the cost of higher complexity at the transmitter and the receiver. Thus, studying the complexity and error rate performance of NOMA-based channel coding transceivers is pivotal. Typical channel coding schemes include low-density parity-check (LDPC) [132], [133], Reed-Solomon codes [132], trellis coded modulation (TCM) [134], polar codes [135], turbo codes [136], and repetition codes [137]. A comprehensive summary for the NOMA work with channel coding is depicted in Table 10.

State-of-the-Art on NOMA with Channel Coding: The authors of [132] propose a novel linear receiver that exploits the constraints of the forward error correcting (FEC) codes to mitigate the SIC error propagation caused by the imperfect CSI at the receiver, where the channel frequency response is estimated by interpolating the responses of the pilot subcarriers. The novel receiver is applicable to symbol and codeword-level SIC. It is designed for a multiple-input multiple-output (MIMO) two-user UL-NOMA based on the minimum output energy criterion that can handle moderate channel estimation errors, where the IUIs are separated from the desired signals by adopting a unique signature based on the FEC codes' constraints. The receiver optimization is formulated as a quadratic programming problem anchored with set of code constraints. Transmit diversity and capacity-achieving LDPC codes are considered. To improve the

performance further, an iterative receiver is designed to recover the Reed-Solomon coded data that is serially concatenated to an LDPC code. To verify the reliability of the proposed detector, an upper bound for the coded BER is derived based on the union bound of the PEPs. The authors of [133] propose probabilistic shaping combined with QAM for N UL-NOMA users in Rayleigh fading channels to improve the SER. Probabilistic shaping assigns the constellation points that have equidistance space different probabilities such that the source generates information symbols with non-uniform probabilities using a constant composition distribution matcher method. To maximize the ergodic constrained capacity, a multi-step optimization is performed to find the optimal probability mass function for each user, where the optimization order is the inverse of the SIC order. At the receiver, maximum a posterior (MAP)-based codeword-level SIC is implemented with an order determined by the large-scale pathloss. Unlike the symbol-level SIC, the codeword-level SIC can ideally cancel the IUI caused by the previously decoded signals due to the powerful error correcting codes as well as the soft channel decoder. Whereas the rest IUIs are assumed to be Gaussian distributed. To validate the reliability of the proposed scheme, closed-form average PEP expressions are derived. Furthermore, a design example combines the proposed system with the practical LDPC codes to study the SER and evaluate the BER performance using Monte-Carlo simulations.

The authors of [134] propose a TCM for two-user DL-NOMA, where the symbols of each user are modulated independently and multiplexed in the power domain. The detection is performed jointly using the Viterbi algorithm where the TCM-NOMA is treated as a regular TCM with the tensor product trellis. Selecting appropriate power coefficients can ensure good decoding performance. Since a larger free distance leads to a better performance at high SNRs, the optimal power coefficients are found to maximize the free distance of the tensor product trellis. A closed-form expression of the free distance of the tensor product trellis is derived.

The authors of [135] propose polar code for the two-user binary Gaussian multiple access channel, where for each user two blocks of polar codes are constructed with unequal power. Code construction with power and rate allocation are jointly optimized to improve performance. To maintain fairness, alternating power allocation over the two blocks is proposed. At the receiver side, hard-decision SIC employing successive cancellation based on adaptive list size is proposed. Upper bound BLER expressions are derived for the finite block length regime assuming BPSK. The authors of [136] design a SIC-free detector for two-user DL-NOMA utilizing turbo codes. The proposed detector is based on the log-likelihood ratios (LLRs) for each bit of the NOMA symbol. These LLRs are derived in closed-form considering QPSK for both users. The symbol-level and codeword-level SIC detectors are the benchmarks. The authors of [137] propose a low-complexity structured coding for two-user DL-NOMA system with BPSK. The coding scheme is based on repetition coding and parity-check, where the far-user's symbol is repeated twice while the 0 and 1 bits of the near-user are mapped to [0, 1] and [1, 0], respectively. Such a scheme exploits the constructive interference for the far-user and eliminates the interference from the near-user. The authors derive the exact closed-form BER and quantify the complexity of the proposed detector.

As can be noted from the surveyed literature, there is still lack of a comprehensive error rate analysis of NOMA with various channel codes, modulation schemes, and a large number of users. In particular, obtaining such a generalized analytical framework has many challenges due to the difficulty of computing the exact LLRs for the bits of each user, particularly when the SIC detector is used.

E. MULTICARRIER DESIGN

In [138], wavelet transform pulse shaping is analyzed for the DL OFDM NOMA as it is more spectrally efficient than the fast Fourier transform (FFT) pulse shaping which requires cyclic prefix. Closed-form BER expressions are derived for both pulse shaping schemes in AWGN channels based on the ED approach, where the presented analysis holds for two-user case with QPSK assuming ideal synchronization. The strong channel user applies SIC to detect its signal, whereas the weak channel user detects its signal assuming that the other user signal being in the noise floor. The effect of the AWGN on the received signal is studied after passing the AWGN components through the discrete Fourier transform (DFT) and discrete wavelet transform (DWT) filter banks and getting their true variances. Since the high frequency components are discarded in the DWT filter banks, the channel effect on the received signal is reduced and the signal recovery is improved.

Maatouk et al. [139] propose combining orthogonal frequency division multiple access (OFDMA) and code division multiple access (CDMA) for DL-NOMA. Unlike conventional NOMA which for example combines two users and uses SIC to cancel the interference, the proposed scheme combines two groups of users with two sets of orthogonal waveforms and uses iterative SIC to cancel the interference between the groups. The users in the OFDMA group can detect their signal directly as the number of the users in the CDMA group is assumed to be small such that the interference is negligible. On the other hand, the users of the CDMA group need to use iterative SIC to cancel the interference. Khansa et al. [140] extend the work by introducing a power split between the two groups that follows the conventional NOMA. Approximate BER expressions are derived for QPSK case in AWGN channel by assuming the interference being a Gaussian-like signal for the OFDMA group of users, while the number of possible sequence errors for the CDMA group is assumed to follow the binomial distribution.

The authors of [141] study combining the generalized frequency division multiple access (GFDMA) waveforms

TABLE 11. Summary of the multicarrier NOMA design work.

[#]	System	Metric	Antennas	Direction	Channel	M	N	Receiver	CSI
[138]	Wavelet Transform OFDM	BER	SISO	DL	AWGN	4	2	Imperf. SIC	Perf.
[139]	OFDMA-CDMA	BER	SISO	DL	AWGN	$16+4$	2	Iterative Hard and Soft SIC	Perf.
[140]	OFDMA-CDMA	BER	SISO	DL	Rayleigh	4	2	Iterative Hard and Soft SIC	Perf.
[141]	GFDMA	BER	SISO	DL,UL	Rayleigh	4	2	Imperf. SIC	Perf.

TABLE 12. Summary of the detector design work.

[#]	Carrier	Metric	Antennas	Direction	Channel	M	N	Receiver	CSI
[142]	Multi	BER	SISO	UL	Rayleigh	$\forall M$	2	Triangular SIC	Perf.
[143]	Multi	BER	SISO	UL	Rayleigh	$\forall M$	3	Triangular SIC	Perf.
[144]	Single	BER	SISO	UL	AWGN	4	2	Time asynchronous SIC	Perf.
[145]	Multi	SER	SISO	UL	Rayleigh	$\forall M$	2	Triangular SIC	Perf.
[146]	Multi	BER	SISO	UL	Rayleigh	$\forall M$	$\forall N$	Triangular SIC	Perf.
[147]	Multi	SER	SISO	UL	AWGN	4	2	JMLD-SIC	-
[148]	Single	SER	SIMO	DL	Rayleigh	$\forall M$	2	Threshold based	Perf.
[149]	Single	BER	SISO	DL	Rayleigh	$\forall M^{\bullet}$	$\forall N$	Improved SIC	Perf.
[150]	Single	SER	SISO	DL,UL	AWGN	4	3	Modified SIC	Perf.

with NOMA, where the information symbol in each subcarrier is shaped using a filter. Analytical conditional BER expressions for the DL and UL are derived considering two-users and QPSK for both users. Perfect SIC and imperfect SIC are considered and their BERs are derived. A comprehensive summary for the mutlicarrier NOMA system designs is shown in Table 11.

F. DETECTOR DESIGN

This subsection focuses on the innovations in the research to improve the performance of the NOMA detectors in different scenarios including asynchronous UL communications [142], [143], [144], [145], [146], synchronous UL communications [147] and DL communications [148], [149], [150]. A comprehensive summary for the NOMA detector designs is presented in Table 12.

1) ASYNCHRONOUS UL COMMUNICATIONS

Haci et al. [142] study the asynchronous UL-NOMA system as perfect synchronization is difficult to achieve for UL users distributed in geographically diverse and dynamic environments. They propose a novel triangular-SIC detector which uses multiple symbols from each interfering user in a triangular pattern to carry out interference cancellation, where iterative soft and hard decision detectors are studied for higher modulation orders. The BER performance analysis is presented in [143] for the three-user case in flat Rayleigh fading considering conventional SIC and the proposed SIC, where besides the receiver power ratios, the BER of the proposed SIC depends also on the iteration number and the time offset between users. It is assumed that the relative time offset between the users is uniformly distributed, and the residual interference is approximated to the Gaussian distribution.

Liu and Beaulieu [144] propose a novel time asynchronous SIC for the asynchronous UL-NOMA. The detector is based on the triangular-SIC introduced by [142], [143] where an optimal time-offset is selected to eliminate the IUI. The optimal time offset is found to be half the symbol duration for the QPSK case. It is worth mentioning that the proposed detector does not introduce signaling overhead nor higher complexity, however, it requires the received symbol timing. Exact BER expressions are derived over AWGN channel considering two-user case with QPSK and imperfect SIC, where no relative phase rotation is assumed between the users. Additionally, a simpler BER approximation is derived for the weak user by relaxing the correlation between the noise samples at the detector. Furthermore, Liu et al. [145] derive closed-form SER expressions over Rayleigh fading channels for the asynchronous UL-NOMA with triangular SIC. The SER expressions are obtained for scenarios involving multiple users and arbitrary M_n-QAM orders. Additionally, a novel parallel triangular SIC detection method is proposed, demonstrating superior interference suppression capabilities compared to the iterative triangular SIC approach.

The authors of [146] propose a three-stage cyclic triangular-SIC detector for the asynchronous UL-NOMA with transmission repetition. The stages are: 1) Optimization: By determining an optimal interference cancellation triangle under QoS constraints, it maximizes the number of data symbols to be decoded at the receiver 2) Decoding using triangular-SIC. 3) Retransmission, where stages 1 and 2 are repeated until all N user data are decoded. The authors present the BER of the proposed detector in integral-form considering M_n-QAM.

2) SYNCHRONOUS UL COMMUNICATIONS

To mitigate the error propagation problem caused by SIC, [147] propose an improved detector to allow much

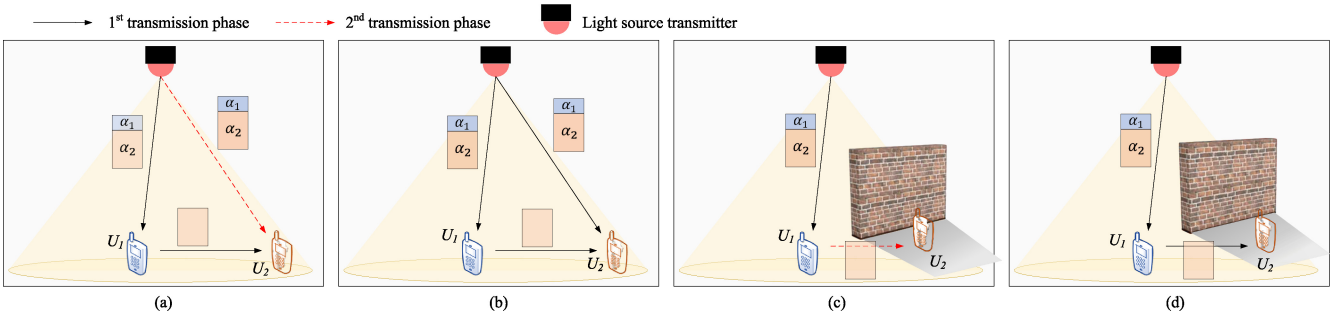

FIGURE 9. Basic DL cooperative O-NOMA; (a) HD relaying and direct link, (b) FD relaying and direct link, (c) HD relaying without direct link, (d) FD relaying without direct link. The near-user can be a dedicated or a user relay.

smaller range of power differences between the UL-NOMA users, as compared with SIC. The proposed detector is based on hard decision JMLD to find decisions on the weak user signal, then using them to cancel the interference from the strong user. Hence, computing the LLRs to find the strong user signal, which is then used to cancel the interference from the weak user signal. Assuming co-phased signals transmitted from the users, the uncoded BER of the SIC and the proposed detector are derived considering QPSK for both users.

3) DL COMMUNICATIONS

The authors of [148] propose a low-complexity threshold based detector to detect the signals of two NOMA users in the DL, where the BS is equipped with a single antenna while the users are equipped with multiple antennas and use M_n-QAM with $M_n \in (4, 16)$. The exponential bound of the $Q(\cdot)$ function is used to derive the SER expressions for Rayleigh fading channels. Al-Dweik et al. [149] study phase-independent NOMA using unipolar amplitude shift keying (ASK) which allows amplitude-coherent detection. Considering two and multiuser systems in ordered SISO Rayleigh fading channels, closed-form BER expressions are derived for three types of detectors, namely JMLD, conventional SIC and improved SIC. The improved SIC cancels interference more effectively than conventional SIC and has identical performance to the JMLD but with lower complexity. Reference [150] introduces a modified SIC detector for an UL-NOMA system. The proposed modified detector incorporates adaptable decision regions and enhance the decoding performance. Exact closed-form SER expressions and approximations are derived for the three-user case over AWGN channels while considering a single antenna at all nodes and QPSK. Furthermore, the study identifies specific scenarios in which the proposed SIC detector demonstrates superior performance compared to the conventional SIC detector.

VI. NOMA INTEGRATION WITH OTHER TECHNOLOGIES

This section briefly presents the main technologies integrated with NOMA and highlights the error rate analytical work. For instance, [11], [12], [151], [152], [153], [154], [155], [156], [157], [158], [159], [160], [161], [162], [163], [164] study optical communications, [165], [166], [167], [168], [169], [170], [171], [172], [173] study IRS and backscatter communications, [174], [175], [176], [177], [178], [179], [180], [181], [182], [183], [184], [185], [186], [187], [188], [189], [42], [190], [191], [192], [193], [194], [195], [196], [197], [198], [199], [200], [201], [202] study cooperative communications, [37], [203], [204], [205], [206], [207], [208], [209], [210], [211], [212], [213], [214], [215], [216], [217], [218], [219], [220], [221] study index modulation (IM), [50], [222], [223], [224], [225], [226], [227], [228], [229], [230], [231], [232], [233], [234], [235], [236], [237], [238], [239], [240], [241], [242], [243], [244] study SPC, and [245], [246], [247], [248], [249], [250], [251] study code-domain NOMA.

A. OPTICAL COMMUNICATIONS

VLC and FSO assisted NOMA systems fall under the umbrella of O-NOMA. A light source like an LED is used to transmit data while photodetectors are used at the receiver to convert the optical signal to electrical. VLC and FSO are considered promising technologies to improve the SER. Additionally, the transmission is highly secure as the light cannot penetrate through the walls, unlike RF signals. Thus, it is foreseen that combining VLC and FSO with NOMA will provide tremendous SE improvements to the communications system.

Fig. 9 depicts the basic structure of a DL cooperative O-NOMA with HD and FD relaying. In the figure, the system comprises a light source transmitter and two users. The near-user has generally a stronger channel than the far-user, and thus, it can act as a relay for the far-user signal. Moreover, it is typically assumed that the direct link between the transmitter and the far-user is either weak or completely absent. If there is a direct link, the O-NOMA symbols will be received by the near- and far-users. The transition process in cooperative networks is typically divided into phases, some phases are designated for initial transmission and the others are for relaying. In this case, the operation mode is denoted as HD. However, if both transmission and relaying are performed simultaneously, the operation mode is denoted as FD. A comprehensive summary of the O-NOMA work is shown in Table 13.

TABLE 13. Summary of the O-NOMA work.

[#]	Metric	Antennas	Direction	Application	M	N	Receiver	CSI
[151]	SER	MISO	DL	Indoor	$2^{\star}$	$\forall N$	Imperf. SIC	Perf.
[152]	BER	SISO	DL	Indoor	$2^{\star}$	$\forall N$	Imperf. SIC	Perf.
[11]	BER	SISO	DL	Indoor	$2^{\star}$	$\forall N$	Imperf. SIC	Imperf.
[153]	BER	SISO	DL	Indoor	$\leq 16^{*}$	2	Imperf. SIC	Perf.
[154]	BER	SISO	DL	Indoor	$\leq 16^{*}, \forall M, \forall M^{\bullet}$	2	Imperf. SIC	Perf.
[155]	SER	SISO	DL	Indoor	$\forall M$	2	Imperf. SIC	Perf.
[12]	BER	SISO	DL	Underwater	$2^{\star}$	2	Imperf. SIC	Perf.
[156]	BER	SISO	DL	Indoor	$2^{\star}$	$\forall N$	Sum and Sample SIC	Perf.
[157]	SER	SISO	DL	Indoor	$2^{\star} + \forall M^{\dagger}$	2	ML, MLD	Perf.
[158]	BER	SISO	DL	Indoor	4	2	Imperf. SIC	Perf.
[159]	BER	2×2	DL	Indoor	$2^{\star}$	3	MRC and SIC	Perf.
[160]	BER	SISO	DL	Indoor	$2^{\star} + \forall M^{\diamond}$	2	Imperf. SIC	Imperf.
[161]	BER	2×2	DL	Indoor	$2^{\star} + \forall M^{\diamond}$	2	MRC and SIC	Imperf.
[162]	BER	MIMO	DL	Indoor	$\forall M$	2	Imperf. SIC	Imperf.
[163]	BER	SISO	DL,UL	Indoor	2	2	Imperf. SIC	Perf.
[164]	BER	SISO	UL	Space	2	2	Imperf. SIC	Perf.

1) VLC

The error rate performance of DL-NOMA for VLC applications is considered in [11], [12], [151], [152], [153], [154], [155], [156], [157], [158], [159], [160], [161], [162], [163]. Huang et al. [151] attempt to characterize the SER by analytically deriving the SER expressions considering multiple LEDs, unipolar transmission and line-of-sight (LoS) optical channels that are corrupted by AWGN. The PDF of the optical channel is obtained using the change of variable method, while the SER derivation is simplified using convolution theory and subsection integral method. Marshoud et al. [152] derive closed-form BER expressions taking into account perfect and imperfect SIC. The work considers a single LED with an arbitrary number of users using unipolar OOK. Marshoud et al. [11] extend the work in [152] to consider noisy CSI as well as outdated CSI, where an approximation is derived for the former, while an upper bound is derived for the latter. Additionally, BER expressions are derived for analog and digital dimming control.

The authors of [153] derive closed-form BER expressions for two-user system considering imperfect SIC and a fixed set of M_n-PSK. The work is extended in [154] to consider modulation schemes such as QAM and PAM. Almohimmah and Alresheedi [155] derive exact closed-form SER for two-user scenario considering imperfect SIC and arbitrary square M_n-QAM. Similarly, Jain et al. [12] derive closed-form BER expressions considering OOK in underwater environments, where the channel is modeled as an exponential generalized gamma distribution. The system is analyzed and validated for parameters such as air bubble levels, gradient temperature and salinity level of the water.

The authors of [156] categorize the users in a cell based on their data rate requirements. Hence, they propose an adjustable bit-rate SC such that each user bit interval is multiple base intervals, where the base interval is the bit interval of the lowest bit rate. Unlike the conventional SIC, the sample-and-sum SIC is introduced to minimize the error propagation caused by the conventional SIC, where each user samples the SC signal at a certain sample rate. Then, these samples will be summed for decoding. Moreover, a modified fixed power allocation is proposed to provide some clear correlation between the effects of adjusting power coefficients and the BER performance. The authors derive closed-form BER expressions for the multiuser scenario with OOK. Furthermore, the authors of [157] propose using OOK for the low data rate user, while MPPM is assigned for the high data rate user. To overcome the error propagation, a SIC-free detector is proposed, where the MPPM user uses soft decision detector, whereas the OOK user sums the detected samples and uses MLD to detect its signal. A closed-form SER expression is derived for the OOK user, while a single-integral form SER expression is derived for the MPPM user. Furthermore, an asymptotic approximation for the probability of the number of erroneously detected slots in one MPPM symbol is derived.

For a two-user system, the authors of [158] propose adjusting the constellation of one user to improve the overall BER. Closed-form BER expressions are derived considering QPSK for both users, and the convexity of the objective function is proved as the Hessian matrix of the objective function is positive semi-definite. Furthermore, the Lagrangian is used to find the optimal constellation parameters, where the optimal parameters are presented for various SNRs.

Dixit and Kumar [159] analyze repetition code with multiple transmitting LEDs system, where MRC is used to combine the signals received by the multiple photodetectors. The BER is studied for the generalized multiuser case considering OOK and imperfect SIC. Additionally, closed-form expressions are derived for the three-user case.

Furthermore, Dixit and Kumar [160] consider a two-user case, where the near- and far-users are assigned OOK and M_n-PPM, respectively. The closed-form BER expressions are derived considering imperfect SIC as well as imperfect CSI. Moreover, this system model is extended for 2×2 MIMO with repetition coding and MRC in [161]. The BER is analyzed for imperfect SIC. Also, dynamic field of view strategies are proposed to control the incident angle of the optical signal in order to improve the performance.

Reference [162] studies the non-linear behavior of the LED in MIMO channels. To address this performance-limiting factor, a pre-distorter is designed using singular value decomposition-based Chebyshev precoding, which is applicable for correlated-channels scenario and arbitrary number of users. Additionally, CR-NOMA power allocation policy is introduced to satisfy the user's QoS requirements. Upper bound BER expressions are derived for square M_n-QAM considering Gaussian residual interference and imperfect CSI.

Reference [173] studies a hybrid RF-VLC NOMA system with physical layer network coding (PLNC). In the first phase, the two users transmit their RF signals to the BS using NOMA. In the second stage, the BS applies PLNC on the received signals and broadcasts an optical signal to both users. Assuming BPSK and considering imperfect SIC, an approximate BER expressions are derived for: 1) The first phase over Rayleigh fading. 2) The second phase over a VLC channel.

2) FSO

The authors of [164] analyze the BER performance of a unique 1-bit feedback based beamforming scheme and novel SIC detection for a 2×1 MISO UL FSO-NOMA system. The beamformer gives higher weights to the antenna with the higher channel gain, while the SIC decoding order is based on the 1-bit feedback to inform the receiver about the instantaneous channel gain order. Hence, the signal with the better channel gain is detected first. Considering subcarrier intensity modulation BPSK, the exact closed-form instantaneous BER expressions are derived, and asymptotic upper bound for the average BER are presented for negative exponential fading channels. In addition, an analytical framework is presented for the average BER. Furthermore, the impact of carrier synchronization errors, and the combined impact of atmospheric turbulence and pointing error are analyzed, and their average BER expressions are presented in integral-form.

B. IRS AND BACKSCATTER COMMUNICATIONS

1) IRS

References [165], [166], [167], [168], [169], [170], [171] study the performance of DL IRS-assisted NOMA system while considering imperfect SIC, a single antenna BS and single antenna users. Additionally, the system model considers that the IRS is divided into groups where each group is responsible for reflecting the signal to one user. A two-user system is considered in [165], [166], [170], [171] while more than two users are considered in [167], [168], [169]. The direct link between the base station and the users is assumed absent in [165], [166], [168], [169], [170], whereas it is assumed available in [167], [171]. Furthermore, the channel phases are shifted using the IRS to improve the SNR at the users while assuming perfect phase estimation and compensation. The authors of [165] consider QPSK and BPSK being assigned for the near- and far-users, respectively. The PDF of the end-to-end channel is based on Rayleigh fading, i.e., base station-IRS and IRS-user, is derived using the central limit theorem to approximate the sum of independent double Rayleigh random variables. However, this approximation is only accurate when a large number of metasurface elements are considered. The BER expressions are presented in a single-integral form using the moment generation function. Bariah et al. [166] present accurate BER approximations for a single metasurface element and multiple (> 10) metasurface elements, where the PDF of the end-to-end channel based on Rayleigh fading, i.e., base station-IRS and IRS-user, is derived. For example, an approximation of the double Rayleigh distribution is used for the single metasurface case, while the central limit theorem is used to approximate the end-to-end channel for the multiple (> 10) metasurface elements. The derived union bound of the PEPs provides a tight approximation of the BER for the two-user case with BPSK while considering various numbers of metasurface elements.

The authors of [167] study a multiuser IRS-assisted NOMA for the DL. Quadrature NOMA is proposed to maximize the diversity order such that the BS multiplexes the odd users using the in-phase component while the even users are multiplexed using the quadrature-phase components. Analytical expressions for the BER are derived over Rician fading channels. The authors of [168] study IRS-NOMA for indoor applications. Exact and asymptotic closed-form BER expressions over the generalized $\kappa - \mu$ fading channels are derived. The BER performance of a simultaneously transmitting and reflecting intelligent reflecting surface (STAR-IRS)-NOMA network has been analyzed in [169]. A mode-switching protocol is employed to facilitate communication between a BS and multiple NOMA users located on either side of it. Closed-form expressions for the BER are derived, for covering both perfect and imperfect SIC scenarios.

Aldabasah et al. [170] study the BER performance considering BPSK where the PDF of the end-to-end channel is derived considering Nakagami-m fading channels. The resulting distribution is approximated to a gamma distribution and it is valid for arbitrary number of metasurfaces. Rito and Li [171] apply alignment techniques to IRS-based DL-NOMA systems. By supporting one user only, the proposed interference cancellation technique enhances the signal for one of the users without degrading the other user's channel. On the other hand, the proposed interference alignment technique allows constructive interference in the channel by 1) dividing the IRS into two parts, 2) aligning the phases of each part to support either user, 3) rotating all phases in the

TABLE 14. Summary of the IRS and backscatter communications work.

[#]	System	Metric	Antennas	Direction	Channel	M	N	Receiver	CSI
[165]	IRS	BER	SISO	DL	Rayleigh	$4+2$	2	Imperf. SIC	Perf.
[166]	IRS	PEP	SISO	DL	Rayleigh	$\forall M$	2	Imperf. SIC	Perf.
[167]	IRS	BER	SISO	DL	Rician	2	4	Imperf. SIC	Perf.
[168]	IRS	BER	SISO	DL	κ-μ fading	4	3	Imperf. SIC	Perf.
[169]	IRS	BER	SISO	DL	Rayleigh	2	$\forall N$	Imperf. SIC	Perf.
[170]	IRS	BER	SISO	DL	Nakagami-m	2	2	Imperf. SIC	Perf.
[171]	IRS	SER	SISO	DL	Rayleigh, Rician	$\forall M$	2	Imperf. SIC	Perf.
[172]	Backscatter Comm	BER	SISO	UL	Nakagam-m	2	2	Imperf. SIC	Perf.
[173]	Backscatter Comm	BER	SISO	PLNC	Exponential	2	2 pairs	JMLD	Perf.

two parts to allow constructive interference between the two parts. Approximate SER expressions of both techniques are derived for the MLD while assuming adjacent symbols errors and M_n-QAM. The end-to-end channel is approximated as gamma distribution since the BS-IRS channels are modeled as Rician distribution, and the BS-users and IRS-users channels are modeled as Rayleigh distribution.

Generally speaking, the error rate analysis of the IRS-based NOMA follows the conventional NOMA except that modeling the end-to-end channel is considered challenging due to the cascaded nature of the IRS channels, which can be heterogeneous in the presence of the direct link. The analysis becomes further complicated when considering imperfect phase estimation and discrete phase compensation.

2) BACKSCATTER COMMUNICATIONS

The authors of [172] study the performance of the UL bistatic backscatter communications-aided NOMA for IoT sensors. Two backscatter nodes are co-located near the carrier emitter assuming interference-free channels. The backscatter nodes operate in two modes, namely the EH mode and the active mode, in which performing intentional impedance mismatch at the antenna input, produces two reflection coefficients to modulate the carrier signal with BPSK. The Nakagami-m fading channel multiplexes the modulated BPSK symbols in the power domain using NOMA. The backscatter reader receives the NOMA symbol and performs SIC for detection. As the analysis of such a problem is challenging, closed-from BER expressions are derived by ignoring the phases of the channels between the backscatter nodes and the backscatter reader. Also, the channels are assumed to be ordered, however, order statistics are not used. Rather than considering double-integration with respect to the Nakagami-m fading coefficients, the sum and difference of the fading coefficients are approximated by another Nakagami-m random variables.

The authors of [173] study the BER performance of a backscatter-assisted NOMA with PLNC. The system model under study considers two clusters and two users per cluster, namely the near and far clusters which want to exchange data. Hence, PLNC is used, where the near cluster pair and the far cluster pair transmit their data to the access point using UL-NOMA in two time slots. Once these symbols are detected using JMLD, PLNC performs exclusive OR operations and sends the PLNC symbols using DL-NOMA in the third time slot. Then the users in each cluster use SIC to detect the symbols. Upper bound BER expressions are derived for the end-to-end system using BPSK and exponential channel. It is worth mentioning that the ambient backscatter is located near the far cluster pair and is only used during the third time slot. A comprehensive summary of the NOMA work with IRS and backscatter communications is given in Table 14.

C. COOPERATIVE COMMUNICATIONS

NOMA naturally aligns with the concept of cooperative communications due to the dependence of both technologies on the distance between various nodes. In cooperative NOMA, strong users cooperate with weak users to improve their SNR by relaying their signals. Fig. 10 depicts the basic structure of a two-user DL cooperative NOMA with HD and FD relaying. The near-user has generally a stronger channel than the far-user, and thus, it can act as a relay for the far-user signal. Moreover, it is typically assumed that the direct link between the BS and the far-user is either weak or completely absent. If there is a direct link, the NOMA symbols will be received by the near- and far-users. The transition process in cooperative networks is typically divided into phases, some phases are designated for initial transmission and the others are for relaying. In this case, the operation mode is denoted as HD. However, if both transmission and relaying are performed simultaneously, the operation mode is denoted as FD.

Cooperative NOMA generally follows OMA, where near-user can adopt AF or DF relaying. The system model for the AF model closely follows OMA, where the relay simply amplifies and forwards the NOMA symbols to the far-user. In the case of DF, the scenario is different because the near-user has to detect the symbols of the both users before re-modulation and transmission. However, since part of the signal belongs only to the near-user, then there is no need to forward this part of the signal to the far-user. Therefore, as shown in Fig. 10, the near-user extracts its own symbols using SIC, and forwards only the signal that corresponds to the far-user. It is also possible to use more efficient designs, where the data forwarding process is designed to be

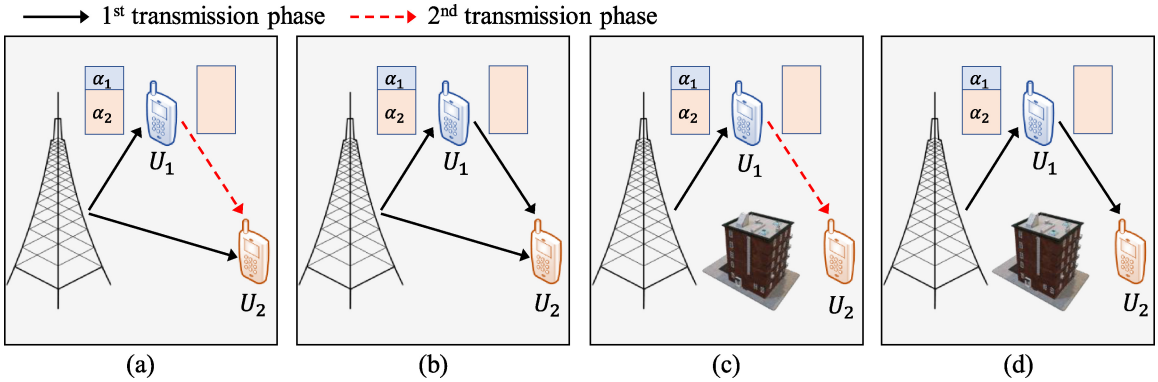

FIGURE 10. Basic DL cooperative NOMA; (a) HD relaying and direct link, (b) FD relaying and direct link, (c) HD relaying without direct link, (d) FD relaying without direct link. The near-user can be a dedicated or a user relay.

conditional on the SINR at the near-user. Therefore, the symbols are forwarded only if the SINR exceeds a predefined threshold.

At the far-user, the receiver design depends on the received signal from the BS and relay. For example, if the direct link exists, and HD-AF is adopted, then the receiver can combine the two signals using a particular combining scheme such as MRC or selection combining (SeC). In the case of DF, the two received signals can still be combined because the far-user power is much larger than the near-user power, which can be considered an additive noise. Finally, the combined signal is applied to a single-user MLD to recover the transmitted data symbols. If no direct link exists between the BS and far-user, then the relayed signal is directly applied to a single-user MLD regardless of the relaying mode. In the case that energy harvesting is considered, the relay can use the energy harvested from the received NOMA signal for cooperation. Therefore, the relay splits the received signal into two segments: 1) for energy harvesting, 2) for signal forwarding process. In cooperative CR NOMA, multiple relays can be considered. Consequently, multiple relays are used to assist the transmission between the secondary BS and secondary usurers.

Literature Review of Cooperative NOMA: Besides the fundamental cooperative NOMA schemes, considerable efforts have been devoted to developing enhanced cooperative NOMA systems for a wide range of applications. A comprehensive summary of the NOMA work with cooperative communications is depicted in Table 15 including the relaying mode and number of relays. Moreover, a cooperative relaying system (CRS) with multiple relays assisting a single-user and a single relay assisting multiple users is shown in Fig. 11.

1) COOPERATIVE NOMA WITH DEDICATED RELAYING

Kara and Kaya [174], [175], consider a diamond-shaped CRS based on NOMA, with two HD-DF relays and a single destination. It is assumed that one relay is located at a far distance from the source, while the other relay is located closer. The transmission is accomplished in two time slots. During

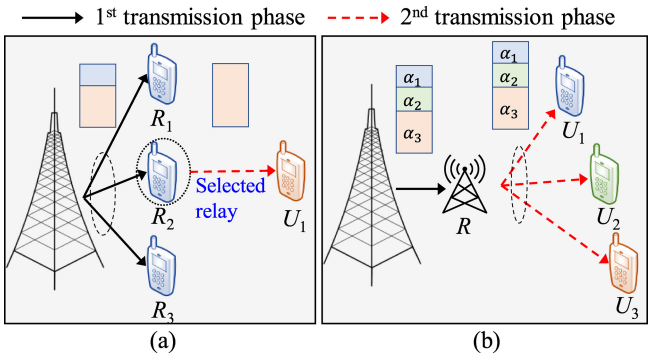

FIGURE 11. CRS system; (a) Multiple relays assisting a single-user, (b) A single relay assisting multiple users.

the first time slot, the source transmits a NOMA symbol of two BPSK modulated signals to both relays. The far relay employs single-user MLD, whereas the near relay uses SIC. In the second time slot, both relays use the UL-NOMA concept to forward the detected information to the destination. Finally, the signal received from the near relay is detected by the destination, while the signal received from the far relay is detected using SIC. For both time slots, the authors derive the BER over a SISO Rayleigh fading channel. Moreover, Kara and Kaya [176] consider a two-user DL-CRS with a single HD-DF relay located closer to the near-user, where no direct link exists between the users and BS. In the first time slot, the PA is applied in a reversed order, i.e., the power allocated to the near-user is larger than the power allocated to the far-user. However, the PA in the second time slot follows the conventional approach. It is worth noting that the SIC decoding order depends on the PA. Exact closed-form BER expression is derived for identical QPSK with imperfect CSI over Rayleigh fading channels.

Kara et al. [177] propose using NOMA for a single-user CRS to overcome the SER degradation inherent to HD mode. In the proposed model, the source multiplexes two consecutive symbols as a NOMA symbol, where the first symbol x_1 is treated as the near-user, and thus it is allocated less power than the second symbol x_2, the NOMA symbol is then transmitted to a HD-DF relay and to the destination. During

TABLE 15. Summary of cooperative SISO NOMA.

[#]	System	Mode	Metric	Direction	Channel	M	N	R	Receiver	CSI
[174], [175]	CRS	HD,DF	BER	DL,UL	Rayleigh	2	1	2	Imperf. SIC	Perf.
[176]	CRS	HD,DF	BER	DL	Rayleigh	4	2	1	Imperf. SIC	Imperf.
[177]	CRS	HD,DF	BER	DL	Nakagami-m	≤ 4	1	1	Imperf. SIC	Perf.
[178]	CRS	HD,AF	PEP	DL	Rayleigh	2	$\forall N$	1	Imperf. SIC	Perf.
[179]	CRS	HD,DF	BER	DL	Rayleigh	2	2	R	Imperf. SIC	Perf.
[180]	CRS	HD,AF	SER	UL	Rayleigh	4	2	1	Imperf. SIC	Perf.
[181]	CRS	HD,DF	BER	DL	Rayleigh	2	2	1	Imperf. SIC	Imperf.
[182]	CRS	HD,DF	BER	UL	Rayleigh	$2, 4$	2	R	ML	Perf.
[183]	CRS	HD,DF	SER	DL	Shadowed Rician	$2, 4$	2	1	Imperf. SIC	Perf.
[184]	CRS	HD,DF	BER	DL	AWGN	2	2	1	Imperf. SIC	Perf.
[185]	CRS	HD,DF	BER	DL	Rayleigh	2	2	1	MRC-Imperf. SIC	Imperf.
[186]	CRS	HD,DF	BER	DL	Rayleigh	$4, 16$	2	1	MRC-Imperf. SIC	Perf.
[187]	CRS	HD,DF	BER	DL	Rayleigh	$4 + 2$	2	1	MRC-Imperf. SIC	Stats.
[188]	CRS	HD,DF	BER,PER	DL	Nakagami-m	2	4	2	Imperf. SIC	Perf.
[189]	CRS	FD,DF	PEP	DL	Rayleigh	2	2	1	Imperf. SIC	Perf.
[190]	CRS	FD,DF	PEP	DL,UL	Nakagami-m	$4 + 2$	2	1	Imperf. SIC	Perf.
[191]	CRS	FD,DF	BER	DL	Rayleigh	$\forall M$, $M^{\bullet}$	2	1	Imperf. SIC	Stats.
[192]	SWIPT	HD,AF/DF	PEP	DL	Rayleigh	2	2	1	Imperf. SIC	Perf.
[193]	SWIPT	HD,AF	PEP	DL	Rayleigh	4	$\forall N$	1	Imperf. SIC	Perf.
[194]	SWIPT	HD,DF	BER	DL	Nakagami-m	2	1	1	Imperf. SIC	Perf.
[195]	SWIPT	HD,DF	BER	DL	Nakagami-m	2	2	1	Imperf. SIC	Perf.
[196]	SWIPT	HD,AF	PEP	DL	Rayleigh	2	$\forall N$	N	Imperf. SIC	Perf.
[197]	SWIPT	HD,AF	PEP	DL	Rayleigh	2	$\forall N$	R	Imperf. SIC	Perf.
[198]	CR	HD,AF	PEP	DL	Rayleigh	4	$\forall N$	R	Imperf. SIC	Perf.
[199]	CR	HD,DF	BER	UL,DL	Rayleigh	4	2	1	Imperf. SIC	Perf.
[200]	CR	HD,DF	BER	DL	Rayleigh	2	2	R	Imperf. SIC	Perf.
[201]	CR	HD,DF	BER	DL	Nakagami-m	2	2	1	Imperf. SIC	Perf.
[202]	VLC	HD,DF	BER	DL	Non-fading	$2^{\star}$	$\forall N$	$N - 1$	MRC-Imperf. SIC	Perf.
[42]	VLC	AF-DF	BER	DL	Gamma-Gamma	2	2	2	Imperf. SIC	Perf.

the first time slot, the destination detects only x_2 while treating x_1 to be in the noise floor. The relay detects x_1 using SIC and forwards it to the destination in the second time slot. Exact closed-form BER expression is derived for BPSK over Nakagami-m fading channels. Further, the authors propose a machine learning PA algorithm to minimize the BER.

The RHIs of a multiuser DL-NOMA CRS that consists of a single HD-AF relay is studied in [178]. The users are considered to be within close proximity of each other, and they do not have a direct link with the BS. Assuming imperfect SIC, PEP expressions are derived over ordered Rayleigh fading channels. In [179], a two-user DL-NOMA CRS with R HD-DF relays is investigated, with each user having a dedicated relay that is selected based on a max-min criterion. It is assumed that no direct link exists between the BS and users. The far-user, which is a high-priority user, applies MLD for detection, while the near-user, which is a delay-tolerant user, applies SIC for detection. The average BER expressions are derived for BPSK over Rayleigh fading channels. In [180], a two-user UL-NOMA CRS with a single HD-AF relay is studied, where both users are at the cell edge and no direct link exists with the BS. In the first time slot, both users transmit their signals to the relay using UL-NOMA. In the second time slot, the relay applies linear noise reduction to the NOMA signal, the signal is then amplified and transmitted to the BS, which uses SIC for detection. Approximate SER is derived analytically which is accurate at high SNRs.

In [181], a two-user DL cooperative NOMA is investigated. The users and the relay have a single antenna each. Moreover, the relay operates in HD mode. The BER expressions are derived assuming Rayleigh fading channels between the transmitter and receivers, with BPSK modulation, imperfect CSI, and imperfect SIC. Althunibat et al. [182] study a two-way relaying system that improves the spectral efficiency by allowing two users to exchange data bi-directionally through two intermediate HD-DF relays in a PLNC fashion. In particular, during the first time slot, each user sends its DL-NOMA intended to the two relays. Consequently, the signals received at the relays follow the UL-NOMA principle. Each relay performs JMLD to detect its signals from the two users and combine them following PLNC principle. During the second time slot, the relays send the PLNC signal to the users following the UL-NOMA principle. Finally, given that each user knows its transmitted signals, it can detect the other user's signal using JMLD. The authors derive closed-form BER expressions

over Rayleigh fading channels. The authors of [183] study a DL-NOMA CRS for hybrid satellite-terrestrial communication. During the first time slot, the satellite transmits to a ground destination and a ground relay. During the second time slot, the ground DF relay simultaneously transmits to the ground destination and a cellular user using DL-NOMA. Assuming imperfect SIC and co-channel interference, the authors derive closed-form SER expressions over shadowed Rician fading channels.

The author of [184] analyzes a two-user DL-NOMA CRS with a HD-DF serving both users. While considering all links to be available and imperfect SIC, closed-form BER expressions are derived for the linear combiner over AWGN channels. Reference [185] considers a similar model to [184] but imperfect CSI is assumed. Both the exact and asymptotic closed-form BER expressions are derived for the Rayleigh fading channels.

2) COOPERATIVE NOMA WITH USER RELAYING

Kara and Kaya [186] study the BER of a two-user DL cooperative NOMA system, where the near-user acts as an opportunistic HD-DF relay for the far-user, forwarding the detected symbols of the far-user if the SINR is greater than a predefined threshold. Assuming that the direct link between the BS and the far use exists, the far-user uses MRC to combine the two signals received from the BS and the relay. Closed-form BER expressions are derived for both users over SISO Rayleigh fading channels assuming M_n-QAM. It is worth noting that the analysis for the near-user is performed considering imperfect SIC. Furthermore, the optimum threshold that minimizes the BER is derived. By relaxing the threshold condition for relaying, the work in [187] derives the BER expressions, where QPSK and BPSK are used by the near- and far-user, respectively.

Jain et al. [188] study the performance of a DL-NOMA CRS that consists of two cell edge users, each of which is assisted by a HD-DF user. The near-far problem is considered such that the relays do not interfere with each other. The near-relay uses SIC for detection, while the far relay uses MLD. The system considers that there is no direct link between the BS and cell-edge users. The authors derive the average BER over Nakagami-m fading channels and present instantaneous PER expressions. The analysis of two-user DL-NOMA CRS is provided in [189], where the near-user acts as a FD-DF for the far-user, which has no link with the BS except through the relay. The relay receives a NOMA signal from the BS for both users and the self-interference signal caused by the FD mode. Both users detect their corresponding signals using SIC. The authors analyze the PEP of the system for both users over Rayleigh fading channels, assuming MLD at the far-user and imperfect SIC at the near-user. In addition, an asymptotic analysis is performed for both users at high SNRs. The analytical expressions are validated for the BPSK case. Sashiganth et al. [190] considered a system model similar to [189] except that UL is also included and the BER is presented in the form of approximation.

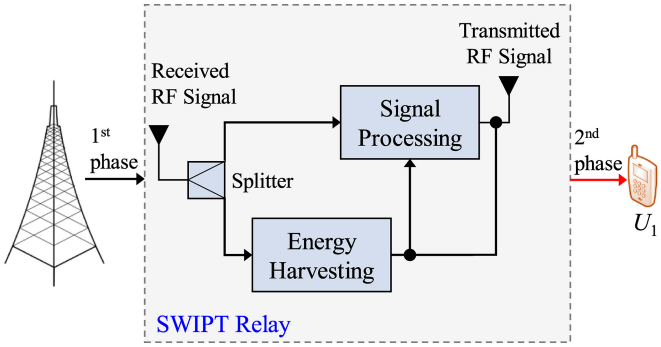

FIGURE 12. Cooperative NOMA with SWIPT-enabled relay.

Reference [191] explores the BER performance of FD cooperative NOMA systems over Rayleigh fading channel. The exact BER expressions are derived, accounting for imperfect SIC and residual self-interference (RSI). The system consists of a BS and a far-user, both with a single antenna, as well as a near-user utilizing multiple antennas to act as a relay in a DF-FD mode. Notably, different modulation schemes, including BPSK for the far-user and QPSK for the near-user. Also, M_n-PAM and M_n-QAM are considered for a comprehensive analysis.

3) SWIPT-BASED CRS

Similar to the system model in [186], [187], the authors of [192] consider the near-user to be a SWIPT-enabled relay for the far-user, where the link between the BS and far-user does not exist. The proposed model is shown in Fig. 12. The union bound on the PEPs over ordered Rayleigh fading channels is derived for the near- and far-user while taking the AF and DF relaying protocols into account. It is worth noting that the analytical results are validated only for BPSK. Moreover, the authors of [193] extend the work to N users, while assuming AF relay. Closed-form PEP expressions are derived over Rayleigh fading channels. In [194], a cooperative NOMA system with SWIPT-enabled relay is investigated. The system model generally follows the one in [177] except that the relay harvests energy from the received NOMA signal during the first phase. Closed-form average BER is derived for BPSK modulation. In addition, machine learning is used to optimize the power sharing-power allocation to minimize the BER. Khennoufa et al. [195] study a cooperative DL-NOMA with EH, where the DF relay harvests the energy from the RF transmitted from the BS. Closed-form BER expressions over Nakagami-m fading channels are derived for a hybrid EH, i.e., power-time splitting, and EH techniques including time-splitting and power-splitting.

A SISO cooperative DL-NOMA for N SWIPT-enabled HD-AF relays and N users is proposed in [196]. The relays harvest energy from the received NOMA signal for a certain time, whereas the residual time is used to amplify and transmit the signal to the users. The exact and approximate PEP

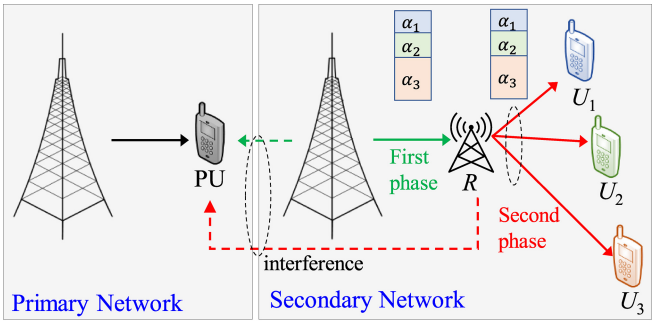

FIGURE 13. A CR-based DL-NOMA proposed in [198].

expressions are derived for all users. In [197], the cooperative NOMA is investigated, where a single SWIPT-enabled relay from the total of R relays is selected during the broadcast phase for cooperation between the transmitter and N users. The relay is selected based on the channel quality between the transmitter and the corresponding relay. Each relay is assumed to operate in HD mode using the AF protocol. Rayleigh fading channel is considered for all links. The work derives an exact PEP expression assuming an imperfect SIC.

4) CR-BASED COOPERATIVE RELAYING

In [198], an underlay CR scenario in a SISO cooperative DL-NOMA is presented. As shown in Fig. 13, the system under consideration is composed of a primary and secondary BSs, as well as one primary and N secondary users served by R AF relays. Transmission power constraints are enforced on the secondary BS and a single selected relay to maintain a tolerable level of interference to the primary network. Accurate PEP expressions are derived and used to evaluate the BER union bound. Üstünbaş and Aygölü [199] propose a cooperative NOMA-based CR butterfly network. The system comprises a primary and secondary transmitters and receivers, and a single relay. The primary transmitter and secondary receiver share a cell, whereas the secondary transmitter and primary receiver share a different cell. During the first time slot, the QPSK modulated symbols are received simultaneously by the relay and nearby receivers. The relay uses MLD to directly detect the secondary transmitter signal, whereas the primary transmitter signal is obtained through SIC. In the second time slot, the relay generates a NOMA symbol from the detected symbols and forwards it to both receivers. Both receivers recover their respective symbols using SIC and MLD. The authors analyzed the BER performance for both users using QPSK modulation and while assuming imperfect SIC.

A two-user cooperative CR based NOMA is presented in [200]. Assuming there is no direct link between the BS and far-user, the communication is established through a single selected HD-AF relay from the R available ones. The NOMA signal is received by the relays and near-user, where the near-user detects its own signal using SIC. Meanwhile, the relay with the maximum SNR with respect to the far-user is selected for cooperation. In the next round, the selected relay forwards the far-user signal through controlled power to avoid interference with the near-user. Exact closed-form BER expression is derived over SISO Rayleigh fading channel for BPSK assuming perfect CSI at the relays. To preserve the near-user QoS, [201] proposes a cooperative spectrum sharing mechanism based on NOMA, where the secondary transmitter cooperates with the primary to achieve full rate through cooperative multiplexing. Under the assumption of perfect CSI, the proposed system is analyzed in terms of average BER for BPSK. A closed-form expression for the BER is obtained through series expansion and numerical integration. Hence, the obtained expression are found to be an accurate approximation for the BER.

5) VLC-BASED COOPERATIVE RELAYING SYSTEM

The authors of [202] study a multiuser cooperative VLC-NOMA. The LED broadcasts the OOK modulated NOMA signal through non-fading channels to N users. The users perform SIC to detect the individual signals. Therefore, the nearest user has to detect the signals of all other users, while the farthest user detects only its own signal. The second round is composed of $N-1$ time slots during which each user forwards the detected signals of other users. The cooperation ensures the link reliability for the far-users. Furthermore, the far-users use MRC and SIC to detect their desired signals. The exact BER of the proposed model is derived under the assumptions of perfect CSI and imperfect SIC.

In [42], the BER of an optical backhauled three-hop cooperative NOMA is derived. The first hop is from the source to the first relay, which is realized using FSO. The second hop between the first and second relay is realized using RF, and finally, the third hop to the end-user is performed using VLC. The RF node acts as an AF relay and the VLC node acts as a DF relay. The adopted system model and performance analysis consider various impairments such as fading caused by the atmospheric turbulence, pointing errors, pathloss, photodiode responsitivity, and AWGN. The BER is evaluated only for a two-user NOMA using BPSK modulation.

Although some work has been conducted to evaluate the error rate of cooperative NOMA networks with some practical constraints such as the imperfect SIC and CSI, most of the reported work is limited to the two-user scenario with low modulation orders. Deriving the error rate for a more generalized scenario where the number of users is more than two and higher order M_n-QAM is generally challenging because the number of cases that have to be considered is massive, particularly when MIMO is incorporated.

D. INDEX MODULATION

IM improves the SE of the communication system by transmitting extra information through the index of the communication resource which could be an antenna, subcarrier or time slot, etc. In such a scheme, the transmitted bit stream is partitioned into two groups, one is mapped to the index

TABLE 16. Summary of conventional spatial modulation (SM) work.

[#]	System	Metric	Antennas	Channel	M	N	Receiver	CSI
[37]	SSK-NOMA	BER,PEP	MIMO	Rayleigh	4	3	MRC-Imperf. SIC	Perf.
[203]	SSK-NOMA	BER,PEP	MIMO	Rayleigh	≤ 4	2	MRC-MLD	Imperf.
[204]	Precoded SM	SER	MIMO	Rayleigh	$\leq 4, 8$	2	Imperf. SIC	Perf.
[205]	SM-NOMA	PEP	MIMO	Rayleigh	4	$\forall N$	Imperf. SIC	Perf.
[206]	SM-NOMA	SER	MIMO	Rayleigh	4	$\forall N$	Imperf. SIC	Perf.

of the activated communication resource, and the other is mapped to a conventional constellation symbol transmitted via the activated communication resource.

1) SM

SM is widely considered as a low-complexity, hardware-efficient and energy-efficient MIMO scheme due to the fact that a single antenna is primarily activated during a transmission. Therefore, one RF chain is required, hence it is hardware efficient, and consequently, the system complexity and energy consumption are reduced. Additionally, SM can be the enabling technology for FD relaying, as one antenna can be the transmitting relay, while the remaining antennas are utilized for reception.

Incorporating SM into NOMA systems can improve the SE without increasing power consumption and implementation complexity. Additionally, while SM systems suffer substantially from IUI, this can be mitigated through NOMA. Thus, combining SM and NOMA leverages the benefits of both schemes. To explain the basic principle of SM-based cooperative NOMA, consider a system with a single transmitter and two users, with the near-user acting as a relay for the far-user, as shown in Fig. 14. The transmitter, relay-user, and far-user each have multiple antennas. The transmission time is divided into two phases if the relay follows the HD protocol, whereas the transmission can be accomplished in a single round if the relay is operated in FD mode. During the first phase, the transmitter broadcasts the SM symbol, which is simultaneously received by the relay and the far-user. The SM symbol is defined as $[0, 0, \ldots, 0, s, 0, \ldots, 0, 0]^T$, where s is the modulated symbol and its location in the vector corresponds to the active antenna index. The relay node employs MLD to produce an estimated $\hat{s}$ for the active antenna index. The relay node then recovers its own data bits from $\hat{s}$. Finally, the relay node forwards the preserved active antenna index in the second phase. Following that, the far-user combines the signal transmitted by the relay-user during the second phase with the signal received from the transmitter during the first phase. The far-user applies MLD to the combined signal to detect its own signal.

State-of-the-Art SM-NOMA: References [37], [203], [204], [205], [206] study SM-NOMA considering DL-MIMO Rayleigh fading channels. Table 16 provides a summary of the work in this part.

Kara and Kaya [37] study the multiuser case in which the users are divided into multiple groups, where the BS communicates with each group within an orthogonal resource block.

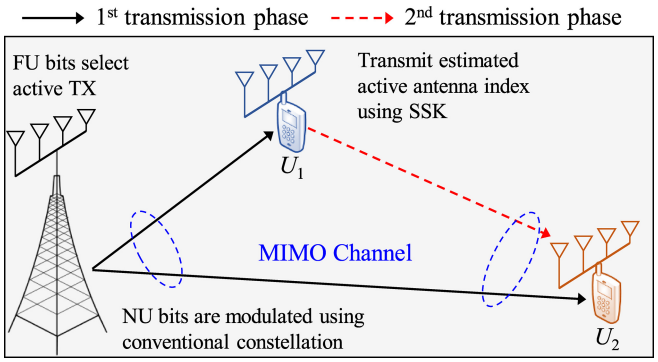

FIGURE 14. SM-NOMA proposed in [208], where FU stands for far-user and NU stands for near-user.

It is assumed that full CSI is available at the receivers, but not at the transmitter. In accordance with SM, the cell edge user's bits are modulated using the index of the activated antenna, whereas the rest of the users' bits are modulated using conventional modulations. The cell edge user performs optimal MLD-based SM detection to detect the index of the transmitting antenna, whereas the other users perform MRC-SIC to detect their own signal. Closed-form BER expressions are derived for the three-user case, while PEP is derived for more than three users. A special case of two-user is treated in [203]. Similarly, [204] considers a two-user case with pre-coded spatial modulation (PSM), where the proposed system employs an efficient power allocation scheme to share all the antennas for DL transmission. The authors derived SER expressions considering imperfect SIC.

The authors of [205] propose a generalised pre-coding quadrature spatial modulation (GPQSM)-NOMA considering N user. The BS generates a NOMA signal using the corresponding normalized powers and the zero-forcing precoding values. The authors propose a low-complexity detection method and derive its PEP expressions. The authors of [206] propose using multiple antennas to broadcast multiple users signals using SM-NOMA with optimal power allocations. To minimize IUI, a complicated SIC technique is employed at the receiver end to detect the signals. The SER for all users using point-to-point M_n-PSK is derived considering imperfect SIC. The resulting SER expressions are used for PA optimization to minimize the average SER for all users.

State-of-the-Art SM-NOMA with CRS: Si et al. [207] study a two-user cooperative SM-NOMA system. Assuming MIMO settings with SM at the BS and the FD relay, simultaneous reception and transmission is enabled at the

TABLE 17. Summary of SM with DL CRS work under perfect CSI conditions.

[#]	Mode	Metric	Antennas	Channel	M	N	R	Receiver
[207]	FD,DF	PEP	MIMO	Rayleigh	$2, 8$	2	1	MLD
[208]	HD,DF	PEP	MIMO	Rayleigh	$\forall M^{\bullet}$, $\forall M$	2	1	MRC-JMLD
[209]	HD,DF	BER	SISO	Rayleigh	2	1	R	Imperf. SIC
[210]	HD,DF	PEP	MIMO	Rayleigh	≤ 8	2	1	Imperf. SIC
[211]	HD,DF	PEP	SIMO	Rayleigh	$2, 4, 16$	$\forall N$	1	Imperf. SIC

relay. A portion of the far-user information bits are used to select the transmitting antenna, while the remaining information bits are applied to the conventional constellation. Afterwards, the BS broadcast the SC signal through the activated antenna, which is then received by the near-user and the relay. The near-user performs SIC to detect its signal, while the relay preserves the signal till the next time slot. The relay receives a new signal from the BS in the next time slot and simultaneously forwards the previous signal to the far-user who in turn uses MLD to detect the received signal. Closed-form PEP expressions are derived for both users under Rayleigh fading, and perfect and imperfect SIC assumptions. The results conclude that the proposed system outperforms MIMO-NOMA with FD relaying and SM-OMA with HD relaying systems.

Furthermore, Li et al. [208] considers the HD mode in which the first time slot includes broadcasting the SM vector by the BS. The near-user receives the SM vector from the BS and tends to detect its own signal and the active antenna index using JMLD. In the second time slot, the near-user acts as a relay by forwarding the active antenna index to the far-user through an space shift keying (SSK) signal. The far-user combines the realizations received from the BS during the first time slot and the near-user during the second time slot. Following that, it recovers its own symbols from the combined signal using MLD. The authors derive closed-form PEP expressions of the proposed system over Rayleigh fading channels.

Reference [209] proposes a distributed SM aided cooperative NOMA, in which the transmitter communicates with a single destination through a relay selected from a pool of R relays. During the first time slot, the transmitter broadcasts a two-user NOMA signal. The relays perform SIC to detect the individual signals, whereas the users only detect strong signal, while the detection of weak signal is postponed until the second time slot. During the second time slot, each relay compares the weak signal it detects to its own unique identity. The relay whose identity matches the weak signal is chosen to transfer data to the destination. The destination jointly detects the realizations received over two time slots. The authors proposed an error-aware MLD at the destination and provided a BER analysis for the proposed system with phase shift keying (PSK)/QAM modulation.

In [210], a cooperative generalized quadrature SM-NOMA is investigated for a two-user scenario in a vehicular network, where the near-user acts as a relay to the far-user. In this scheme, the transmitted bits are divided into three groups: one group is applied to a conventional modulator, and the other two are applied to antenna activation for the real and imaginary parts of the modulated signal vector. The received SM signal is recovered through JMLD. Using a simplified approximation of the complex Q-function, the conditional PEP is derived considering PAM and QAM.

Can et al. [211] investigate a DL-CRS-NOMA considering N users and a DF relay. In the first time slot, SM-based media-based modulation (MBM) technique is used for transmission to the relay to improve the BER. Such technique relies on a single transmitting antenna and multiple RF mirrors at the BS and multiple receiving antennas at the relay. In this method, the transmitted bits are partitioned into two groups, the first of which is used to select the active channel state, while the remaining ones are mapped to M_n-QAM constellation. Assuming a perfect CSI the relay can jointly detects the active channel state index and the M_n-QAM symbol using JMLD. In the second time slot, the relay combines the users M_n-QAM symbols in a NOMA symbol and forward it to all the users, where the users perform SIC to detect their desired signals. Closed-form PEP expressions are derived over Rayleigh fading channels. Table 17 provides a summary of the work in this part.

2) IM-OFDM/TDMA/CDMA/PD

State-of-the-Art NOMA-based IM-OFDM: Chen et al. [212] study a two-user cooperative NOMA-based IM-OFDM system. During the first time slot, the BS transmits the IM-OFDM information in a NOMA fashion to both users. The near-user performs SIC to detect its signal, while the far-user retains the received signal till the next slot. During the second time slot, the near-user acts as a relay and forwards the far-users signal. The far-user uses MRC-MLD to combine the signals received in the two time slots and detect its desired signal. Tight closed-form upper bound BER expressions are derived for both users over Rayleigh fading channels. Furthermore, Chen et al. [213] extend the work presented in [212] by proposing a low-complexity greedy detector, where they present tight closed-form upper bound BER expressions.

The authors of [214] derive the PEP of a DL two-user IM-OFDM-NOMA system over Rayleigh fading channels considering. Assuming the far-user symbols embedded in the indices of the activated subcarriers as well as the NOMA signal, the far-user performs JMLD to jointly detect its data from the OFDM signal and the indices of the active subcarrier. The near-user on the other hand performs SIC to

TABLE 18. Summary of the IM-OFDM/TDMA/CDMA/PD work.

[#]	System	Metric	Antennas	Direction	Channel	M	N	Receiver	CSI
[212]	IM-OFDM	PEP	SISO	DL	Rayleigh	$\leq 16^*$	2	Imperf. SIC	Perf.
[213]	IM-OFDM	PEP	SISO	DL	Rayleigh	$\leq 16^*$	2	Greedy detector	Perf.
[214]	IM-OFDM	PEP	SISO	DL	Rayleigh	2	2	Imperf. SIC	Perf.
[215]	IM-OFDM	PEP	SIMO	UL	Rayleigh	$\forall M, M^*$	$\forall N$	JMLD	Imperf.
[216]	IM-OFDM	BER	SISO	UL	Rayleigh	2	2	MRC	Perf.
[217]	IM-SC-FDMA	PEP	SISO	UL	Rayleigh	2	2	JMLD,Imperf. SIC	Perf.
[218]	IM-OFDMA	PEP	SISO	DL	Rayleigh	$\forall M^*$	$\forall N$	JMLD	Stats.
[219]	IM-TDMA	PEP	SISO	UL	Rayleigh	$\forall M^*, \forall M$	$\forall N$	JMLD	Perf.
[220]	CPI-SCMA	PEP	SISO	UL	Rayleigh	≤ 4	$\forall N$	JMLD	Perf.
[221]	IM-PD	PEP	SISO	UL	Rayleigh	$\forall M^\bullet$	2	Imperf. SIC	Perf.

detect its own signal. Furthermore, the authors of [215] consider N users in UL with SIMO settings. Assuming a single active subcarrier, closed-form PEP expressions are derived over Rayleigh fading channels considering JMLD for all users.

Doğan et al. [216] propose an IM-OFDM-NOMA system to reduce the impact of collision in GFA for ultra-reliable low latency communication (URLLC). Assuming a delay-sensitive user and a delay-tolerating user, the former is allowed GFA which results in collisions between the two users. Therefore, to alleviate the adverse effects of collisions, the users are multiplexed through IM-OFDM. To obtain the frequency-domain signal for the delay-sensitive user, a portion of the bits are mapped to the standard constellation, which is then transmitted to the BS via a Rayleigh fading channel. To improve the delay-sensitive user's SNR, the NOMA signals received over multiple transmissions are combined and detected using MRC-MLD. The BER and SINR of the delay-sensitive user is analyzed. The probability of a subcarrier being active or inactive is taken into account when computing the average BER, which is derived in closed-form for BPSK and M_n-QAM modulations. On the other hand, Shahab et al. [217] propose an IM-IM-single-carrier frequency division multiple access (SC-FDMA)-NOMA system to support massive machine type communication (mMTC). Assuming two-user system, the users' signals are detected at the BS by applying JMLD. Closed-form PEP expressions are derived for both the JMLD and SIC-based detectors.

The authors of [218] study an IM-OFDMA-NOMA with N users in the DL. The available bandwidth is divided into multiple orthogonal subcarriers, where the adjacent subcarriers are pooled to serve a subset of N users. For each user, the BS broadcasts a block of bits. These bits are split into two parts, where the first part is applied to a conventional M_n-PSK modulator, while the second is used to determine the subcarriers' subset for transmission. The modulated symbols of different users on the same subcarriers are multiplexed in power-domain. The users perform optimal JMLD to estimate the individual signals. Average PEP expressions are derived over Rayleigh fading channels.

State-of-the-Art NOMA-based IM-TDMA: Althunibat et al. [219] propose an IM-time division multiple access (TDMA)-NOMA technique for UL communications. Assuming N users, the BS receives a signal from each user sending concurrently during a common transmission slot. The BS then performs JMLD to estimate the individual signals. Closed-form PEP expressions are derived over Rayleigh fading channel.

State-of-the-Art NOMA-based IM-CDMA: Lai et al. [220] propose a codeword position index (CPI)-based sparse code multiple access (SCMA) in which the information bits of each user are sent using a codebook and the indices of the codeword positions. The proposed scheme follows the NOMA principle in each time slot. Closed-form PEP expressions are derived over Rayleigh fading channels. Table 18 provides a comprehensive summary of the work on IM-OFDM/TDMA/CDMA.

State-of-the-Art NOMA-based IM-PD: Reference [221] propose a DL-NOMA system, which consists of a BS, a near-user, and a far-user, each equipped with a single antenna. Unlike traditional NOMA, the BS uses random power level selection from a predefined set to improve SE. As a result, the transmitter conveys $\log_2$(number of power levels) additional bits alongside the actual transmitted symbols. Since the users are unaware of the dynamically changing power levels, a distinct constellation is designed for each power level to distinguish between them. The error rate performance of the system is evaluated using conditional PEP analysis, with a Rayleigh fading channel and M_n-PAM modulation.

E. SHORT PACKET COMMUNICATIONS

According to Shannon capacity theorem, the probability of decoding error approaches zero when the block length approaches infinity [50]. Therefore, the error probability deteriorates by reducing the block length. This type of communications is referred to as SPC and is crucial for URLLC applications. Hence, the error probability associated with SPC cannot be ignored. SPC is investigated in the context of NOMA to highlight the throughput and the error rate performance. Table 19 provides a summary of the work in this part.

TABLE 19. Summary of the SPC-NOMA work.

[#]	System	Metric	Antennas	Direction	Channel	N	Receiver	CSI
[50]	SPC	BLER	SISO	DL	AWGN	2	Imperf. SIC	Perf.
[222]	SPC	BLER	SISO	DL	Rayleigh	2	Imperf. SIC	Perf.
[223]	SPC	BLER	SISO	DL	Nakagami-m	$\forall N$	Imperf. SIC	Perf.
[224]	SPC	BLER	MIMO	DL	Nakagami-m	2	Imperf. SIC	Perf.
[225]	SPC	BLER	SISO	DL	Rayleigh	2	Imperf. SIC	Perf.
[226]	SPC	BLER	SISO	DL	Rayleigh	2	Imperf. SIC	Perf.
[227]	SPC	BLER	SISO	UL	Rayleigh	$\forall N$	Imperf. SIC	Imperf.
[228]	SPC	BLER	SISO	UL	Various	2	Perf. SIC	Not available
[229]	SPC	BLER	SISO	UL	Rayleigh	2	MRC-Imperf. SIC	Perf.
[230]	CRS	BLER	SISO	DL	Rayleigh	2	MRC,SeC-Imperf. SIC	Perf.
[231]	CRS	BLER	SISO	DL	Rayleigh	2	MRC,SeC-Imperf. SIC	Perf.
[232]	CRS	BLER	SISO	DL	Nakagami-m	2	Imperf. SIC	Perf.
[233]	CRS	BLER	SISO	DL	Rayleigh	2	MRC-Perf. SIC	Perf.
[234]	CRS	BLER	MIMO	UL	Rayleigh	2	Partial SIC	Perf.
[235]	CR	BLER	SISO	DL	Rayleigh	2	Imperf. SIC	Imperf.
[236]	CR	BLER	SISO	DL	Nakagami-m	$\forall N$	Imperf. SIC	Perf.
[237]	CR	BLER	SISO	DL	Nakagami-m	2	Imperf. SIC	Imperf.
[238]	VLC	BLER	SISO	DL	VLC channel	2	Imperf. SIC	Perf.
[239]	VLC	BLER	SISO	DL	VLC channel	2	Imperf. SIC	Imperf.
[240]	IRS	BLER	SISO	DL	Rayleigh	2	Imperf. SIC	Perf.
[241]	IRS	BLER	SISO	DL	Rayleigh	$\forall N$	Imperf. SIC	Perf.
[242]	IRS	BLER	SISO	DL	Nakagami-m	2	Imperf. SIC	Perf.
[243]	IRS	BLER	SISO	DL	Rician	2	Perf. SIC	Stats.
[244]	IRS	BLER	SISO	DL	Nakagami-m	2	Perf. SIC	Perf.

State-of-the-Art on NOMA-based SPC: The average BLER is analyzed for the DL-NOMA with SPC in [50], [222], [223], [224], [225], [226], [230], [235]. It is obtained by considering a linear approximation of the instantaneous BLER, PDF and cumulative distribution function (CDF) of users. It is noted that the derived expressions are a function of SINR, block length, and target rate.

A two-user DL NOMA system employing SPC is studied in [50], [222]. The authors of [50] analyzed the users' error probabilities in AWGN channels for coded system, and uncoded system given that imperfect SIC is considered and QPSK is adopted. In both cases, a PA optimization problem is formulated with the objective of minimizing the error probability. On the other hand, Reference [222] considered Rayleigh fading channels. It is demonstrated that the blocklength can be represented as the function of users' power coefficients. The authors formulate an optimization problem in which the objective is to minimize the blocklength under average BLER constraints. Consequently, a closed-form expression for average BLER is derived to solve the optimization problem and to determine the best minimum blocklength for each user.

A multiuser DL-NOMA with SPC is investigated in [223] considering Nakagami-m fading channels. The authors derived analytical expressions for the average BLER considering perfect SIC. The expressions are obtained by utilizing the conditional BLER and the PDF. A linear function is used to approximate the complex integration required for the derivation. The CDF is constructed using the derived average BLER.

Yuan et al. [224] study the BLER performance of a DL-NOMA system considering SPC with Alamouti space-time block code. The BS is equipped with two antennas, while the two users have single antenna. Nakagami-m fading channel is assumed, where the channel remains constant across a two-symbol period. The instantaneous BLER is approximated and the CDF of the SINR under imperfect SIC assumption is derived. Closed-form BLER expressions are derived for both users using the instantaneous BLER and the corresponding CDFs. Furthermore, asymptotic expressions for the average BLER are derived to obtain the expressions for the minimum blocklengths for both users.

A secure two-user DL-NOMA with SPC is investigated in [225]. It is assumed that the far-user can eavesdrop on the signal transmitted to the near-user. While assuming imperfect SIC, and perfect CSI knowledge at all ends, the average secure BLER of the near-user for detecting and decoding its signal is derived over Rayleigh fading channels. Finally, an asymptotic average secure BLER is derived for the near-user via linear approximations. In [226], a hybrid long and short packet communication DL-NOMA is proposed, in which the near-user requests a long packet while the far-user requests a

short packet. The analytical expression of the average BLER for the far-user is derived over Rayleigh fading channel considering linear approximations to simplify the analysis.

The performance of a two-user UL-NOMA system is presented in [228]. All nodes are equipped with a single antenna. A unified analysis is conducted for SPC for various fading channels, including lognormal-Nakagami-m, generalized K_G, $\eta-\mu$, Nakagami-q (Hoyt), $\kappa-\mu$, Rician, Nakagami-m, and Rayleigh fading. While assuming imperfect CSI at the users, closed-form BLER expressions are derived. In [227], the authors analyze the performance of an N-user UL-NOMA system with SPC under the influence of channel estimation errors and RHI. The users are divided into several clusters, each consisting of a fixed number of users. The article proposes two decoding schemes: 1) fixed-order decoding, where the decoding order is determined based on the power levels, 2) dynamic decoding order, where the decoding order is determined by the instantaneous received powers. Closed-form BLER expressions are derived over Rayleigh fading channels.

The authors of [229] study the performance of a two-user UL-NOMA with hybrid automatic repeat request (HARQ) using SPC. Upon reception of negative acknowledgement by both users from the BS, the proposed scheme allows the higher power user to retransmit up to L times, while the lower power user transmits a new packet. The lower power user is allowed to retransmit only when the higher power user stops retransmission. The closed-form expressions for BLER are obtained for Rayleigh fading channels by employing a Markov model, assuming ideal CSI knowledge at all nodes, and utilizing MRC as well as imperfect SIC.

State-of-the-Art on SPC with CRS-NOMA: The authors of [230] study SPC for a two-user DL cooperative NOMA with user relaying. During the first time slot, the BS transmits a NOMA signal to both users. During the second time slot, the near-user acts as a HD-DF relay for the far-user after detecting the signals using SIC. The far-user combines the two received realizations during the two slots and combines them using SeC and MRC. The authors derive closed-form expressions for the BLER over Rayleigh fading channels considering linear approximation. In addition, an asymptotic BLER is computed for long packets.

Another SPC with DL-NOMA is discussed in [231]. The model consists of one source node, two NOMA users, and one selective DF-HD relay, where all nodes are equipped with a single antenna. While assuming perfect CSI at all nodes, the BLER is derived under Rayleigh fading channels and imperfect SIC conditions. Furthermore, separate analyses are performed at the far-user for SeC and MRC. In [232], an analytical framework for SPC with CRS-DL-NOMA over Nakagami-m fading channels is presented. The system consists of a source node, two NOMA users, and multiple DF-HD relays, each with a single antenna. The transmission is split into two time slots. During the first time slot, the transmitter broadcasts a NOMA signal to both users. If the far-user signal is successfully decoded by the near-user, it then implements SIC to obtain its signal; otherwise, the entire received NOMA sequence is cached. At the same time, the relays directly decode the received NOMA sequence to obtain the far-user signal. If failed to decode the far-user's signal, the relay is selected for transmission in the second time slot based on the resultant SINR at the relays and received SNR at the far-user. Otherwise, the relay is chosen based on the distance between the relays and the near-user, as well as the distance between the transmitter and the near-user. The goal of relay selection is to improve the near-user's reliability. The average BLER expressions are derived for the users under perfect and imperfect SIC assumptions.

Furthermore, DL-NOMA assisted SPC system is proposed in [233]. The system consists of a source and two NOMA users, with the near-user acting as a DF-FD relay and thus experiencing RSI. The fading channels between the nodes follow the Rayleigh distribution. The model assumes perfect SIC and perfect CSI conditions. There are two types of RSI models considered. One in which the RSI link is assumed to be free of fading and the other in which the RSI link follows Rayleigh fading. The expressions for average BLER are derived to evaluate the performance of the proposed system.

The authors of [234] present a novel approach, which involves a partial DF-AF relaying technique for a two-user UL-NOMA with SPC. In the first time slot, both users transmit their signals to the relay. The relay then employs partial SIC to decode the signal with higher receive power and re-encodes this within the received signal employing a modified PA. During the second time slot, the relay transmits this new NOMA signal to the BS. The BS then utilizes MRC and SIC to successfully decode the signals of the users. Upon a comparative analysis with the conventional DF, it is observed that the proposed technique is distinguished by its reduced complexity and enhanced security. Assuming that both the relay and the BS have multiple antennas, the authors derive closed-form BLER expressions over Rayleigh fading channels.

State-of-the-Art on SPC with CR-NOMA: In [235], a DL wireless-powered CR-NOMA IoT network with SPC is presented. The system consists of a BS, a secondary source node, multiple primary users and two secondary NOMA users. The secondary source node uses the energy harvested from the BS to transmit information to the near- and far-user using NOMA. All nodes, excluding the BS, are assumed to be equipped with a single antenna and to be operating in HD mode. The secondary source node adjusts its transmission power to avoid interfering with the primary users and meet their QoS requirements. The proposed system operates in two phases. The first phase involves the EH, while the second phase is the information transmission to the secondary users using NOMA. The authors derive approximate and asymptotic average BLER expressions. To obtain these expressions, the CDF is derived by using a linear approximation of the instantaneous BLER expression in order to

TABLE 20. Summary of the code domain NOMA work.

[#]	System	Metric	Antennas	Direction	Channel	M	N	Receiver	CSI
[245]	SCMA	PEP	SISO	DL,UL	Rayleigh	≤ 4	$\forall N$	JMLD	Perf.
[246]	SM-SCMA	PEP	MIMO	UL	Rayleigh	4	$\forall N$	MLD, MAP, MPA	Perf.
[247]	SCMA	BER	SISO	DL	One-sided Gaussian, Rayleigh	$\forall M$	$\forall N$	MPA	Perf.
[248]	SCMA	BER	SISO	DL	AWGN	≤ 16	$\forall N$	MPA	Perf.
[249]	SCMA	BER	SISO	DL	Rayleigh	≤ 16	$\forall N$	MPA	Perf.
[250]	SCMA	BER	SISO	UL	Rayleigh	4	$\forall N$	Multiple decision SIC	Perf.
[251]	MUSA	BER	SISO	UL	AWGN	4	$\forall N$	Imperf. SIC	Perf.

deal with the complex Q-function. In addition, the concept of first order Riemann integral approximation is used to handle the multiple integration involved in the CDF. Finally, the simulation results are compared to the analytical solution and to the real-time configuration results obtained using the deep neural network technique.

The authors of [236] study the performance of an CR-NOMA with SPC. The system consists of a primary network with a primary user and a secondary network with secondary users. In an underlay fashion, the secondary network uses NOMA for broadcasting to the secondary users with a tolerable interference at the primary user. Assuming perfect CSI, closed-form BLER expressions are derived for the imperfect SIC over Nakagami-*m* fading channels. On the other hand, the authors of [237] consider the effect of imperfect CSI and analyze the BLER.

State-of-the-Art on SPC with VLC-NOMA: A theoretical framework is proposed in [238] to assess the efficiency of SPC in a DL-VLC system employing NOMA. It is assumed that perfect CSI is known to the transmitter and the users. In this system, a single transmitting LED establishes communication over VLC channel with two single-photodiode users. Under the assumption of imperfect SIC and perfect CSI, closed-form expressions for BLER are derived. Furthermore, the performance of the same system under the assumption of imperfect CSI knowledge is studied in [239].

State-of-the-Art on SPC with IRS-aided NOMA: Vu et al. [240] study the STAR-IRS-enabled NOMA with SPC. Assuming perfect knowledge of CSI and perfect SIC, approximate and asymptotic closed-form BLER expressions are derived for the discrete phase shift model over Rayleigh fading channels, where the direct link between the two users and BS is assumed absent. Furthermore, Vu et al. extend the work to multiple users in [241]. The authors of [242] consider the two-user scenario with imperfect SIC and derive closed-form BLER expressions for the continuous phase model over Nakagami-*m* fading channels, where the direct link between the BS and one of the users only is assumed available. Similarly, the authors of [243] consider a two-user model but with perfect SIC and statistical CSI knowledge. The authors derive closed-form BLER expressions for the continuous and discrete phase models over Rician fading channels, where the direct link between the users and BS is assumed absent. Yuan et al. [244] consider an IRS-aided NOMA with SPC. Considering a two-user DL system, the near-user has a direct link with the BS only, while the far-user has a direct link with the IRS only that is configured to support the far-user. Assuming perfect SIC and CSI, the authors derive closed-form BLER expressions continuous and discrete phase models over Nakagami-*m* fading channels.

F. CODE DOMAIN

SCMA is a recently proposed multi-carrier NOMA scheme to serve multiple users simultaneously by employing different codebooks. The information bits of each user in the SCMA aided NOMA system are mapped to multidimensional complex codewords using a predefined codebook. Table 20 provides a summary of the work in this part.

State-of-the-Art NOMA-based SCMA: In [245], multidimensional constellations are studied for the DL and UL directions, where the PEP expressions are derived over Rayleigh fading channels. The PEP is initially derived for a single-user, considering MLD then it is extended for the multiuser scenario considering JMLD.

In [246], a SM-SCMA system is proposed for a single-cell UL communication. Each user activates one of the transmit antennas following the SSK approach, where the remaining bits are applied to conventional modulation to be transmitted using the activated antenna. The authors derive PEP expressions over frequency selective Rayleigh fading channels for three different detectors: 1) MLD, 2) MAP detector, 3) low-complexity near-optimal message passing algorithm (MPA) detector. In [247], the BER performance of an impulsive noise-impaired DL SCMA is provided. The binary sequence is converted to codewords, which are then superimposed to create the SC signal and broadcast through the wireless channel. At the receiver, MPA-based detector is formulated using the maximum correntropy criterion. By invoking the concept of generalized SNR, the BER can be derived by noting that LLR is proportional to the SNR with a scaling factor. Hence, the BER can be approximated. The authors of [248] study a multiuser DL-SCMA system. Closed-form BER expressions are derived over AWGN channel for the star-QAM considering MPA-based detector. Such detector minimizes the IUI and BER by defining the decision regions.

Furthermore, [249] proposes a novel DL-SCMA codebook design criterion with large minimum ED using star-QAM, where the design is based on PEP. Approximate BER expressions are derived over Rayleigh fading channels for the

MPA-based detector based on the moment-generation function technique and the CDF of the phase angle in the SCMA constellation. Ling et al. [250] propose a multiple decision SIC for the UL SCMA to mitigate the error propagation problem of the conventional SIC, where multiple codeword candidates are considered rather than one. A trade-off between complexity and performance is achieved by selecting candidates that have probabilities greater than a predefined threshold.

Using non-orthogonal spreading sequences, multiple-user shared access (MUSA) is proposed for the UL GFA in [251]. The power allocation is optimized to minimize the overall system BER under two constraints: 1) total power constraint and 2) minimum difference in received power between strong and interfering signals. At the receiver, SIC is employed in conjunction with the linear minimum mean square error (MMSE) detector.

VII. ERROR RATE LITERATURE CLASSIFICATION

This section aims to highlight the different NOMA system model traits considered by the researchers. These traits are classified into six categories which are:

- Antennas setup
- Number of users
- Error performance metric
- Modulation scheme
- Channel model
- Receiver design

Fig. 15 illustrates the different categories in a snowflake diagram which counts the number of papers that consider a certain trait for each category. This looks like a compass to guide the readers to the most common assumptions made in the research community for NOMA systems. It is worthy to mention that the scale is logarithmic in the figure.

It can be seen in Fig. 15a, that SISO is the most considered antennas setup by researchers, while MISO is the least considered. This is because MISO-NOMA beamforming requires optimization, which makes it challenging to derive closed-form expressions for the error performance metrics. Hence, it can be seen as a promising direction for NOMA error rate analysis research. Furthermore, as can be noted from Fig. 15b two-user NOMA system is mostly considered by researchers to minimize the receiver complexity since the complexity of the SIC chain increases when more users are assumed. Interestingly, the arbitrary number of users is also considered by some researchers to verify the performance of the NOMA system in extremely overloaded scenarios.

The BER is exhaustively studied by the researchers to validate the error performance of NOMA according to Fig. 15c, whereas BLER is the least studied. In addition, the PEP analysis has been considered widely to evaluate the NOMA system performance when the BER and SER expressions are difficult to obtain or intractable. The statistics show that the BLER, which is mostly considered for SPC, did not receive remarkable attention by the research community compared to other error rate metrics. Hence, it can be seen as a promising direction for study. Further, Fig. 15d shows that QAM is used very frequently in the literature due to its energy packing capability and energy efficiency. The other modulation schemes such as OOK and PSK are mostly used by VLC systems which received significant attention.

Fig. 15e shows that Rayleigh fading channel is the most considered channel in the literature, since it is widely accepted for modeling the non-LoS wireless channel. The second mostly adopted channel model is the AWGN channel, which is commonly accepted to derive the closed-form instantaneous error rate performance. While deriving the average error rate performance might be challenging for UL-NOMA systems, it is accepted to consider mathematical approximation or single integral-form expressions. It is worthy to mention that channel models such as Nakagami-m and other generalized channel models can capture several models by tuning the channel parameters, which gives better insights into the system performance in different scenarios. However, deriving the average error rate performance becomes challenging. Furthermore, Fig. 15f shows that the imperfect SIC receiver assumption is dominating over the other receiver assumptions. The reason is that such a receiver captures the error propagation issue faced in practical scenarios. In addition, its complexity is much lower compared to the JMLD. It is worthy to mention that MRC is used mostly to combine the transmitting or receiving diversity signals. Many researchers focused on enhancing the receiver, which is under others trait.

VIII. FUTURE DIRECTIONS AND OPEN RESEARCH PROBLEMS

This section aims to highlight future directions and open research problems of NOMA systems while focusing on the error rate performance. These future directions include the error rate performance analysis of NOMA integrated with IRS, joint radar-communications, millimeter wave (mmWave) and terahertz (THz) communications. Moreover, the open research problems include the design and analysis of low complexity detectors for NOMA systems, as well as the error rate performance analysis of the non-ideal NOMA systems due to hardware imperfections. Furthermore, error rate analysis of new NOMA variants and machine learning-enabled NOMA are presented as possible future directions.

A. HYBRID IRS

As discussed in Section II, IRS can enhance the system performance by controlling the propagation of signals in the environment via passive smart metasurface elements. However, there are several challenges, such as acquiring channel estimates between all metasurface elements and users. Since the IRS is passive, it cannot transmit pilot/training signals to facilitate channel estimation. Hence, novel channel estimation methods should be considered for IRS, such as estimating the cascaded user-IRS-BS channels,

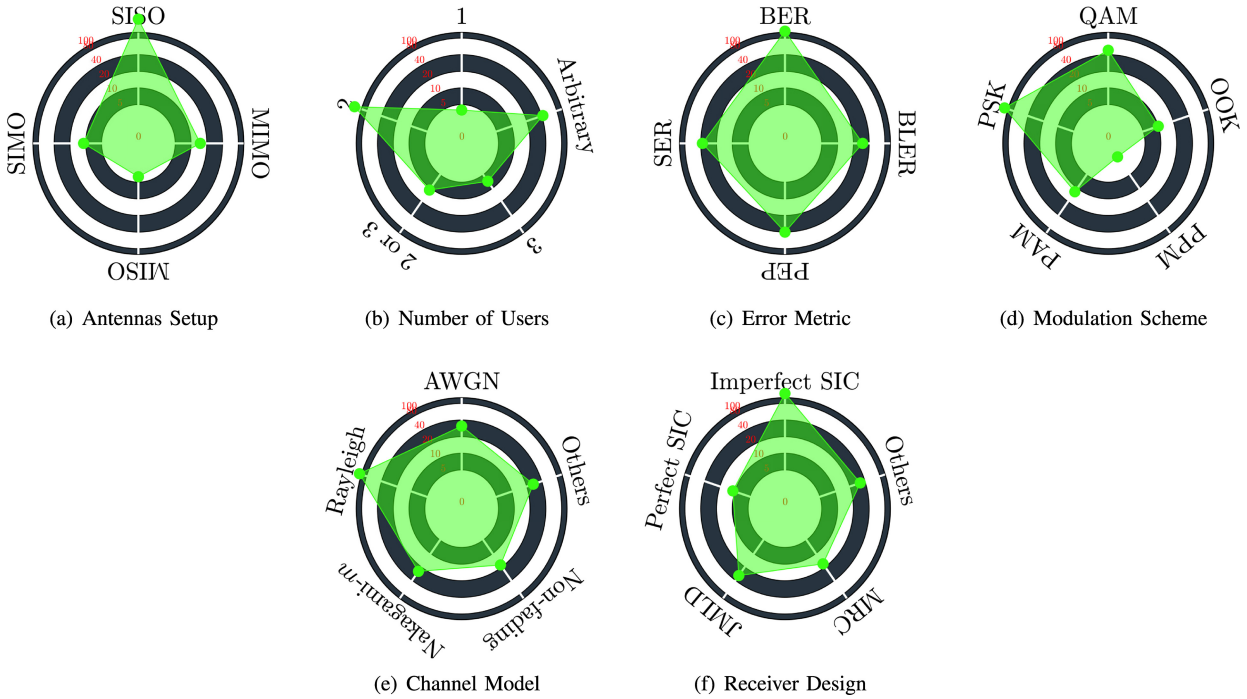

(a) Antennas Setup (b) Number of Users (c) Error Metric (d) Modulation Scheme

(e) Channel Model (f) Receiver Design

FIGURE 15. Error rate work classification counter based on: (a) Antenna setup. (b) Number of users. (c) Error metric. (d) Modulation scheme. (e) Channel model. (f) Receiver design.

or by considering semi-passive IRS models which have sensing capabilities [252]. Also, the phase cannot be controlled continuously in practice. Therefore, it is crucial to consider quantized phase control.

The error rate performance of IRS-assisted NOMA has been investigated for the DL direction only, where the assumptions of continuous and perfect phase are assumed [165], [166]. Hence, analyzing the error rate performance under imperfect and quantized phase is worth studying to get better practical insights. Moreover, the design and analysis for the UL direction is a promising direction as well. Furthermore, studying the system performance while considering the direct link between the users and the BS is still an open research question. Hence, the design and analysis of the dual function IRS in DL and UL-NOMA systems is attractive.

B. JOINT RADAR-COMMUNICATIONS SYSTEMS

Joint radar-communications systems is promising to solve the spectrum scarcity problem as both tasks are processed on the same frequency band. Hence, a single beamformer can be optimized to satisfy the requirements for both signals. For example, a certain error rate performance or sum-rate requirements for the communications part, while certain sensing power for the sensing part. While NOMA is used to serve multiple users, it can also be used for sensing simultaneously [253]. Investigating the error performance of the communications part and the effectiveness of the sensing part of the NOMA-based joint radar-communications system while considering proper signaling is still an open research problem.

C. MMWAVE AND THZ COMMUNICATIONS

Higher frequency bands such as mmWave bands are currently used in the 5G standard to satisfy the growth in higher data requirements, since wider bandwidths are available at such frequencies. However, current trends indicate that THz bands, which are wider than millimeter bands, are considered a key technology for future wireless networks [25]. Nonetheless, the propagation limitations become more challenging and the communications would be directional and take place mostly in LoS environments. Therefore, the near-far problem would exist even if the users are relatively in close proximity. Consequently, studying the best conditions for pairing the NOMA users under certain error rate performance requirements can provide a better understanding of the practical scenarios in which NOMA performance would be maximized. Furthermore, including technologies such as cooperative communications and IRS can be used to improve the network coverage.

D. LOW COMPLEXITY DETECTORS

One of the crucial concerns for deploying NOMA with more than two-user per resource block is the associated detectors' complexity. While either SIC or JMLD computational complexities might limit the applications of NOMA, designing new detectors with lower complexity for the UL or DL is a promising research direction. Most importantly is the UL, since JMLD is introduced as a solution for the SIC error floor problem [36]. However, it should be noted that the adoption of NOMA in standards and industry has been limited due to its trade-off between performance gain and complexity [254], [255]. These practical considerations highlight

the need to address the complexity issue while maintaining acceptable performance. Therefore, further research and development are required to explore low complexity detectors for NOMA systems, providing motivation and future directions for error rate analysis.

E. HARDWARE IMPERFECTIONS

Although several articles studied the impact of imperfect SIC and channel estimation errors as seen in Fig. 15, the literature works studying the impact of RHI, I/Q imbalance and phase noise are limited [125], [126], [178], [227]. In addition, problems including frame synchronization, time synchronization and carrier synchronization over the performance of NOMA systems are missing from the literature. Furthermore, the works of OFDM-NOMA systems reported in this survey mostly assume ideal conditions in terms of time and frequency synchronization, as well as cyclic prefix (CP) length which is assumed to be longer than the channel maximum delay spread, and hence the inter-symbol interference is removed perfectly. However, such ideal conditions cannot be achieved in practical scenarios, where imperfect time and frequency synchronization are likely to occur. Additionally, OFDM-NOMA is prone to user mobility, which introduces Doppler shift and loss of subcarriers orthogonality. Applying orthogonal time frequency space (OTFS) and studying the error rate performance of NOMA systems under the previously mentioned imperfections can be important directions for future research

F. VARIANTS

While NOMA is mainly recognized as a beyond 5G multiple access technique due to its ability to augment the SE of communication systems, its advantages are not limited to SE enhancement only, they extend to other several aspects of the communication systems such as reliability, energy efficiency and latency. In the following, we highlight several more general variants of NOMA that may offer significant improvements to the communications system.

1) MULTIRATE NOMA

Multirate NOMA has been introduced to improve the reliability of the NOMA system [256]. Unlike conventional NOMA systems, mutlirate NOMA allows pairing users with different symbol rates, thus the energy dimension is exploited as another degree of freedom when performing PA. Error rate analysis of multirate NOMA systems for UL and DL, as well as the design of optimal low-complexity detectors, are still open research problems. Further problems that need investigation are user pairing, optimal PA and modulation orders selection.

2) NOM

Nonorthogonal multiplexing (NOM) has been proposed for HARQ-based wireless systems to allow multiplexing new packet transmission with retransmissions such that the energy efficiency and latency are improved [257]. While [258] considers generalizing NOM to more than two packets, the PA is assumed fixed during the retransmissions. Allowing adaptive power and considering higher modulation orders can improve performance further. Nonetheless, the design of a low-complexity detector and low-complexity algorithm to solve the PA and the number of multiplexed packets are important research directions.

3) RSMA

While noting that the sheer number of articles reported in this survey deals with SISO settings as can be seen in Fig. 15a, NOMA is effective for SISO designs and its SE reduces for most of the multiple antennas scenarios [259]. Clerckx et al. [260] presented rate-splitting multiple access (RSMA) as another variant of NOMA for and OMA for multiple antenna settings, where it is based on splitting the user's message into different parts such as common and private parts, each of which can be handled independently, leading to increasing both efficiency and reliability. Consequently, RSMA promises to achieve higher multiplexing gains and rates, robustness to user deployment settings, and serve a larger number of users [261], [262], [263]. In addition, latency caused by the long chain of SIC in NOMA is reduced due to more efficient use of SIC. Therefore, researchers are invited to study the error rate performance of RSMA for SIMO, MISO and MIMO settings.

G. MACHINE LEARNING

While both statistical-based analysis and machine learning-based analysis of NOMA are reported in the literature, the latter has the potential to revolutionize the performance of NOMA by leveraging data-driven models and advanced algorithms. More specifically, machine learning is used in prediction and optimization problems such as channel estimation, adaptive modulation, constellation design, and classification [264] as well as receiver design [265]. Nonetheless, analyzing the performance of machine learning-based approaches using the traditional error rate metrics including BER, SER and BLER can be very complicated due to the black-box nature of machine learning-based approaches. Therefore, adopting model-dependent evaluation metrics such as accuracy, computational complexity, and reliability besides the hybrid analytical approach can provide a comprehensive understanding of NOMA error rate performance.

Furthermore, evaluating the error rate of machine learning-enabled NOMA has the following challenges. For instance, limited labeled data, NOMA system complexity, scalability issues, generalization across diverse environments, and real-time processing constraints. Since NOMA networks have a dynamic nature, acquiring labeled data is challenging, and modeling interference management and resource allocation complexities is complicated. Scaling techniques to handle

numerous users while ensuring generalization across scenarios is complex. In addition, real-time analysis is required for effective resource allocation.

IX. CONCLUSION

To summarize, this article surveys the state-of-the-art work in the literature of NOMA focusing on papers that are concerned with the error rate performance of NOMA systems. A comprehensive summary and tutorial are firstly presented for the conventional NOMA scheme in both the DL and UL directions. Also, improved NOMA schemes are discussed including labeling, constellation rotation, interference alignment, channel coding multicarrier NOMA system design and detector design. Furthermore, a comprehensive survey is provided on the integration of NOMA and other technologies such as optical communications, IRS and backscatter communications, cooperative communications, IM, SPC and code domain. Finally, future research directions and open NOMA research problems are presented.

APPENDIX I: ACRONYMS

Notation	Description
M_n-PAM	M-ary pulse amplitude modulation
M_n-PPM	M-ary pulse position modulation
M_n-PSK	M-ary phase shift keying
M_n-QAM	M-ary quadrature amplitude modulation
4G	fourth generation
5G	fifth generation
AF	amplify-and-forward
ASK	amplitude shift keying
AWGN	additive white Gaussian noise
BER	bit error rate
BLER	block error rate
BPSK	binary phase shift keying
BS	base station
CDF	cumulative distribution function
CDMA	code division multiple access
CP	cyclic prefix
CPI	codeword position index
CR	cognitive radio
CRS	cooperative relaying system
CSI	channel state information
DF	decode-and-forward
DFT	discrete Fourier transform
DL	downlink
DWT	discrete wavelet transform
ED	Euclidean distance
EH	energy harvesting
FD	full-duplex
FEC	forward error correcting
FFT	fast Fourier transform
FSO	free space optical
GFA	grant free access
GFDMA	generalized frequency division multiple access
GGN	generalized Gaussian noise
GPQSM	generalised pre-coding quadrature spatial modulation
HARQ	hybrid automatic repeat request
HD	half-duplex
IM	index modulation
IoT	Internet of Things
IRS	intelligent reflecting surface
IUI	inter-user interference
JMLD	joint-multiuser maximum likelihood detector
LDPC	low-density parity-check
LED	light emitting diode
LLR	log-likelihood ratio
LoS	line-of-sight
MAP	maximum a posterior
MBM	media-based modulation
MI	mutual information
MIMO	multiple-input multiple-output
MISO	multiple-input single-output
ML	maximum likelihood
MLD	maximum likelihood detector
MMSE	minimum mean square error
mMTC	massive machine type communication
mmWave	millimeter wave
MPA	message passing algorithm
MPPM	multiple pulse position modulation
MRC	maximal ratio combining
MUSA	multiple-user shared access
NOM	nonorthogonal multiplexing
NOMA	non-orthogonal multiple access
O-NOMA	optical-NOMA
OFDM	orthogonal frequency division multiplexing
OFDMA	orthogonal frequency division multiple access
OMA	orthogonal multiple access
OOK	on-off keying
OSTBC	orthogonal space-time block code
OTFS	orthogonal time frequency space
PA	power assignment
PAM	pulse amplitude modulation
PCB	power coefficient bound
PD	power domain
PDF	probability density function
PEP	pairwise error probability
PER	packet error rate
PLNC	physical layer network coding
PMF	probability mass function
PSK	phase shift keying
PSM	precoded spatial modulation
QAM	quadrature amplitude modulation
QoS	quality of service
QPSK	quadrature-phase shift keying
RF	radio frequency
RHI	residual hardware impairment
RSI	residual self-interference
RSMA	rate-splitting multiple access
SC	superposition coding

SC-FDMA	single-carrier frequency division multiple access
SCMA	sparse code multiple access
SDR	software-defined-radio
SE	spectral efficiency
SeC	selection combining
SER	symbol error rate
SIC	successive interference cancellation
SIMO	single-input-multiple-output
SINR	signal-to-interference-plus-noise ratio
SISO	single-input-single-output
SM	spatial modulation
SNR	signal-to-noise ratio
SPC	short packet communication
SSK	space shift keying
STAR-IRS	simultaneously transmitting and reflecting intelligent reflecting surface
STLC	space-time line code
SWIPT	simultaneous wireless information and power transfer
TCM	trellis coded modulation
TDMA	time division multiple access
THz	terahertz
TM	transmission mode
UL	uplink
URLLC	ultra-reliable low latency communication
V2V	vehicle-to-vehicle
VLC	visible light communication
WIT	wireless information transfer
WPT	wireless power transfer

REFERENCES

[1] W. Saad, M. Bennis, and M. Chen, "A vision of 6G wireless systems: Applications, trends, technologies, and open research problems," *IEEE Netw.*, vol. 34, no. 3, pp. 134–142, May/Jun. 2020.

[2] S. Dang, O. Amin, B. Shihada, and M.-S. Alouini, "What should 6G be?" *Nature Electron.*, vol. 3, no. 1, pp. 20–29, 2020.

[3] "Ericsson mobility report, Q2 update, August 2021," Ericsson, Stockholm, Sweden, Rep., 2021. [Online]. Available: https://www.ericsson.com/en/mobility-report

[4] "Cisco annual Internet report (2018–2023)," Cisco, San Jose, CA, USA, Rep., 2020. [Online]. Available: https://www.cisco.com/c/en/us/solutions/collateral/executive-perspectives/annual-internet-report/white-paper-c11-741490.pdf

[5] A. Benjebbour, K. Saito, A. Li, Y. Kishiyama, and T. Nakamura, "Non-orthogonal multiple access (NOMA): Concept, performance evaluation and experimental trials," in *Proc. Int. Conf. Wireless Netw. Mobile Commun. (WINCOM)*, Marrakech, Morocco, 2016, pp. 1–6.

[6] Z. Ding et al., "Application of non-orthogonal multiple access in LTE and 5G networks," *IEEE Commun. Mag.*, vol. 55, no. 2, pp. 185–191, Feb. 2017.

[7] M. Vaezi, R. Schober, Z. Ding, and H. V. Poor, "Non-orthogonal multiple access: Common myths and critical questions," *IEEE Wireless Commun.*, vol. 26, no. 5, pp. 174–180, Oct. 2019.

[8] Z. Xiang, W. Yang, Y. Cai, Z. Ding, Y. Song, and Y. Zou, "NOMA-assisted secure short-packet communications in IoT," *IEEE Wireless Commun.*, vol. 27, no. 4, pp. 8–15, Aug. 2020.

[9] A. I. Perez-Neira, M. Caus, and M. A. Vazquez, "Non-orthogonal transmission techniques for Multibeam satellite systems," *IEEE Commun. Mag.*, vol. 57, no. 12, pp. 58–63, Dec. 2019.

[10] Y. Liu, Z. Qin, Y. Cai, Y. Gao, G. Y. Li, and A. Nallanathan, "UAV communications based on non-orthogonal multiple access," *IEEE Wireless Commun.*, vol. 26, no. 1, pp. 52–57, Feb. 2019.

[11] H. Marshoud, P. C. Sofotasios, S. Muhaidat, G. K. Karagiannidis, and B. S. Sharif, "On the performance of visible light communication systems with non-orthogonal multiple access," *IEEE Trans. Wireless Commun.*, vol. 16, no. 10, pp. 6350–6364, Oct. 2017.

[12] M. Jain, N. Sharma, A. Gupta, D. Rawal, and P. Garg, "Performance analysis of NOMA assisted underwater visible light communication system," *IEEE Wireless Commun. Lett.*, vol. 9, no. 8, pp. 1291–1294, Aug. 2020.

[13] L. Dai, B. Wang, Y. Yuan, S. Han, I. Chih-lin, and Z. Wang, "Non-orthogonal multiple access for 5G: Solutions, challenges, opportunities, and future research trends," *IEEE Commun. Mag.*, vol. 53, no. 9, pp. 74–81, Sep. 2015.

[14] Y. Wang, B. Ren, S. Sun, S. Kang, and X. Yue, "Analysis of non-orthogonal multiple access for 5G," *China Commun.*, vol. 13, pp. 52–66, Jan. 2016.

[15] S. M. R. Islam, N. Avazov, O. A. Dobre, and K.-S. Kwak, "Power-domain non-orthogonal multiple access (NOMA) in 5G systems: Potentials and challenges," *IEEE Commun. Surveys Tuts.*, vol. 19, no. 2, pp. 721–742, 2nd Quart., 2017.

[16] Z. Ding, X. Lei, G. K. Karagiannidis, R. Schober, J. Yuan, and V. K. Bhargava, "A survey on non-orthogonal multiple access for 5G networks: Research challenges and future trends," *IEEE J. Sel. Areas Commun.*, vol. 35, no. 10, pp. 2181–2195, Oct. 2017.

[17] W. Shin, M. Vaezi, B. Lee, D. J. Love, J. Lee, and H. V. Poor, "Non-orthogonal multiple access in multi-cell networks: Theory, performance, and practical challenges," *IEEE Commun. Mag.*, vol. 55, no. 10, pp. 176–183, Oct. 2017.

[18] Y. Liu, Z. Qin, M. Elkashlan, Z. Ding, A. Nallanathan, and L. Hanzo, "Nonorthogonal multiple access for 5G and beyond," *Proc. IEEE*, vol. 105, no. 12, pp. 2347–2381, Dec. 2017.

[19] S. M. R. Islam, M. Zeng, O. A. Dobre, and K.-S. Kwak, "Resource allocation for downlink NOMA systems: Key techniques and open issues," *IEEE Wireless Commun.*, vol. 25, no. 2, pp. 40–47, Apr. 2018.

[20] M. Basharat, W. Ejaz, M. Naeem, A. M. Khattak, and A. Anpalagan, "A survey and taxonomy on nonorthogonal multiple-access schemes for 5G networks," *Trans. Emerg. Telecommun. Technol.*, vol. 29, no. 1, 2018, Art. no. e3202. [Online]. Available: https://onlinelibrary.wiley.com/doi/abs/10.1002/ett.3202

[21] L. Dai, B. Wang, Z. Ding, Z. Wang, S. Chen, and L. Hanzo, "A survey of non-orthogonal multiple access for 5G," *IEEE Commun. Surveys Tuts.*, vol. 20, no. 3, pp. 2294–2323, 3rd Quart., 2018.

[22] Y. Cai, Z. Qin, F. Cui, G. Y. Li, and J. A. McCann, "Modulation and multiple access for 5G networks," *IEEE Commun. Surveys Tuts.*, vol. 20, no. 1, pp. 629–646, 1st Quart., 2018.

[23] N. Ye, H. Han, L. Zhao, and A.-H. Wang, "Uplink nonorthogonal multiple access technologies toward 5G: A survey," *Wireless Commun. Mobile Comput.*, vol. 2018, Jun. 2018, Art. no. 6187580. [Online]. Available: https://doi.org/10.1155/2018/6187580

[24] M. Vaezi, G. A. Aruma Baduge, Y. Liu, A. Arafa, F. Fang, and Z. Ding, "Interplay between NOMA and other emerging technologies: A survey," *IEEE Trans. Cogn. Commun. Netw.*, vol. 5, no. 4, pp. 900–919, Dec. 2019.

[25] O. Maraqa, A. S. Rajasekaran, S. Al-Ahmadi, H. Yanikomeroglu, and S. M. Sait, "A survey of rate-optimal power domain NOMA with enabling technologies of future wireless networks," *IEEE Commun. Surveys Tuts.*, vol. 22, no. 4, pp. 2192–2235, 4th Quart., 2020.

[26] M. B. Shahab, R. Abbas, M. Shirvanimoghaddam, and S. J. Johnson, "Grant-free non-orthogonal multiple access for IoT: A survey," *IEEE Commun. Surveys Tuts.*, vol. 22, no. 3, pp. 1805–1838, 3rd Quart., 2020.

[27] B. Makki, K. Chitti, A. Behravan, and M.-S. Alouini, "A survey of NOMA: Current status and open research challenges," *IEEE Open J. Commun. Soc.*, vol. 1, pp. 179–189, Jan. 2020.

[28] M. Liaqat, K. A. Noordin, T. Abdul Latef, and K. Dimyati, "Power-domain non orthogonal multiple access (PD-NOMA) in cooperative networks: An overview," *Wireless Netw.*, vol. 26, pp. 181–203, Jan. 2020.

[29] A. Akbar, S. Jangsher, and F. A. Bhatti, "NOMA and 5G emerging technologies: A survey on issues and solution techniques," *Comput. Netw.*, vol. 190, May 2021, Art. no. 107950.

[30] H. Sadat, M. Abaza, A. Mansour, and A. Alfalou, "A survey of NOMA for VLC systems: Research challenges and future trends," *Sensors*, vol. 22, no. 4, p. 1395, Feb. 2022. [Online]. Available: https://www.mdpi.com/1424--8220/22/4/1395

[31] S. A. H. Mohsan, Y. Li, A. V. Shvetsov, J. Varela-Aldás, S. M. Mostafa, and A. Elfikky, "A survey of deep learning based NOMA: State of the art, key aspects, open challenges and future trends," *Sensors*, vol. 23, no. 6, p. 2946, Mar. 2023. [Online]. Available: https://www.mdpi.com/1424--8220/23/6/2946

[32] M. Vaezi, Z. Ding, and H. V. Poor, *Multiple Access Techniques for 5G Wireless Networks and Beyond*. Cham, Switzerland: Springer, 2019, vol. 159.

[33] T. Assaf, A. Al-Dweik, M. S. E. Moursi, H. Zeineldin, and M. Al-Jarrah, "NOMA receiver design for delay-sensitive systems," *IEEE Syst. J.*, vol. 15, no. 4, pp. 5606–5617, Dec. 2021.

[34] H. Yahya, E. Alsusa, and A. Al-Dweik, "Exact BER analysis of NOMA with arbitrary number of users and modulation orders," *IEEE Trans. Commun.*, vol. 69, no. 9, pp. 6330–6344, Sep. 2021.

[35] Y. Qi, X. Zhang, and M. Vaezi, "Over-the-air implementation of NOMA: New experiments and future directions," *IEEE Access*, vol. 9, pp. 135828–135844, 2021.

[36] H. Semira, F. Kara, H. Kaya, and H. Yanikomeroglu, "Multi-user joint maximum-likelihood detection in uplink NOMA-IoT networks: Removing the error floor," *IEEE Wireless Commun. Lett.*, vol. 10, no. 11, pp. 2459–2463, Nov. 2021.

[37] F. Kara and H. Kaya, "Performance analysis of SSK-NOMA," *IEEE Trans. Veh. Technol.*, vol. 68, no. 7, pp. 6231–6242, Jul. 2019.

[38] C. Pan et al., "Reconfigurable intelligent surfaces for 6G systems: Principles, applications, and research directions," *IEEE Commun. Mag.*, vol. 59, no. 6, pp. 14–20, Jun. 2021.

[39] F. Jameel, S. Zeb, W. U. Khan, S. A. Hassan, Z. Chang, and J. Liu, "NOMA-enabled backscatter communications: Toward battery-free IoT networks," *IEEE Internet Things Mag.*, vol. 3, no. 4, pp. 95–101, Dec. 2020.

[40] Z. Ding and H. Vincent Poor, "A simple design of IRS-NOMA transmission," *IEEE Commun. Lett.*, vol. 24, no. 5, pp. 1119–1123, May 2020.

[41] H. Marshoud, S. Muhaidat, P. C. Sofotasios, S. Hussain, M. A. Imran, and B. S. Sharif, "Optical non-orthogonal multiple access for visible light communication," *IEEE Wireless Commun.*, vol. 25, no. 2, pp. 82–88, Apr. 2018.

[42] M. Le-Tran, T.-H. Vu, and S. Kim, "Performance analysis of optical backhauled cooperative NOMA visible light communication," *IEEE Trans. Veh. Technol.*, vol. 70, no. 12, pp. 12932–12945, Dec. 2021.

[43] M. A. Khalighi and M. Uysal, "Survey on free space optical communication: A communication theory perspective," *IEEE Commun. Surveys Tuts.*, vol. 16, no. 4, pp. 2231–2258, 4th Quart., 2014.

[44] M. A. Al-Jarrah, A. Al-Dweik, K.-H. Park, and M.-S. Alouini, "Amplitude-coherent detection for optical wireless communications: Opportunities and limitations," *IEEE Open J. Commun. Soc.*, vol. 1, pp. 550–562, 2020.

[45] M. Zeng, W. Hao, O. A. Dobre, and Z. Ding, "Cooperative NOMA: State of the art, key techniques, and open challenges," *IEEE Netw.*, vol. 34, no. 5, pp. 205–211, Sep./Oct. 2020.

[46] F. Kara and H. Kaya, "BER performances of downlink and uplink NOMA in the presence of SIC errors over fading channels," *IET Commun.*, vol. 12, no. 15, pp. 1834–1844, Sep. 2018.

[47] I. Lee and J. Kim, "Average symbol error rate analysis for non-orthogonal multiple access with *M*-Ary QAM signals in rayleigh fading channels," *IEEE Commun. Lett.*, vol. 23, no. 8, pp. 1328–1331, Aug. 2019.

[48] E. C. Cejudo, H. Zhu, and O. Alluhaibi, "On the power allocation and constellation selection in downlink NOMA," in *Proc. IEEE Veh. Technol. Conf. (VTC)*, Toronto, ON, Canada, Sep. 2017, pp. 1–5.

[49] Q. He, Y. Hu, and A. Schmeink, "Closed-form symbol error rate expressions for non-orthogonal multiple access systems," *IEEE Trans. Veh. Technol.*, vol. 68, no. 7, pp. 6775–6789, Jul. 2019.

[50] Y. Wang, J. Wang, L. Ma, Y. Huang, and C. Zhao, "Minimum error performance of downlink non-orthogonal multiple access systems," in *Proc. IEEE Veh. Technol. Conf. (VTC)*, Honolulu, HI, USA, Sep. 2019, pp. 1–5.

[51] L. Bariah, S. Muhaidat, and A. Al-Dweik, "Error probability analysis of non-orthogonal multiple access over Nakagami-*m* fading channels," *IEEE Trans. Commun.*, vol. 67, no. 2, pp. 1586–1599, Feb. 2019.

[52] L. Bariah, B. Selim, L. Mohjazi, S. Muhaidat, P. C. Sofotasios, and W. Hamouda, "Pairwise error probability of non-orthogonal multiple access with i/Q imbalance," in *Proc. U.K./China Emerg. Technol. (UCET)*, Glasgow, U.K., Aug. 2019, pp. 1–4.

[53] L. Bariah, S. Muhaidat, P. C. Sofotasios, S. Gurugopinath, W. Hamouda, and H. Yanikomeroglu, "Non-orthogonal multiple access in the presence of additive generalized Gaussian noise," *IEEE Commun. Lett.*, vol. 24, no. 10, pp. 2137–2141, Oct. 2020.

[54] A. Almohamad, S. Althunibat, M. Hasna, and K. Qaraqe, "On the error performance of non-orthogonal multiple access systems," in *Proc. Int. Conf. Inf. Commun. Technol. Converg. (ICTC)*, Oct. 2020, pp. 116–121.

[55] K. Lee, J. S. Yeom, B. C. Jung, and J. Joung, "A novel non-orthogonal multiple access with space-time line codes for massive IoT networks," in *Proc. IEEE Veh. Technol. Conf. (VTC)*, Honolulu, HI, USA, Sep. 2019, pp. 1–5.

[56] Y. Iraqi and A. Al-Dweik, "Power allocation for reliable SIC detection of rectangular QAM-based NOMA systems," *IEEE Trans. Veh. Technol.*, vol. 70, no. 8, pp. 8355–8360, Aug. 2021.

[57] F. Kara and H. Kaya, "A true power allocation constraint for non-orthogonal multiple access with M-QAM signalling," in *Proc. IEEE Microw. Theory Techn. Wireless Commun. (MTTW)*, vol. 1, Riga, Latvia, Oct. 2020, pp. 7–12.

[58] A. Chauhan and A. Jaiswal, "Power allocation constraint and error rate analysis for multi-user PD-NOMA system employing *M*–Ary PSK," *IEEE Commun. Lett.*, vol. 27, no. 5, pp. 1452–1456, May 2023.

[59] H. Yahya, E. Alsusa, A. Al-Dweik, and M. Debbah, "Cognitive NOMA with blind transmission-mode identification," *IEEE Trans. Commun.*, vol. 71, no. 4, pp. 2042–2058, Apr. 2023.

[60] A. Hilario-Tacuri, "Closed-form expressions for symbol error rate of two-user NOMA systems," in *Proc. IEEE Int. Conf. Electron. Elect. Eng. Comput. (INTERCON)*, Lima, Peru, Sep. 2021, pp. 1–4.

[61] S. Bisen, P. Shaik, J. Jose, J. Nebhen, O. Krejcar, and V. Bhatia, "ASER analysis of generalized hexagonal QAM schemes for NOMA systems over Nakagami-*m* fading channels," *Int. J. Commun. Syst.*, vol. 36, no. 6, Jan. 2023, Art. no. e5440.

[62] T. Assaf, A. J. Al-Dweik, M. S. E. Moursi, H. Zeineldin, and M. Al-Jarrah, "Exact bit error-rate analysis of two-user NOMA using QAM with arbitrary modulation orders," *IEEE Commun. Lett.*, vol. 24, no. 12, pp. 2705–2709, Dec. 2020.

[63] M. Jain, S. Soni, N. Sharma, and D. Rawal, "Performance analysis at far and near user in NOMA based system in presence of SIC error," *Int. J. Electron. Commun.*, vol. 114, Feb. 2020, Art. no. 152993.

[64] A. Hilario-Tacuri, J. Maldonado, M. Revollo, and H. Chambi, "Bit error rate analysis of NOMA-OFDM in 5G systems with non-linear HPA with memory," *IEEE Access*, vol. 9, pp. 83709–83717, Jun. 2021.

[65] K. Chung, "Impact of channel estimation errors on SIC performance of NOMA in 5G systems," *J. Converg. Inf. Technol.*, vol. 10, no. 9, pp. 22–27, Sep. 2020. [Online]. Available: https://doi.org/10.22156/CS4SMB.2020.10.09.022

[66] K. Chung, "Optimal detection for NOMA systems with correlated information sources of interactive mobile users," *J. Korea Inst. Electron. Commun. Sci.*, vol. 15, no. 4, pp. 651–658, Aug. 2020. [Online]. Available: http://dx.doi.org/10.13067/JKIECS.2020.15.4.651

[67] K. Chung, "On negative correlation bit-to-symbol(:B2S) mapping for NOMA with correlated information sources in 5G systems," *J. Korea Inst. Electron. Commun. Sci.*, vol. 15, no. 5, pp. 881–888, Oct. 2020. [Online]. Available: http://dx.doi.org/10.13067/JKIECS.2020.15.5.881

[68] N. Jaiswal and N. Purohit, "Performance analysis of NOMA-enabled vehicular communication systems with transmit antenna selection over double Nakagami-*m* fading," *IEEE Trans. Veh. Technol.*, vol. 70, no. 12, pp. 12725–12741, Dec. 2021.

[69] R. Makkar, V. Kotha, D. Rawal, V. K. Chakka, and N. Sharma, "Performance analysis of OSTBC in NOMA assisted downlink system with SIC errors," in *Proc. IEEE Veh. Technol. Conf. (VTC)*, London, U.K., Sep. 2022, pp. 1–5.

[70] A. Abushattal, S. Althunibat, M. Qaraqe, and H. Arslan, "A secure downlink NOMA scheme against unknown internal eavesdroppers," *IEEE Wireless Commun. Lett.*, vol. 10, no. 6, pp. 1281–1285, Jun. 2021.

[71] T. Alshamaseen, S. Althunibat, M. Qaraqe, and H. Alashaary, "Phase-assisted NOMA based key distribution for IoT networks," *Trans. Emerg. Telecommun. Technol.*, vol. 34, Apr. 2023, Art. no. e4738.

[72] A. M. A. Alkhazzar and H. Aghaeinia, "Symbol error rate analysis of non-orthogonal multiple access systems," *Phys. Commun.*, vol. 46, Jun. 2021, Art. no. 101295. [Online]. Available: https://www.sciencedirect.com/science/article/pii/S187449072100032X

[73] T. Assaf, A. Al-Dweik, M. E. Moursi, and H. Zeineldin, "Exact BER performance analysis for downlink NOMA systems over Nakagami-m fading channels," *IEEE Access*, vol. 7, pp. 134539–134555, Sep. 2019.

[74] J.-R. Garnier, A. Fabre, H. Farès, and R. Bonnefoi, "On the performance of QPSK modulation over Downlink NOMA: From error probability derivation to SDR-based validation," *IEEE Access*, vol. 8, pp. 66495–66507, Mar. 2020.

[75] M. Aldababsa, C. Göztepe, G. K. Kurt, and O. Kucur, "Bit error rate for NOMA network," *IEEE Commun. Lett.*, vol. 24, no. 6, pp. 1188–1191, Jun. 2020.

[76] N. Jaiswal and N. Purohit, "Performance of downlink NOMA-enabled vehicular communications over double rayleigh fading channels," *IET Commun.*, vol. 14, no. 20, pp. 3652–3660, Sep. 2020.

[77] S. Mukhtar and G. R. Begh, "On the performance analysis of downlink NOMA system over non-homogenous fading channel," in *Proc. IEEE Int. Conf. Comput. Power Commun. Technol. (GUCON)*, Kuala Lumpur, Malaysia, Nov. 2021, pp. 1–6.

[78] A. S. Alqahtani and E. Alsusa, "Performance analysis of downlink NOMA system over α-η-μ generalized fading channel," in *Proc. IEEE Veh. Technol. Conf. (VTC)*, Antwerp, Belgium, May 2020, pp. 1–5.

[79] B. M. ElHalawany, F. Jameel, D. B. da Costa, U. S. Dias, and K. Wu, "Performance analysis of Downlink NOMA systems over κ-μ shadowed fading channels," *IEEE Trans Veh. Technol.*, vol. 69, no. 1, pp. 1046–1050, Jan. 2020.

[80] X. Yan, H. Xiao, C. Wang, K. An, A. T. Chronopoulos, and G. Zheng, "Performance analysis of NOMA-based land mobile satellite networks," *IEEE Access*, vol. 6, pp. 31327–31339, Jun. 2018.

[81] A. Alqahtani, E. Alsusa, A. Al-Dweik, and M. Al-Jarrah, "Performance analysis for Downlink NOMA over α-μ generalized fading channels," *IEEE Trans. Veh. Technol.*, vol. 70, no. 7, pp. 6814–6825, Jul. 2021.

[82] P. Kumar and K. Dhaka, "Average BER analysis of NOMA systems under TWDP fading," in *Proc. Nat. Conf. Commun. (NCC)*, Guwahati, India, Feb. 2023, pp. 1–6.

[83] K. Aslan and T. Gucluoglu, "Performance analysis of downlink-NOMA over generalized-k fading channels," *Phys. Commun.*, vol. 48, Oct. 2021, Art. no. 101414.

[84] X. Wang, F. Labeau, and L. Mei, "Closed-form BER expressions of QPSK constellation for uplink non-orthogonal multiple access," *IEEE Commun. Lett.*, vol. 21, no. 10, pp. 2242–2245, Oct. 2017.

[85] X. Chen, H. Yin, and G. Wei, "Impact of frequency offset on the performance of uplink OFDM-NOMA systems," in *Proc. IEEE Int. Conf. Comput. Commun. (ICCC)*, Chengdu, China, Dec. 2018, pp. 168–173.

[86] F. Wei, T. Zhou, T. Xu, and H. Hu, "BER analysis for uplink NOMA in asymmetric channels," *IEEE Commun. Lett.*, vol. 24, no. 11, pp. 2435–2439, Nov. 2020.

[87] R. P. Sirigina, A. S. Madhukumar, and M. Bowyer, "BER analysis of interference-limited synchronous wireless networks with line-of-sight links," *IEEE Commun. Lett.*, vol. 23, no. 3, pp. 542–545, Mar. 2019.

[88] J. S. Yeom, H. S. Jang, K. S. Ko, and B. C. Jung, "BER performance of uplink NOMA with joint maximum-likelihood detector," *IEEE Trans. Veh. Technol.*, vol. 68, no. 10, pp. 10295–10300, Oct. 2019.

[89] C. Liu and N. C. Beaulieu, "Exact SER and BER analysis on jointly optimal maximum likelihood detection of two QPSK signals with phase offset," *IEEE Trans. Veh. Technol.*, vol. 70, no. 11, pp. 11695–11709, Nov. 2021.

[90] P. Shachi, T. Sanjana, K. R. Sudhindra, and M. N. Suma, "Outage and error-rate analysis of NOMA-inspired multicarrier underlay cognitive radio system," *IEEE Access*, vol. 10, pp. 113956–113968, Nov. 2022.

[91] H. Semira, F. Kara, H. Kaya, and H. Yanikomeroglu, "Error performance analysis of multiuser detection in uplink-NOMA with adaptive M-QAM," *IEEE Wireless Commun. Lett.*, vol. 11, no. 8, pp. 1654–1658, Aug. 2022.

[92] E. C. Cejudo, H. Zhu, and J. Wang, "Resource allocation in Multicarrier NOMA systems based on optimal channel gain ratios," *IEEE Trans. Wireless Commun.*, vol. 21, no. 1, pp. 635–650, Jan. 2022.

[93] T. Assaf, A. Al-Dweik, M. S. E. Moursi, and H. Zeineldin, "Efficient bit loading algorithm for OFDM-NOMA systems with BER constraints," *IEEE Trans. Veh. Technol.*, vol. 71, no. 1, pp. 423–436, Jan. 2022.

[94] H. Yahya, E. Alsusa, and A. Al-Dweik, "Design and analysis of NOMA with adaptive modulation and power under BLER constraints," *IEEE Trans. Veh. Technol.*, vol. 71, no. 10, pp. 11228–11233, Oct. 2022.

[95] H. Yahya, E. A. Alsusa, and A. Al-Dweik, "Min-max design and analysis of NOMA with adaptive modulation under BLER constraints," in *Proc. IEEE Veh. Technol. Conf. (VTC)*, London, U.K., Sep. 2022, pp. 1–5.

[96] W. Yu, H. Jia, and L. Musavian, "Joint adaptive M-QAM modulation and power adaptation for a Downlink NOMA network," *IEEE Trans. Commun.*, vol. 70, no. 2, pp. 783–796, Feb. 2022.

[97] K. Wang, T. Zhou, T. Xu, H. Hu, and X. Tao, "Asymmetric adaptive modulation for uplink NOMA systems," *IEEE Trans. Commun.*, vol. 69, no. 11, pp. 7222–7235, Nov. 2021.

[98] Y. Wang, J. Wang, D. W. Kwan Ng, R. Schober, and X. Gao, "A minimum error probability NOMA design," *IEEE Trans. Wireless Commun.*, vol. 20, no. 7, pp. 4221–4237, Jul. 2021.

[99] A. K. Dutta, "MBER criterion assisted power NOMA design and performance analysis with estimated channel," *IEEE Trans. Veh. Technol.*, vol. 68, no. 12, pp. 11816–11826, Dec. 2019.

[100] Z. Dong, H. Chen, J. K. Zhang, L. Huang, and B. Vucetic, "Uplink non-orthogonal multiple access with finite-alphabet inputs," *IEEE Trans. Wireless Commun.*, vol. 17, no. 9, pp. 5743–5758, Sep. 2018.

[101] C. Wang, Y. Wang, and P. Xiao, "Power allocation based on SINR balancing for NOMA systems with imperfect channel estimation," in *Proc. Int. Conf. Signal Process. Commun. Syst. (ICSPCS)*, Gold Coast, QLD, Australia, Dec. 2019, pp. 1–6.

[102] S. Shieh, C. Lin, Y. Huang, and C. Wang, "On gray labeling for downlink non-orthogonal multiple access without SIC," *IEEE Commun. Lett.*, vol. 20, no. 9, pp. 1721–1724, Sep. 2016.

[103] W. Han, Y. Wang, D. Tang, R. Hou, and X. Ma, "Study of the symbol error rate/bit error rate in non-orthogonal multiple access (NOMA) systems," in *Proc. IEEE/CIC Int. Conf. Commun. China (ICCC Workshops)*, Beijing, China, Aug. 2018, pp. 101–106.

[104] W. Han, X. Ma, D. Tang, and N. Zhao, "Study of SER and BER in NOMA systems," *IEEE Trans. Veh. Technol.*, vol. 70, no. 4, pp. 3325–3340, Apr. 2021.

[105] J. Yeom, E. Chu, B. Jung, and H. Jin, "Performance analysis of diversity-controlled multi-user superposition transmission for 5G wireless networks," *Sensors*, vol. 18, no. 2, p. 536, Feb. 2018. [Online]. Available: http://www.mdpi.com/1424--8220/18/2/536

[106] Q. Gao, M. Jia, Q. Guo, and X. Gu, "On the analysis and optimization of BER performance of symmetrical coding based NOMA," in *Proc. IEEE Wireless Commun. Netw. Conf. Workshops (WCNCW)*, May 2021, pp. 1–6.

[107] J. Zhang, X. Wang, T. Hasegawa, and T. Kubo, "Downlink non-orthogonal multiple access (NOMA) constellation rotation," in *Proc. IEEE Veh. Technol. Conf. (VTC)*, Montreal, QC, Canada, Sep. 2016, pp. 1–5.

[108] Y. Chang and K. Fukawa, "Non-orthogonal multiple access with phase rotation employing joint MUD and SIC," in *Proc. IEEE Veh. Technol. Conf. (VTC)*, Porto, Portugal, Jun. 2018, pp. 1–5.

[109] Y. Chang and K. Fukawa, "Phase rotated non-orthogonal multiple access for 3-user superposition signals," in *Proc. IEEE Veh. Technol. Conf. (VTC)*, Honolulu, HI, USA, Sep. 2019, pp. 1–5.

[110] B. K. Ng and C. T. Lam, "On joint modulation design in two-user non-orthogonal multiple access channels," in *Proc. Int. Symp. Wireless Commun. Syst. (ISWCS)*, Poznan, Poland, Oct. 2016, pp. 65–69.

[111] B. K. Ng and C.-T. Lam, "Joint power and modulation optimization in two-user non-orthogonal multiple access channels: A minimum error probability approach," *IEEE Trans. Veh. Technol.*, vol. 67, no. 11, pp. 10693–10703, Nov. 2018.

[112] X. Guan, Q. Yang, Y. Hong, and C. C.-K. Chan, "Non-orthogonal multiple access with phase pre-distortion in visible light communication," *Opt. Exp.*, vol. 24, no. 22, pp. 25816–25823, Oct. 2016. [Online]. Available: http://www.osapublishing.org/oe/abstract.cfm?URI=oe-24--22-25816

[113] M. Qiu, Y.-C. Huang, and J. Yuan, "Downlink NOMA without SIC for fast fading channels: Lattice partitions with algebraic rotations," in *Proc. IEEE Int. Conf. Commun. (ICC)*, Shanghai, China, Jul. 2019, pp. 1–6.

[114] M. Qiu, Y. C. Huang, and J. Yuan, "Downlink non-orthogonal multiple access without SIC for block fading channels: An algebraic rotation approach," *IEEE Trans. Wireless Commun.*, vol. 18, no. 8, pp. 3903–3918, Aug. 2019.

[115] N. Ye, A. Wang, X. Li, W. Liu, X. Hou, and H. Yu, "On constellation rotation of NOMA with SIC receiver," *IEEE Commun. Lett.*, vol. 22, no. 3, pp. 514–517, Mar. 2018.

[116] S. Ozyurt and O. Kucur, "Quadrature NOMA: A low-complexity multiple access technique with coordinate interleaving," *IEEE Wireless Commun. Lett.*, vol. 9, no. 9, pp. 1452–1456, Sep. 2020.

[117] H. Y. Lee and S. Y. Shin, "A novel user grouping in phase rotation based downlink NOMA," *IEEE Access*, vol. 10, pp. 27211–27222, Mar. 2022.

[118] K.-H. Lee, J. S. Yeom, J. Joung, and B. C. Jung, "Performance analysis of uplink NOMA with constellation–rotated STLC for IoT networks," *IEEE Open J. Commun. Soc.*, vol. 3, pp. 705–717, Apr. 2022.

[119] B. R. Reddy, S. P. Dash, and D. Ghose, "Optimal rotated M-PSK signaling for multi-user receive diversity system over correlated Rician fading channels," *IEEE Commun. Lett.*, vol. 27, no. 3, pp. 1006–1010, Mar. 2023.

[120] A. Chauhan and A. Jaiswal, "Non-orthogonal multiple access: A constellation domain multiplexing approach," in *Proc. IEEE Int. Symp. Pers. Indoor Mobile Radio Commun. (PIMRC)*, London, U.K., Aug./Sep. 2020, pp. 1–6.

[121] C. H. Lin, S. L. Shieh, T. C. Chi, and P. N. Chen, "Optimal inter-constellation rotation based on minimum distance criterion for uplink NOMA," *IEEE Trans. Veh. Technol.*, vol. 68, no. 1, pp. 525–539, Jan. 2019.

[122] H.-P. Liu, S.-L. Shieh, C.-H. Lin, and P.-N. Chen, "A minimum distance criterion based constellation design for uplink NOMA," in *Proc. IEEE Veh. Technol. Conf. (VTC)*, Honolulu, HI, USA, Nov. 2019, pp. 1–5.

[123] H.-P. Liu, Y.-C. Huang, S.-L. Shieh, and P.-N. Chen, "Power-domain downlink NOMA constellation design with heterogeneous reliability requirements," in *Proc. Int. Conf. Signal Process. Commun. Syst. (ICSPCS)*, Adelaide, SA, Australia, Feb. 2021, pp. 1–6.

[124] E. Khorov, A. Kureev, I. Levitsky, and I. F. Akyildiz, "Prototyping and experimental study of non-orthogonal multiple access in wi-Fi networks," *IEEE Netw.*, vol. 34, no. 4, pp. 210–217, Jul./Aug. 2020.

[125] A. Kureev, I. Levitsky, and E. Khorov, "Experimental study of constellation rotation in NOMA Wi-Fi networks," *J. Commun. Technol. Electron.*, vol. 65, pp. 1525–1530, Jan. 2020.

[126] E. Khorov, A. Kureev, I. Levitsky, and I. F. Akyildiz, "A phase noise resistant constellation rotation method and its experimental validation for NOMA Wi-Fi," *IEEE J. Sel. Areas Commun.*, vol. 40, no. 4, pp. 1346–1354, Apr. 2022.

[127] Y. Zhao, J. Hu, Z. Ding, and K. Yang, "Constellation rotation aided modulation design for the multi-user SWIPT-NOMA," in *Proc. IEEE Int. Commun. Conf. (ICC)*, Kansas City, MO, USA, May 2018, pp. 1–6.

[128] Y. Zhao, J. Hu, Z. Ding, and K. Yang, "Joint interleaver and modulation design for multi-user SWIPT-NOMA," *IEEE Trans. Commun.*, vol. 67, no. 10, pp. 7288–7301, Oct. 2019.

[129] X. Wan, X. Zhu, Y. Jiang, Y. Liu, and J. Zhao, "An interference alignment and ICA-based semiblind dual-user downlink NOMA system for high-reliability low-latency IoT," *IEEE Internet Things J.*, vol. 7, no. 11, pp. 10837–10851, Nov. 2020.

[130] H. Yahya, A. Al-Dweik, and E. Alsusa, "Power-tolerant NOMA using data-aware adaptive power assignment for IoT systems," *IEEE Internet Things J.*, vol. 8, no. 19, pp. 14896–14907, Oct. 2021.

[131] H. Yahya, E. Alsusa, and A. Al-Dweik, "Enhanced non-orthogonal multiple access using data-aware power assignment," in *Proc. Int. Symp. Netw. Comput. Commun. (ISNCC)*, pp. 1–6, Nov. 2021.

[132] P. Li, Z. Ding, and K. Feng, "Enhanced receiver based on FEC code constraints for uplink NOMA with imperfect CSI," *IEEE Trans. Wireless Commun.*, vol. 18, no. 10, pp. 4790–4802, Oct. 2019.

[133] K. Xiao, B. Xia, L. Ma, and Y. Wei, "Design and analysis of probabilistic shaping scheme for uplink nonorthogonal multiple access systems," *IEEE Trans. Commun.*, vol. 67, no. 12, pp. 8818–8833, Dec. 2019.

[134] X. Zou, M. Ganji, and H. Jafarkhani, "Trellis-coded non-orthogonal multiple access," *IEEE Wireless Commun. Lett.*, vol. 9, no. 4, pp. 538–542, Apr. 2020.

[135] B. K. Ng and C.-T. Lam, "A new two-user binary polar coded multiple access scheme with power and rate allocation," *IEEE Wireless Commun. Lett.*, vol. 10, no. 10, pp. 2299–2303, Oct. 2021.

[136] C. Yan, A. Harada, A. Benjebbour, Y. Lan, A. Li, and H. Jiang, "Receiver design for downlink non-orthogonal multiple access (NOMA)," in *Proc. IEEE Veh. Technol. Conf. (VTC)*, Jul. 2015, pp. 1–6.

[137] W. Abd-Alaziz, B. A. Jebur, H. Fakhrey, Z. Mei, and K. Rabie, "A low-complexity coding scheme for NOMA," *IEEE Syst. J.*, early access, Apr. 12, 2023, doi: 10.1109/JSYST.2023.3262174.

[138] S. Baig, U. Ali, H. M. Asif, A. A. Khan, and S. Mumtaz, "Closed-form BER expression for Fourier and wavelet transform-based pulse-shaped data in Downlink NOMA," *IEEE Commun. Lett.*, vol. 23, no. 4, pp. 592–595, Apr. 2019.

[139] A. Maatouk, E. Caliskan, M. Koca, M. Assaad, G. Gui, and H. Sari, "Frequency-domain NOMA with two sets of orthogonal signal waveforms," *IEEE Commun. Lett.*, vol. 22, no. 5, pp. 906–909, May 2018.

[140] A. A. Khansa, X. Chen, Y. Yin, G. Gui, and H. Sari, "Performance analysis of power-domain NOMA and NOMA-2000 on AWGN and Rayleigh fading channels," *Phys. Commun.*, vol. 43, Dec. 2020, Art. no. 101185.

[141] X. Zhang, Z. Wang, X. Ning, and H. Xie, "On the performance of GFDM assisted NOMA schemes," *IEEE Access*, vol. 8, pp. 88961–88968, May 2020.

[142] H. Haci, H. Zhu, and J. Wang, "A novel interference cancellation technique for non-orthogonal multiple access (NOMA)," in *Proc. IEEE Global Commun. Conf. (GLOBECOM)*, San Diego, CA, USA, Feb. 2016, pp. 1–6.

[143] H. Haci, H. Zhu, and J. Wang, "Performance of non-orthogonal multiple access with a novel asynchronous interference cancellation technique," *IEEE Trans. Commun.*, vol. 65, no. 3, pp. 1319–1335, Mar. 2017.

[144] C. Liu and N. C. Beaulieu, "Exact BER performance for symbol-asynchronous two-user non-orthogonal multiple access," *IEEE Commun. Lett.*, vol. 25, no. 3, pp. 764–768, Mar. 2021.

[145] C. Liu, N. C. Beaulieu, J. Cheng, S. Wu, C. Jiang, and H. Yang, "An analysis of the error rate performance for uplink asynchronous signal detection in non-orthogonal multiple access," *IEEE Trans. Commun.*, vol. 70, no. 7, pp. 4591–4606, Jul. 2022.

[146] V. Basnayake, D. N. K. Jayakody, H. Mabed, A. Kumar, and T. D. Ponnimbaduge Perera, "M-Ary QAM asynchronous-NOMA D2D network with cyclic triangular-SIC decoding scheme," *IEEE Access*, vol. 11, pp. 6045–6059, Jan. 2023.

[147] H. S. Ghazi and K. W. Wesoløwski, "Improved detection in successive interference cancellation NOMA OFDM receiver," *IEEE Access*, vol. 7, pp. 103325–103335, Jul. 2019.

[148] H. Xu and N. Pillay, "Threshold based signal detection and the average symbol error probability for downlink NOMA systems with M-ary QAM," *IEEE Access*, vol. 8, pp. 156677–156685, Aug. 2020.

[149] A. Al-Dweik, Y. Iraqi, K.-H. Park, M. Al-Jarrah, E. Alsusa, and M.-S. Alouini, "Efficient NOMA design without channel phase information using amplitude-coherent detection," *IEEE Trans. Commun.*, vol. 70, no. 1, pp. 245–263, Jan. 2022.

[150] R. Campello, G. Carlini, C. E. C. Souza, C. Pimentel, and D. P. B. Chaves, "Successive interference cancellation decoding with adaptable decision regions for NOMA schemes," *IEEE Access*, vol. 10, pp. 2051–2062, Jan. 2022.

[151] H. Huang, J. Wang, J. Wang, J. Yang, J. Xiong, and G. Gui, "Symbol error rate performance analysis of non-orthogonal multiple access for visible light communications," *China Commun.*, vol. 14, no. 12, pp. 153–161, Dec. 2017.

[152] H. Marshoud, P. C. Sofotasios, S. Muhaidat, G. K. Karagiannidis, and B. S. Sharif, "Error performance of NOMA VLC systems," in *Proc. IEEE Int. Conf. Commun. (ICC)*, Paris, France, May 2017, pp. 1–6.

[153] X. Liu, Y. Wang, F. Zhou, and R. Q. Hu, "BER analysis for NOMA-enabled visible light communication systems with M-PSK," in *Proc. Int. Conf. Wireless Commun. Signal Process. (WCSP)*, Hangzhou, China, Oct. 2018, pp. 1–7.

[154] X. Liu, Z. Chen, Y. Wang, F. Zhou, Y. Luo, and R. Q. Hu, "BER analysis of NOMA-enabled visible light communication systems with different modulations," *IEEE Trans. Veh. Technol.*, vol. 68, no. 11, pp. 10807–10821, Nov. 2019.

[155] E. M. Almohimmah and M. T. Alresheedi, "Error analysis of NOMA-based VLC systems with higher order modulation schemes," *IEEE Access*, vol. 8, pp. 2792–2803, Dec. 2020.

[156] T. Cao, H. Zhang, and J. Song, "BER performance analysis for Downlink nonorthogonal multiple access with error propagation mitigated method in visible light communications," *IEEE Trans. Veh. Technol.*, vol. 70, no. 9, pp. 9190–9206, Sep. 2021.

[157] J. Song, T. Cao, and H. Zhang, "Performance analysis of a low-complexity nonorthogonal multiple access scheme in visible light communication downlinks using pulse modulations," *Intell. Converg. Netw.*, vol. 2, no. 1, pp. 50–65, Mar. 2021.

[158] H. Ren et al., "Performance improvement of NOMA visible light communication system by adjusting superposition constellation: A convex optimization approach," *Opt. Exp.*, vol. 26, no. 23, pp. 29796–29806, Nov. 2018. [Online]. Available: http://www.osapublishing.org/oe/abstract.cfm?URI=oe-26--23-29796

[159] V. Dixit and A. Kumar, "An exact error analysis of multi-user RC/MRC based MIMO-NOMA-VLC system with imperfect SIC," *IEEE Access*, vol. 9, pp. 136710–136720, Oct. 2021.

[160] V. Dixit and A. Kumar, "An exact BER analysis of NOMA-VLC system with imperfect SIC and CSI," *Int. J. Electron. Commun.*, vol. 138, pp. 1434–8411, Aug. 2021. [Online]. Available: https://doi.org/10.1016/j.aeue.2021.153864

[161] V. Dixit and A. Kumar, "BER analysis of dynamic FOV based MIMO-NOMA-VLC system," *Int. J. Electron. Commun.*, vol. 142, Dec. 2021, Art. no. 153989. [Online]. Available: https://www.sciencedirect.com/science/article/pii/S1434841121003861

[162] R. Mitra and V. Bhatia, "Precoded Chebyshev-NLMS-based predistorter for nonlinear LED compensation in NOMA-VLC," *IEEE Trans. Commun.*, vol. 65, no. 11, pp. 4845–4856, Nov. 2017.

[163] S. Rajkumar, P. Tennakoon, and D. N. K. Jayakody, "NOMA-PLNC based visible light communications," in *Proc. Conf. Cloud Internet Things (CIoT)*, Lisbon, Portugal, Apr. 2023, pp. 183–189.

[164] P. Saxena and M. R. Bhatnagar, "1-bit feedback-based beamforming scheme for an uplink FSO-NOMA system with SIC errors," *Appl. Opt.*, vol. 59, no. 36, pp. 11274–11291, Dec. 2020. [Online]. Available: http://ao.osa.org/abstract.cfm?URI=ao-59--36-11274

[165] V. C. Thirumavalavan and T. S. Jayaraman, "BER analysis of reconfigurable intelligent surface assisted downlink power domain NOMA system," in *Proc. Int. Conf. Commun. Syst. Netw. (COMSNETS)*, Bengaluru, India, Mar. 2020, pp. 519–522.

[166] L. Bariah, S. Muhaidat, P. C. Sofotasios, F. E. Bouanani, O. A. Dobre, and W. Hamouda, "Large intelligent surface-assisted nonorthogonal multiple access for 6G networks: Performance analysis," *IEEE Internet Things J.*, vol. 8, no. 7, pp. 5129–5140, Apr. 2021.

[167] A. Chauhan, S. Ghosh, and A. Jaiswal, "RIS partition-assisted non-orthogonal multiple access (NOMA) and quadrature-NOMA with imperfect SIC," *IEEE Trans. Wireless Commun.*, vol. 22, no. 7, pp. 4371–4386, Jul. 2023.

[168] A. Alqahtani and E. Alsusa, "On the quality of service and experience in IRS-NOMA over $\kappa - \mu$ generalized fading channels," *IEEE Open J. Commun. Soc.*, vol. 3, pp. 2272–2283, Nov. 2022.

[169] M. Aldababsa, A. Khaleel, and E. Basar, "STAR-RIS-NOMA networks: An error performance perspective," *IEEE Commun. Lett.*, vol. 26, no. 8, pp. 1784–1788, Aug. 2022.

[170] M. Aldababsa, A. A. Mwais, and M. Obaid, "Performance of STAR-RIS assisted NOMA networks in Nakagami-*m* fading channels," *Int. J. Electron. Commun.*, vol. 166, Jul. 2023, Art. no. 154685. [Online]. Available: https://www.sciencedirect.com/science/article/pii/S1434841123001590

[171] B. Y. D. Rito and K. H. Li, "RIS-assisted NOMA with interference-cancellation and interference-alignment scheme," *IEEE Commun. Lett.*, vol. 27, no. 3, pp. 1011–1015, Mar. 2023.

[172] A. W. Nazar, S. A. Hassan, H. Jung, A. Mahmood, and M. Gidlund, "BER analysis of a backscatter communication system with non-orthogonal multiple access," *IEEE Trans. Green Commun. Netw.*, vol. 5, no. 2, pp. 574–586, Jun. 2021.

[173] S. Rajkumar and D. N. K. Jayakody, "Backscatter assisted NOMA-PLNC based wireless networks," *Sensors*, vol. 21, no. 22, p. 7589, Nov. 2021. [Online]. Available: https://www.mdpi.com/1424--8220/21/22/7589

[174] F. Kara and H. Kaya, "Error probability analysis of NOMA-based diamond relaying network," *IEEE Trans. Veh. Technol.*, vol. 69, no. 2, pp. 2280–2285, Feb. 2020.

[175] F. Kara and H. Kaya, "Improved error performance in NOMA-based diamond relaying," in *Proc. IEEE Microw. Theory Techn. Wireless Commun. (MTTW)*, vol. 1. Riga, Latvia, Oct. 2020, pp. 151–156.

[176] F. Kara and H. Kaya, "Improved user fairness in decode-forward relaying non-orthogonal multiple access schemes with imperfect SIC and CSI," *IEEE Access*, vol. 8, pp. 97540–97556, May 2020.

[177] F. Kara, H. Kaya, and H. Yanikomeroglu, "A lightweight machine learning assisted power optimization for minimum error in NOMA-CRS over Nakagami-*m* channels," *IEEE Trans. Veh. Technol.*, vol. 70, no. 10, pp. 11067–11072, Oct. 2021.

[178] L. Mohjazi, L. Bariah, S. Muhaidat, P. C. Sofotasios, O. Onireti, and M. A. Imran, "Error probability analysis of non-orthogonal multiple access for relaying networks with residual hardware impairments," in *Proc. IEEE Int. Symp. Pers. Indoor Mobile Radio Commun. (PIMRC)*, Istanbul, Turkey, Sep. 2019, pp. 1–6.

[179] M. Shen, Z. Huang, X. Lei, and L. Fan, "BER analysis of NOMA with max-min relay selection," *China Commun.*, vol. 18, no. 7, pp. 172–182, Jul. 2021.

[180] D. Zhu, Y. Yao, L. Xu, H. Zhang, H. Fang, and X. Li, "Analysis of asymptotically tight approximation SER for cooperative NOMA systems," in *Proc. IEEE Int. Conf. Commun. Technol. (ICCT)*, Xi'an, China, Oct. 2019, pp. 34–39.

[181] S. Beddiaf et al., "A unified performance analysis of cooperative NOMA with practical constraints: Hardware impairment, imperfect SIC and CSI," *IEEE Access*, vol. 10, pp. 132931–132948, 2022.

[182] S. Althunibat, H. Hassan, T. Khattab, and N. Zorba, "A new NOMA-based two-way relaying scheme," *IEEE Trans. Veh. Technol.*, early access, Apr. 5, 2023, doi: 10.1109/TVT.2023.3264905.

[183] R. Chai, L. Liu, F. Zou, J. Li, and Q. Chen, "Performance analysis of NOMA-based hybrid satellite-terrestrial relay networks with CCI," *IEEE Trans. Netw. Sci. Eng.*, vol. 10, no. 4, pp. 2016–2029, Jul./Aug. 2023.

[184] A. Olfat, "Resource allocation and BER performance analysis of NOMA based cooperative networks," *Telecommun. Syst.*, pp. 1–13, 2023.

[185] S. Soni, R. Makkar, D. Rawal, and N. Sharma, "Performance analysis of selective DF cooperative NOMA in presence of practical impairments," *IEEE Syst. J.*, vol. 83, pp. 227–239, Jul. 2023.

[186] F. Kara and H. Kaya, "Threshold-based selective cooperative-NOMA," *IEEE Commun. Lett.*, vol. 23, no. 7, pp. 1263–1266, Jul. 2019.

[187] F. Kara and H. Kaya, "On the error performance of cooperative-NOMA with statistical CSIT," *IEEE Commun. Lett.*, vol. 23, no. 1, pp. 128–131, Jan. 2019.

[188] M. Jain, N. Sharma, A. Gupta, D. Rawal, and P. Garg, "Performance analysis of NOMA assisted mobile ad hoc networks for sustainable future radio access," *IEEE Trans. Sustain. Comput.*, vol. 6, no. 2, pp. 347–357, Apr.-Jun. 2021.

[189] M. Li, S. Huang, L. Tian, O. Alhussein, and S. Muhaidat, "Error rate performance of NOMA system with full-duplex cooperative relaying," *Phys. Commun.*, vol. 49, Dec. 2021, Art. no. 101447.

[190] M. Sashiganth, S. Thiruvengadam, and D. S. Kumar, "BER analysis of full duplex NOMA downlink and uplink co-operative user relaying systems over Nakagami-m fading environment," *Phys. Commun.*, vol. 38, Feb. 2020, Art. no. 100963.

[191] A. A. Hamza, I. Dayoub, I. Alouani, and A. Amrouche, "On the error rate performance of full-duplex cooperative NOMA in wireless networks," *IEEE Trans. Commun.*, vol. 70, no. 3, pp. 1742–1758, Mar. 2022.

[192] S. Li, L. Bariah, S. Muhaidat, P. Sofotasios, J. Liang, and A. Wang, "Error analysis of NOMA-based user cooperation with SWIPT," in *Proc. Int. Conf. Distrib. Comput. Sensor Syst. (DCOSS)*, May 2019, pp. 507–513.

[193] L. Bariah, S. Muhaidat, and A. Al-Dweik, "Error probability analysis of NOMA-based relay networks with SWIPT," *IEEE Commun. Lett.*, vol. 23, no. 7, pp. 1223–1226, Jul. 2019.

[194] F. Kara, "Error performance of cooperative relaying systems empowered by SWIPT and NOMA," *Phys. Commun.*, vol. 49, Dec. 2021, Art. no. 101450.

[195] F. Khennoufa, A. Khelil, K. Rabie, H. Kaya, and X. Li, "An efficient hybrid energy harvesting protocol for cooperative NOMA systems: Error and outage performance," *Phys. Commun.*, vol. 58, Jun. 2023, Art. no. 102061.

[196] S. Li, A. Wang, and J. Liang, "PEP analysis of AF relay NOMA systems employing order statistics of cascaded channels," *Electron.*, vol. 8, no. 6, p. 695, Jun. 2019. [Online]. Available: https://www.mdpi.com/2079--9292/8/6/695

[197] S. Li, L. Bariah, S. Muhaidat, P. C. Sofotasios, J. Liang, and A. Wang, "SWIPT-enabled cooperative NOMA with *m*th best relay selection," *IEEE Open J. Commun. Soc.*, vol. 1, pp. 1798–1807, Nov. 2020.

[198] L. Bariah, S. Muhaidat, and A. Al-Dweik, "Error performance of NOMA-based cognitive radio networks with partial relay selection and interference power constraints," *IEEE Trans. Commun.*, vol. 68, no. 2, pp. 765–777, Feb. 2020.

[199] S. Üstünbaş and U. Aygölü, "BER analysis of non-orthogonal multiple access-based cognitive butterfly network," *Electron. Lett.*, vol. 56, no. 7, pp. 357–360, Mar. 2020. [Online]. Available: https://onlinelibrary.wiley.com/doi/10.1049/el.2019.3618

[200] K. Sultan, "Best relay selection schemes for NOMA based cognitive relay networks in underlay spectrum sharing," *IEEE Access*, vol. 8, pp. 190160–190172, Oct. 2020.

[201] S. Dhanasekaran and T. R. Sushma, "Performance analysis of cell-Center users in NOMA based-spectrum sharing protocol," *IEEE Commun. Lett.*, vol. 24, no. 1, pp. 52–56, Jan. 2020.

[202] H. Sadat, M. Abaza, S. M. Gasser, and H. ElBadawy, "Performance analysis of cooperative non-orthogonal multiple access in visible light communication," *Appl. Sci.*, vol. 9, no. 19, p. 4004, Sep. 2019. [Online]. Available: https://www.mdpi.com/2076--3417/9/19/4004

[203] F. Kara and H. Kaya, "Spatial multiple access (SMA): Enhancing performances of MIMO-NOMA systems," in *Proc. Int. Conf. Telecomm. Signal Process. (TSP)*, Budapest, Hungary, Jul. 2019, pp. 466–471.

[204] P. Yang, Y. Xiao, M. Xiao, and Z. Ma, "NOMA-aided precoded spatial modulation for downlink MIMO transmissions," *IEEE J. Sel. Topics Signal Process.*, vol. 13, no. 3, pp. 729–738, Jun. 2019.

[205] J. Li, J. Hou, L. Fan, Y. Yan, X. Q. Jiang, and H. Hai, "NOMA-aided generalized pre-coded quadrature spatial modulation for downlink communication systems," *China Commun.*, vol. 17, no. 11, pp. 120–130, Nov. 2020.

[206] X. Zhu, Z. Wang, and J. Cao, "NOMA-based spatial modulation," *IEEE Access*, vol. 5, pp. 3790–3800, Mar. 2017.

[207] Q. Si, M. Jin, Y. Chen, N. Zhao, and X. Wang, "Performance analysis of spatial modulation aided NOMA with full-duplex relay," *IEEE Trans. Veh. Technol.*, vol. 69, no. 5, pp. 5683–5687, May 2020.

[208] Q. Li, M. Wen, E. Basar, H. V. Poor, and F. Chen, "Spatial modulation-aided cooperative NOMA: Performance analysis and comparative study," *IEEE J. Sel. Topics Signal Process.*, vol. 13, no. 3, pp. 715–728, Jun. 2019.

[209] A. Shehni and M. F. Flanagan, "Distributed spatial modulation aided NOMA," in *Proc. Eur. Conf. Netw. Commun. (EuCNC)*, Valencia, Spain, Jun. 2019, pp. 325–330.

[210] J. Li, S. Dang, Y. Yan, Y. Peng, S. Al-Rubaye, and A. Tsourdos, "Generalized quadrature spatial modulation and its application to vehicular networks with NOMA," *IEEE Trans. Intell. Transp. Syst.*, vol. 22, no. 7, pp. 4030–4039, Jul. 2021.

[211] M. Can, I. Altunbas, and E. Basar, "NOMA-based downlink relaying with media-based modulation," *Phys. Commun.*, vol. 41, Aug. 2020, Art. no. 101116.

[212] X. Chen, M. Wen, T. Mao, and S. Dang, "Spectrum resource allocation based on cooperative NOMA with index modulation," *IEEE Trans. Cogn. Commun. Netw.*, vol. 6, no. 3, pp. 946–958, Sep. 2020.

[213] X. Chen, M. Wen, and S. Dang, "On the performance of cooperative OFDM-NOMA system with index modulation," *IEEE Wireless Commun. Lett.*, vol. 9, no. 9, pp. 1346–1350, Sep. 2020.

[214] A. Tusha, S. Doğan, and H. Arslan, "A hybrid Downlink NOMA with OFDM and OFDM-IM for beyond 5G wireless networks," *IEEE Signal Process. Lett.*, vol. 27, pp. 491–495, 2020.

[215] Y.-K. Bae, J. S. Yeom, and B. C. Jung, "Performance analysis of uplink index-modulated NOMA for 6G wireless communications," *IEEE Wireless Commun. Lett.*, early access, May 16, 2023, doi: 10.1109/LWC.2023.3275944.

[216] S. Doğan, A. Tusha, and H. Arslan, "NOMA with index modulation for uplink URLLC through grant-free access," *IEEE J. Sel. Topics Signal Process.*, vol. 13, no. 6, pp. 1249–1257, Oct. 2019.

[217] M. B. Shahab, S. J. Johnson, M. Shirvanimoghaddam, M. Chafii, E. Basar, and M. Dohler, "Index modulation aided uplink NOMA for massive machine type communications," *IEEE Wireless Commun. Lett.*, vol. 9, no. 12, pp. 2159–2162, Dec. 2020.

[218] A. Almohamad, S. Althunibat, M. Hasna, and K. Qaraqe, "A downlink index-modulation based nonorthogonal multiple access scheme," in *Proc. IEEE Int. Symp. Pers. Indoor Mobile Radio Commun. (PIMRC)*, London, U.K., Aug./Sep. 2020, pp. 1–6.

[219] S. Althunibat, R. Mesleh, and T. F. Rahman, "A novel uplink multiple access technique based on index-modulation concept," *IEEE Trans. Commun.*, vol. 67, no. 7, pp. 4848–4855, Jul. 2019.

[220] K. Lai, J. Lei, L. Wen, and G. Chen, "Codeword position index modulation design for sparse code multiple access system," *IEEE Trans. Veh. Technol.*, vol. 69, no. 11, pp. 13273–13288, Nov. 2020.

[221] X. Pei, Y. Chen, M. Wen, H. Yu, E. Panayirci, and H. V. Poor, "Next-generation multiple access based on NOMA with power level modulation," *IEEE J. Sel. Areas Commun.*, vol. 40, no. 4, pp. 1072–1083, Apr. 2022.

[222] Y. Yu, H. Chen, Y. Li, Z. Ding, and B. Vucetic, "On the performance of non-orthogonal multiple access in short-packet communications," *IEEE Commun. Lett.*, vol. 22, no. 3, pp. 590–593, Mar. 2018.

[223] J. Zheng, Q. Zhang, and J. Qin, "Average block error rate of downlink NOMA short-packet communication systems in Nakagami-m fading channels" *IEEE Commun. Lett.*, vol. 23, no. 10, pp. 1712–1716, Oct. 2019.

[224] L. Yuan, Z. Zheng, N. Yang, and J. Zhang, "Performance analysis of short-packet non-orthogonal multiple access with Alamouti space-time block coding," *IEEE Trans. Veh. Technol.*, vol. 70, no. 3, pp. 2900–2905, Mar. 2021.

[225] X. Lai, T. Wu, Q. Zhang, and J. Qin, "Average secure BLER analysis of NOMA Downlink short-packet communication systems in flat rayleigh fading channels," *IEEE Trans. Wireless Commun.*, vol. 20, no. 5, pp. 2948–2960, May 2021.

[226] X. Lai, Q. Zhang, and J. Qin, "Downlink NOMA networks with hybrid long-packet and short-packet communications in flat rayleigh fading channels," *IEEE Syst. J.*, vol. 14, no. 3, pp. 3410–3413, Sep. 2020.

[227] N. P. Le and K. N. Le, "Uplink NOMA short-packet communications with residual hardware impairments and channel estimation errors," *IEEE Trans. Veh. Technol.*, vol. 71, no. 4, pp. 4057–4072, Apr. 2022.

[228] N. P. Le and K. N. Le, "Performance analysis of NOMA short-packet communications with QoS-based SIC detecting order," *IEEE Wireless Commun. Lett.*, vol. 11, no. 3, pp. 617–621, Mar. 2022.

[229] F. Ghanami, S. Poursheikhali, and M. Shirvanimoghaddam, "Dynamic NOMA-HARQ in the finite blocklength regime: Performance analysis and optimization," *IEEE Commun. Lett.*, vol. 27, no. 4, pp. 1220–1224, Apr. 2023.

[230] X. Lai, Q. Zhang, and J. Qin, "Cooperative NOMA short-packet communications in flat Rayleigh fading channels," *IEEE Trans. Veh. Technol.*, vol. 68, no. 6, pp. 6182–6186, Jun. 2019.

[231] T.-H. Vu, T.-V. Nguyen, T.-T. Nguyen, V. N. Q. Bao, and S. Kim, "Short-packet communications in NOMA-CDRT IoT networks with Cochannel interference and imperfect SIC," *IEEE Trans. Veh. Technol.*, vol. 71, no. 5, pp. 5552–5557, May 2022.

[232] T.-H. Vu, T.-V. Nguyen, T.-T. Nguyen, D. B. da Costa, and S. Kim, "Performance analysis of short-packet NOMA-based CDRT networks over Nakagami-*m* fading channels," *IEEE Trans. Veh. Technol.*, vol. 71, no. 12, pp. 12928–12942, Dec. 2022.

[233] L. Yuan, Q. Du, and F. Fang, "Performance analysis of full-duplex cooperative NOMA short-packet communications," *IEEE Trans. Veh. Technol.*, vol. 71, no. 12, pp. 13409–13414, Dec. 2022.

[234] T.-H. Vu, T.-T. Nguyen, Q.-V. Pham, D. B. da Costa, and S. Kim, "A novel partial decode-and-amplify NOMA-inspired relaying protocol for uplink short-packet communications," *IEEE Wireless Commun. Lett.*, vol. 12, no. 7, pp. 1244–1248, Jul. 2023.

[235] T.-H. Vu, T.-V. Nguyen, T.-T. Nguyen, and S. Kim, "Performance analysis and deep learning design of wireless powered cognitive NOMA IoT short-packet communications with imperfect CSI and SIC," *IEEE Internet Things J.*, vol. 9, no. 13, pp. 10464–10479, Jul. 2022.

[236] Z. Xiang et al., "Cognitive radio-inspired NOMA in short-packet communications," *IEEE Trans. Veh. Technol.*, early access, May 24, 2023, doi: 10.1109/TVT.2023.3279439.

[237] C. Xia, Z. Xiang, J. Meng, H. Liu, and G. Pan, "NOMA-assisted cognitive short-packet communication with node mobility and imperfect channel estimation," *IEEE Trans. Veh. Technol.*, early access, Apr. 25, 2023, doi: 10.1109/TVT.2023.3270349.

[238] G. N. Tran and S. Kim, "Performance analysis of short packets in NOMA VLC systems," *IEEE Access*, vol. 10, pp. 6505–6517, Jan. 2022.

[239] G. N. Tran and S. Kim, "Performance evaluation of short packet communications in NOMA VLC systems with imperfect CSI," *IEEE Access*, vol. 10, pp. 49781–49793, May 2022.

[240] T.-H. Vu, T.-V. Nguyen, D. B. D. Costa, and S. Kim, "Intelligent reflecting surface-aided short-packet non-orthogonal multiple access systems," *IEEE Trans. Veh. Technol.*, vol. 71, no. 4, pp. 4500–4505, Apr. 2022.

[241] T.-H. Vu, T.-V. Nguyen, Q.-V. Pham, D. B. da Costa, and S. Kim, "STAR-RIS-enabled short-packet NOMA systems," *IEEE Trans. Veh. Technol.*, early access, May 23, 2023, doi: 10.1109/TVT.2023.3278737.

[242] F. Karim, S. K. Singh, K. Singh, S. Prakriya, and M. F. Flanagan, "On the performance of STAR-RIS-aided NOMA at finite blocklength," *IEEE Wireless Commun. Lett.*, vol. 12, no. 5, pp. 868–872, May 2023.

[243] J. Xu, L. Yuan, N. Yang, N. Yang, and Y. Guo, "Performance analysis of STAR-IRS aided NOMA short-packet communications with statistical CSI," *IEEE Trans. Veh. Technol.*, early access, Apr. 13, 2023, doi: 10.1109/TVT.2023.3266830.

[244] L. Yuan, Q. Du, N. Yang, F. Fang, and N. Yang, "Performance analysis of IRS-aided short-packet NOMA systems over Nakagami-*m* fading channels," *IEEE Trans. Veh. Technol.*, vol. 72, no. 6, pp. 8228–8233, Jun. 2023.

[245] J. Bao, Z. Ma, G. K. Karagiannidis, M. Xiao, and Z. Zhu, "Joint multiuser detection of multidimensional constellations over fading channels," *IEEE Trans. Commun.*, vol. 65, no. 1, pp. 161–172, Jan. 2017.

[246] Y. Liu, L. Yang, P. Xiao, H. Haas, and L. Hanzo, "Spatial modulated Multicarrier sparse code-division multiple access," *IEEE Trans. Wireless Commun.*, vol. 19, no. 1, pp. 610–623, Jan. 2020.

[247] E. Sfeir, R. Mitra, G. Kaddoum, and V. Bhatia, "Performance analysis of maximum-Correntropy based detection for SCMA," *IEEE Commun. Lett.*, vol. 25, no. 4, pp. 1114–1118, Apr. 2021.

[248] L. Yu, P. Fan, X. Lei, and P. T. Mathiopoulos, "BER analysis of SCMA systems with Codebooks based on star-QAM signaling constellations," *IEEE Commun. Lett.*, vol. 21, no. 9, pp. 1925–1928, Sep. 2017.

[249] L. Yu, P. Fan, D. Cai, and Z. Ma, "Design and analysis of SCMA Codebook based on star-QAM signaling constellations," *IEEE Trans. Veh. Technol.*, vol. 67, no. 11, pp. 10543–10553, Nov. 2018.

[250] B. Ling, C. Dong, J. Dai, and J. Lin, "Multiple decision aided successive interference cancellation receiver for NOMA systems," *IEEE Wireless Commun. Lett.*, vol. 6, no. 4, pp. 498–501, Aug. 2017.

[251] W. B. Ameur, P. Mary, M. Dumay, J. Hélard, and J. Schwoerer, "Power allocation for BER minimization in an uplink MUSA scenario," in *Proc. IEEE Veh. Technol. Conf. (VTC)*, Antwerp, Belgium, May 2020, pp. 1–5.

[252] Q. Wu, S. Zhang, B. Zheng, C. You, and R. Zhang, "Intelligent reflecting surface-aided wireless communications: A tutorial," *IEEE Trans. Commun.*, vol. 69, no. 5, pp. 3313–3351, May 2021.

[253] Z. Wang, Y. Liu, X. Mu, Z. Ding, and O. A. Dobre, "NOMA empowered integrated sensing and communication," *IEEE Commun. Lett.*, vol. 26, no. 3, pp. 677–681, Mar. 2022.

[254] "Study on downlink multiuser superposition transmission (MUST) for LTE (release 13)," 3GPP, Sophia Antipolis, France, 3GPP Rep. 36.859, 2015. [Online]. Available: https://www.3gpp.org/ftp/Specs/archive/36_series/36.859/

[255] H. Lee, S. Kim, and J.-H. Lim, "Multiuser superposition transmission (MUST) for LTE-a systems," in *Proc. IEEE Int. Conf. Commun. (ICC)*, Kuala Lumpur, Malaysia, May 2016, pp. 1–6.

[256] A. Al-Dweik, E. Alsusa, O. A. Dobre, and R. Hamila. "Multirate NOMA for improving connectivity in 6G communications networks." 2023. [Online]. Available: https://www.techrxiv.org/articles/preprint/Multirate_NOMA_for_Improving_Connectivity_in_6G_Communications_Networks/22258660

[257] A. Al-Dweik and Y. Iraqi, "High throughput wireless links for time-sensitive WSNs with reliable data requirements," *IEEE Sensors J.*, vol. 21, no. 21, pp. 24890–24898, Nov. 2021.

[258] H. Yahya, A. Al-Dweik, Y. Iraqi, E. Alsusa, and A. Ahmed, "A power and spectrum efficient uplink transmission scheme for QoS-constrained IoT networks," *IEEE Internet Things J.*, vol. 9, no. 18, pp. 17425–17439, Sep. 2022.

[259] B. Clerckx et al., "Is NOMA efficient in multi-antenna networks? a critical look at next generation multiple access techniques," *IEEE Open J. Commun. Soc.*, vol. 2, pp. 1310–1343, 2021.

[260] B. Clerckx et al., "A primer on rate-splitting multiple access: Tutorial, myths, and frequently asked questions," *IEEE J. Sel. Areas Commun.*, vol. 41, no. 5, pp. 1265–1308, May 2023.

[261] F. Xiao, X. Li, L. Yang, H. Liu, and T. A. Tsiftsis, "Outage performance analysis of RSMA-aided semi-grant-free transmission systems," *IEEE Open J. Commun. Soc.*, vol. 4, pp. 253–268, 2023.

[262] A. Bansal, K. Singh, B. Clerckx, C.-P. Li, and M.-S. Alouini, "Rate-splitting multiple access for intelligent reflecting surface aided multi-user communications," *IEEE Trans. Veh. Technol.*, vol. 70, no. 9, pp. 9217–9229, Sep. 2021.

[263] A. Bansal, K. Singh, and C.-P. Li, "Analysis of hierarchical rate splitting for intelligent reflecting surfaces-aided downlink multiuser MISO communications," *IEEE Open J. Commun. Soc.*, vol. 2, pp. 785–798, 2021.

[264] M. Choi, D. Yoon, and J. Kim, "Blind signal classification for non-orthogonal multiple access in vehicular networks," *IEEE Trans. Veh. Technol.*, vol. 68, no. 10, pp. 9722–9734, Oct. 2019.

[265] C.-P. Wei, H. Yang, C.-P. Li, and Y.-M. Chen, "SCMA decoding via deep learning," *IEEE Wireless Commun. Lett.*, vol. 10, no. 4, pp. 878–881, Apr. 2021.

HAMAD YAHYA (Graduate Student Member, IEEE) was born in Sharjah, UAE, in 1997. He received the B.Sc. degree in electrical engineering/communications from Ajman University, Ajman, UAE, in 2018, where he was the top of the class and the M.Sc. degree (with Distinction) in communications and signal processing from The University of Manchester, Manchester, U.K., in 2019, where he is currently pursuing the Ph.D. degree in electrical and electronic engineering.

He is also a Research Associate with the Communication Systems Group with The University of Manchester. His research interests include wireless communications for future wireless networks, optimization, and visible light communications. He received the Best Student and the Best Project Prizes from the Department of Electrical and Electronic Engineering, The University of Manchester. He was nominated for the Distinguished Achievement Award in 2019, where he was among the top 14 postgraduate taught students across the Faculty of Science and Engineering. He is the recipient of the M.Sc. Success Scholarship from The University of Manchester.

ASHFAQ AHMED (Senior Member, IEEE) received the M.S. and Ph.D. degrees from the Department of Electronics and Telecommunications, Politecnico di Torino, Torino, Italy, in 2010 and 2014, respectively.

He is currently affiliated with the Center for Cyber-Physical Systems, Department of Electrical Engineering and Computer Science, Khalifa University, Abu Dhabi, UAE. He worked as an Assistant Professor with the Department of Electrical and Computer Engineering, COMSATS University Islamabad, Wah campus, Pakistan, from March 2014 to March 2021. His research interests include hardware security, security protocols, computational intelligence, evolutionary algorithms, convex optimization, resource allocation, and applied optimization for 5G and beyond 5G applications, cloud computing, and physical layer wireless communication. He has hands-on experience with simulation and modeling of optimization problems, as well as working with a variety of optimization toolboxes, including the MATLAB optimization toolbox and the OPTI toolbox. He also developed heuristics and applied several meta-heuristics to various optimization problems.

EMAD ALSUSA (Senior Member, IEEE) received the Ph.D. degree in telecommunications from the University of Bath, U.K., in 2000. In 2000, he was appointed to work on developing high data rates systems as part of an Industrial Project based at Edinburgh University. He joined Manchester University (then UMIST) as a Faculty Member in September 2003, where his current rank is a Reader with the Communications Engineering Group. His research work has resulted in over 200 journals and refereed conference publications mainly in top IEEE transactions and conferences. He has supervised over 30 Ph.D.s to successful completion. His research interests lie in the area of Communications Systems with a focus on Physical, MAC and Network Layers including developing techniques and algorithms for array signal detection, channel estimation and equalization, adaptive signal precoding, interference avoidance through novel radio resource management techniques, cognitive radio, and energy and spectrum optimization techniques. Applications of his research include cellular networks, IoT, Industry 4.0, and powerline communications. He has received a number of awards, including the Best Paper Award in the international Symposium on Power Line Communications 2016 and the Wireless Communications and Networks Conference 2019. He is an Editor of the IEEE WIRELESS COMMUNICATIONS LETTERS, a Fellow of the U.K. Higher Academy of Education, and the TPC Track Chair of a number of conferences, such as VTC'16, GISN'16, PIMRC'17, and Globecom'18, as well as the General Co-Chair of the OnlineGreenCom'16 Conference. He is currently the U.K. representative in the International Union of Radio Science and the Co-Chair of the IEEE Special Working Group on RF Energy Harvesting.

ARAFAT AL-DWEIK (Senior Member, IEEE) received the M.S. (Summa Cum Laude) and the Ph.D. (Magna Cum Laude) degrees in electrical engineering from Cleveland State University, Cleveland, OH, USA, in 1998 and 2001, respectively.

He is currently with the Department of Electrical Engineering and Computer Science, Khalifa University, Abu Dhabi, UAE. He also worked with Efficient Channel Coding, Inc., Cleveland; the Department of Information Technology, Arab American University, Jenin, Palestine; and the University of Guelph, ON, Canada. He is a Visiting Research Fellow with the School of Electrical, Electronic, and Computer Engineering, Newcastle University, Newcastle upon Tyne, U.K, and a Research Professor with Western University, London, ON, Canada, and the University of Guelph, Guelph, Canada. He has extensive research experience in various areas of wireless communications that include modulation techniques, channel modeling and characterization, synchronization and channel estimation techniques, OFDM technology, error detection and correction techniques, MIMO, and resource allocation for wireless networks.

Dr. Al-Dweik was the recipient of the Hijjawi Award for Applied Sciences in 2003, the Fulbright Alumni Development Grant in 2003 and 2005, the Dubai Award for Sustainable Transportation in 2016, and the UAE Leader-Founder Award in 2019. He was awarded the Fulbright scholarship from 1997 to 1999. He serves as an Associate Editor for the IEEE TRANSACTIONS ON VEHICULAR TECHNOLOGY and the *IET Communications*. He is a Registered Professional Engineer in the Province of Ontario, Canada. He is a member of Tau Beta Pi and Eta Kappa Nu.

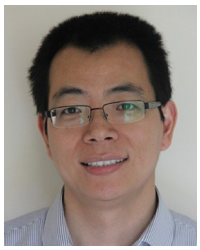

ZHIGUO DING (Fellow, IEEE) received the B.Eng. degree from the Beijing University of Posts and Telecommunications, Beijing, China, in 2000, and the Ph.D. degree from Imperial College London, London, U.K., in 2005. He is currently a Professor of Communications with Khalifa University, and has also been affiliated with the University of Manchester and Princeton University. His research interests are 5G networks, game theory, cooperative and energy-harvesting networks, and statistical signal processing. He recently received the EU Marie Curie Fellowship for the term from 2012 to 2014, the Top IEEE TVT Editor in 2017, the IEEE Heinrich Hertz Award in 2018, the IEEE Jack Neubauer Memorial Award in 2018, the IEEE Best Signal Processing Letter Award in 2018, the Friedrich Wilhelm Bessel Research Award in 2020, and the IEEE SPCC Technical Recognition Award in 2021. He is serving as an Area Editor for the IEEE OPEN JOURNAL OF THE COMMUNICATIONS SOCIETY and an Editor for IEEE TRANSACTIONS ON VEHICULAR TECHNOLOGY and IEEE WIRELESS COMMUNICATION LETTERS, IEEE TRANSACTIONS ON COMMUNICATIONS, and IEEE COMMUNICATION LETTERS from 2013 to 2016. He is a Distinguished Lecturer of IEEE ComSoc and a Web of Science Highly Cited Researcher in two categories in 2021.